Understanding and anticipating change in aquatic ecosystems

By

Ryan D. Batt

A dissertation submitted in partial fulfillment of

the requirements for the degree of

Doctor of Philosophy

(Limnology and Marine Sciences)

at the

UNIVERSITY OF WISCONSIN – MADISON

2014

Date of final oral examination: April 29, 2014

The dissertation is approved by the following members of the Final Oral Committee:

Stephen R. Carpenter, Professor, Zoology

Paul C. Hanson, Research Professor, Center for Limnology

James P. Hurley, Associate Professor, Civil and Environmental Engineering

Anthony R. Ives, Professor, Zoology

M. Jake Vander Zanden, Professor, Zoology

Table of Contents

Acknowledgements

During my years at the Center for Limnology, my committee was an unyielding source of wisdom and positive energy. For that support, I thank Steve Carpenter, Paul Hanson, Jim Hurley, Tony Ives, and Jake Vander Zanden. Insightful conversations with these individuals have greatly improved my research, and perhaps more important, continually reinvigorated my curiosity and passion for research. And for that, I am thankful.

I also thank all of the staff at UW–Madison who have helped me sift through confusion and guided me through hoops. Without them, I'd be (more) broke, unhealthy, lost, and I probably would have missed every important deadline as a graduate student. Thank you so much.

I've been incredibly fortunate to learn from Steve Carpenter, Mike Pace, and Jon Cole via my research at UNDERC. From them I've learned a lot of science and many life lessons, including how to appreciate bourbon and pork related humor. You taught me that, yes, science does involve facts and skill … but that science is also about friends, fun, humility, and humor (including towards one's self). I've never stopped learning from you, and doubt I ever will.

I love to talk (there you go, Mike), especially about science. There is a long list of people who have been willing to discuss my research with me, and I thank those who have enthusiastically engaged in protracted, stimulating discussion of my research: Luke Winslow, Jason Kurtzweil, Grace Wilkinson, Tim Cline, Arden Patton, Jereme Gaeta, Alex Latzka, Dan Oele, Cal Buelo, Sapna Sharma, Sam Oliver, Robert Johnson, David Seekell, Katie Deyoung, Jordan Read, Kevin

Rose, Amanda Stone, Emily Read, Tyler Tunney, Ben Kraemer. I'm certainly forgetting to mention some people here, but I haven't forgotten what they've meant to me.

Luke, we've had a ton of crazy, off-the-wall, and just downright interesting conversations about science and life … and even more cheeky exchanges first thing in the morning (perfect way to start the day, WS). Jason, you've been there since day 1, always in the thick of things helping me make sense of it all. Jereme, you've always been there to provide sound advice whenever I needed it. Grace, we were buds from the get-go – our conversations have covered a lot of subject matter, and you've been there for me at some key times. Kornis, you were a great office mate – beer, LoL, and of course, pennies.

And finally, my family, especially Mom, Dad, Madison, Sean, Nana, and Papa. The support and encouragement you've given me over the years has been essential to my health, happiness and professional motivation … probably more than you know. I love you.

Abstract

Ecosystem change can be understood through many approaches, including mechanistic analyses of ecosystem processes, the study of generic indicators of approaching change, or using past observations to gauge the scale and frequency of extreme events. My dissertation focuses on aspects of these three approaches to understanding change in lake ecosystems.

Metabolism is a fundamental process that occurs in all ecosystems. The metalimnion of some lakes can have high concentrations of chlorophyll and dissolved oxygen, which may be associated with high rates of primary production. However, metalimnetic metabolism is rarely quantified. Estimates of aquatic metabolism are facilitated by automated sensor technology, but time series collected from the metalimnion of a lake can be extremely noisy. We developed a metabolism model that uses a Kalman filter to estimate metabolism, and found that the metalimnion of Ward Lake is the locus of intense primary production. This model is able to reliably estimate metabolism from noisy metalimnetic time series.

The organic matter in lakes originates from a variety of habitats, including the surrounding terrestrial ecosystem. Ward Lake is a small, naturally productive lake that contains organic matter derived from a wide variety of primary producers – terrestrial material, macrophytes, benthic algae, and phytoplankton in the epilimnion and metalimnion comprise the base of the food web. We quantified the contribution of these resources to zooplankton, a snail, and fishes using stable isotopes of carbon, nitrogen, and hydrogen. Resource support varied among consumers, and fishes tended to integrate over resources more thoroughly than other consumers. Few studies investigate the energetic roles of macrophytes and metalimnetic phytoplankton, but we found that these resources made substantial contributions to consumer biomass. Thus, a variety of resources can support the food web of a naturally productive lake.

Latent low-quality resources may become energetically important to a food web when resource availability declines, which is a mechanism that is theorized to stabilize food webs. To test the potential for alternative resources to support consumers, we experimentally darkened Ward Lake, whose consumers had relied heavily on algal resources. Declining oxygen and chlorophyll along with increasing pCO_2 indicated reduced availability of resources and a shift to heterotrophy. A specialist copepod maintained high reliance on phytoplankton resources, but most other consumers (*Chaoborus* spp., a snail, fishes) received increased support from alternatives like floating-leafed macrophytes and terrestrial material. These shifts highlight the potential for increased support by alternative resources, which may provide a mechanism that stabilizes ecosystems.

Regime shifts are large and sudden ecosystem changes that involve thresholds, and theory suggests that statistical indicators of changing resilience can be detected near thresholds. However, these statistical indicators are data-hungry, may not be evident in all variables, and the variables showing signs of declining resilience may vary across types of regime shifts. Thus, data collection is a major challenge to the application of indicators of declining resilience. Automated measures of metabolism could be a solution to the challenge of data collection – metabolism is a variable that is central to a variety of ecosystem processes, and can be estimated from automated sensors, which can simultaneously measure a variety of variables with little increase in cost or effort. We examined the capacity of automated measures of metabolism to assess resilience during an experimentally-induced transition in a whole-lake manipulation. A trophic cascade was induced in a planktivore-dominated lake by slowly adding piscivorous bass, while a nearby bass-dominated lake remained unmanipulated and served as a reference ecosystem during the four-year experiment. We used the sensors to monitor variables related to metabolism (oxygen,

chlorophyll, pH), as well as to estimate metabolic rates. We were unable to detect indicators of changing resilience from the estimates of metabolic rates. However, we detected indicators of declining resilience in the directly measured variables in the manipulated lake prior to the completion of the regime shift. Therefore, automated sensors and variables related to metabolism may be useful for detecting approaching ecosystem thresholds.

An ecosystem can be greatly impacted by a single, large event. Massive events are more likely to be present in time series with extremes that follow fat-tailed probability distributions. As a result, the thickness of the tails of a distribution (tailedness) is often assessed for abiotic variables to gauge the size and frequency of disturbances like floods. However, the tailedness of biological time series is not well characterized. We analyzed 595 long-term lake time series spanning meteorological, physical, chemical, and biological variables, and show that a range of tailedness can be found in all variable types. Biological variables were the most fat-tailed time series in our data set, and were estimated to exceed their historical records more frequently than the other categories. Furthermore, we found that presuming a normal or log-normal distribution for ecological time series can result in a skewed perception of the time that will pass between recording breaking events. Even if a large event cannot be predicted, it is useful to know that it is possible. Thus, undue surprise from ecological extremes may be avoided by accounting for the tailedness of ecosystem variables, including biological populations.

Introduction

Ecosystem functioning is essential for human welfare. Therefore, understanding how and why ecosystems change is of utmost importance. My dissertation focuses on lake ecosystems and how they change.

One way to anticipate ecosystem change is through a mechanistic understanding. We can learn how an ecosystem works by treating it like a jigsaw puzzle: we study its components and join them as we find links, thereby allowing a clear picture to emerge from distinct pieces. Certain types of pieces serve the same functions across puzzles – corner and edge pieces form the edge of a puzzle, just like primary producers serve as the energetic basis of a food web. For the interior of the puzzle, we define characteristics that permit a logical connection between pieces, like color or shape. Big changes in one piece of an ecosystem reveal mechanisms that link it to other pieces, helping us to anticipate the consequences of future changes. However, some big changes are extremely difficult to anticipate from studying mechanisms alone, making the puzzle approach ineffective. In these situations, it may be better to look for generic signals of impending change, or to simply know that a big change is possible.

The first three chapters of my dissertation focus on studying ecosystem dynamics as a jigsaw puzzle, while in the last two I search for generic patterns that provide information on the timing or magnitude of big change. In the first chapter I find an edge piece to the puzzle by developing an approach for quantifying primary production. In the second chapter I use stable isotopes to figure out how the energetic edges of the food web feed into the consumers of a small lake. In the third chapter I again connect energetic edges to consumers using stable isotopes, but I also experiment with the color of the lake to understand how these connections can change when primary production declines. In the fourth chapter I use the dynamics of primary producers

to detect generic indicators of an ecosystem regime shift. In the fifth chapter I study a variety of ecosystem time series in order to determine what types of variables are most capable of producing surprisingly large events. Together, the chapters take several approaches to understanding ecosystem change.

Chapter 1: Kalman filter metabolism. Metabolism is a process common to all ecosystems, and includes net ecosystem production, respiration, and primary production. Primary producers necessarily comprise the ultimate source of organic energy in food webs. Thus, identifying loci of primary production is a critical step towards understanding food web and ecosystem functioning.

Sometimes a narrow band of the metalimnion of a lake will contain an exceptionally high concentration of chlorophyll and oxygen, indicating high primary producer biomass, and possibly high primary production. Metalimnetic primary production and its contribution to the rest of the food web are rarely quantified, but metalimnetic primary production can be substantial (Fee 1976). However, estimating metalimnetic primary production with modern free-water sensor methods can be challenging. A sensor suspended in the metalimnion of a lake can be subjected to large amount of noise as internal waves vertically displace the sensor, causing it to move between several sublayers of the metalimnion. Because the metalimnetic chlorophyll and oxygen maximum is a spatially discrete and abrupt phenomenon (adjacent layers have exceptionally *low* oxygen or chlorophyll), the resultant data are noisy, and this noise severely confounds conventional models for estimating metabolism from sensor data. To solve this problem, the first chapter of my dissertation employs a statistical technique known as a Kalman

filter to reliably estimate metabolism in the presence of noise. I applied this technique to the metalimnion of Ward Lake, which I found to have high rates of primary production.

Chapter 2: Resources supporting Ward Lake. The organic matter in lake ecosystems is derived from a variety of plant forms growing in a variety of lake habitats, and even includes organic matter originating from the surrounding terrestrial ecosystem. Ward Lake presented a variety of resources to its consumers: phytoplankton growing in the epilimnion and metalimnion, benthic algae, macrophytes, and terrestrial organic matter were present in this ecosystem. The contributions of some of these resources, such as metalimnetic phytoplankton and macrophytes, are not often quantified. Using stable isotopes as food web tracers, I found that all of these resources contributed to the consumers of Ward Lake, especially the algal resources. These results contribute to a small but growing body of evidence that metalimnetic and macrophyte resources support lake food webs.

Chapter 3: Resources supporting a lake dyed blue. Although many types of resources supported consumers in Ward Lake, some resources like terrestrial organic matter did not support many consumers, despite being abundant. Resources like terrestrial material are not generally considered to be high-quality resources for lake consumers. However, latent resources may become more important in times when the heavily-used high-quality resources become less abundant – a phenomenon which is known to contribute to the stabilization of food web dynamics.

Could the consumers of Ward Lake rely on these energetic alternatives? To test the potential for alternative resources to support a food web, we added a dye, Aquashade, to Ward

Lake in 2012. After Ward Lake was darkened and the abundance of important local resources (e.g., phytoplankton) declined, consumers were more greatly supported by alternative resources. This experiment demonstrates that alternative resources can support consumers when high-quality resources are depleted, which highlights support by alternative resources as a plausible mechanism for stabilizing food webs.

Chapter 4: Using sensors to detect declining resilience. The first three chapters of my dissertation describe a method for estimating primary production, and how primary production is linked to the flow of energy through a food web. These connections are mechanisms that aid in understanding how ecosystems might respond to particular environmental changes (e.g., darkening water). However, ecosystem regime shifts comprise a class of large ecosystem changes that can be sudden and difficult to reverse, but equally difficult to predict mechanistically. During a regime shift, an ecosystem can undergo sudden change as a small change in a key variable crosses a threshold. The exact location of this tipping point is hard to identify, which is what makes mechanistic prediction of regime shifts so difficult.

However, as a system approaches a tipping point, it loses resilience. This loss in resilience manifests itself as sluggish dynamics in key ecosystem variables, which in turn can be quantified through statistics like temporal variance and autocorrelation (Dakos et al. 2012). These leading indicators of declining resilience are promising for anticipating regime shifts, but data collection remains a large challenge to accurately computing indicator statistics, and thus to detecting changes in resilience. Furthermore, not all types of variables will show clear signs of declining resilience, and the variables showing changing resilience may differ among types of regime shifts.

Metabolism is a variable that is central to a variety of ecosystem processes, and can be estimated from automated sensors, which can simultaneously measure a variety of variables with little increase in cost or effort. As such, if changes in resilience could be detected in metabolism and associated variables, automated sensors may greatly facilitate the application of early warning theory in a management scenario. In my fourth chapter I used automated sensor data associated with ecosystem metabolism to detect changing resilience in a food web undergoing an experimentally induced regime shift.

Chapter 5: Fat tails. Previous chapters focused on mechanisms that guide ecosystems through change, and an approach to anticipating ecosystem change even when a precise mechanism is unknown. However, sometimes ecosystems are subjected to – or produce – large, surprising events. All variables have a set of largest observations over time – annual maxima, for example, may constitute such a set of extremes.

The tail of the distribution of extremes (henceforth tailedness) reflects a variable's propensity to exceed its historical precedent: a fat-tailed variable is more likely to massively exceed its record, whereas a thin-tailed variable is much more likely to break its record by a small margin (Coles 2001). Similarly, fat-tailed variables are likely to break their current record value more frequently than thin-tailed variables. Ecosystems can change drastically as a result of a single large event, which has made tailedness an important topic of study in environmental sciences. However, tailedness is typically evaluated for abiotic perturbations to ecosystems, but rarely assessed for the biotic components of ecosystems, like biological populations.

In the fifth chapter of my dissertation I present an analysis of 595 time series from the North Temperate Lakes Long Term Ecological Research database. My analysis is the first to

show that time series of vertebrate populations can be fat-tailed, and that biological variables are more fat-tailed than abiotic variables measured in the same ecosystems. The presence of fat-tailed biological variables could profoundly affect how we manage for ecosystem resilience, particularly because a variety of ecosystems are subject to regime shifts triggered by critical densities of biological populations (Folke et al. 2004, Carpenter et al. 2012). Managing for ecosystem resilience could be facilitated by investigating the mechanisms that generate fat tails, and by recognizing that fat tails exist in a variety of ecosystem variables, including biological populations.

Literature Cited in Introduction

Batt, R. D., and S. R. Carpenter. 2012. Free-water lake metabolism: Addressing noisy time series with a Kalman filter. Limnology and Oceanography: Methods 10:20–30.

Batt, R. D., S. R. Carpenter, J. J. Cole, M. L. Pace, T. J. Cline, R. A. Johnson, and D. a. Seekell. 2012. Resources supporting the food web of a naturally productive lake. Limnology and Oceanography 57:1443–1452.

Batt, R. D., S. R. Carpenter, J. J. Cole, M. L. Pace, and R. A. Johnson. 2013. Changes in ecosystem resilience detected in automated measures of ecosystem metabolism during a whole-lake manipulation. Proceedings of the National Academy of Sciences of the United States of America 110:17398–17403.

Carpenter, S., K. Arrow, S. Barrett, R. Biggs, W. Brock, A.-S. Crépin, G. Engström, C. Folke, T. Hughes, N. Kautsky, C.-Z. Li, G. McCarney, K. Meng, K.-G. Mäler, S. Polasky, M. Scheffer, J. Shogren, T. Sterner, J. Vincent, B. Walker, A. Xepapadeas, and A. Zeeuw. 2012. General Resilience to Cope with Extreme Events. Sustainability 4:3248–3259.

Coles, S. 2001. An introduction to statistical modeling of extreme values. Springer, London.

Dakos, V., S. R. Carpenter, W. a. Brock, A. M. Ellison, V. Guttal, A. R. Ives, S. Kéfi, V. Livina, D. a. Seekell, E. H. van Nes, and M. Scheffer. 2012. Methods for detecting early warnings of critical transitions in time series illustrated using simulated ecological data. PLoS ONE 7:e41010.

Fee, E. J. 1976. The vertical and seasonal distribution of chlorophyll in lakes of the Experimental Lakes Area, northwestern Ontario: Implications for primary production estimates. Limnology and Oceanography 21:767–783.

Folke, C., S. Carpenter, B. Walker, M. Scheffer, T. Elmqvist, L. Gunderson, and C. S. Holling. 2004. Regime Shifts, Resilience, and Biodiversity in Ecosystem Management. Annual Review of Ecology, Evolution, and Systematics 35:557–581.

Chapter 1: Free-water lake metabolism: addressing noisy time series with a Kalman filter*

Abstract

Whole-ecosystem metabolism is often estimated in lakes using high-frequency free-water measurements of dissolved oxygen (DO) taken in the upper mixed layer. DO dynamics in the metalimnion are not adequately captured by measurements made in the upper mixed layer, which could reduce the accuracy of whole-lake metabolism estimates made from such data. However, estimating metabolism from metalimnetic DO time series can be challenging because of high variability (noise). This study used simulated and field data to determine if metabolism estimates from metalimnetic data containing noise can be improved by accounting for both process and observation error in models. When DO time series exhibited high variability, free-water metabolism estimates obtained using a Kalman filter (which accounts for both process and observation error) were substantially more accurate than estimates obtained from models that did not account for error or accounted for process error only.

*Published as: Batt, R. D. and S.R. Carpenter. 2012. Free-water lake metabolism: addressing noisy time series with a Kalman filter. *Limnology and Oceanography: Methods* **10**: 20-30, doi: 10.4319/lom.2012.10.20

Introduction

Metabolism is a fundamental ecosystem process that describes the collective fixation and mineralization of carbon by all organisms in a given ecosystem. Whole-lake metabolism characterizes the origin and fate of energy in lake food webs (Schindler et al. 1972; Cole et al. 2000; Pace et al. 2004), and quantifies part of the role that lakes play in global carbon cycling (Cole et al. 2007). Ecosystem metabolism has been measured in aquatic ecosystems for decades using free-water measurements of dissolved oxygen (DO) concentration (Odum 1956). In recent years, free-water methods for estimating metabolism have become increasingly more common as technological advances have increased the availability of sensors (known as sondes) capable of making high-frequency measurements of DO over extended deployments. Free-water methods are less constrained by the questions of scale and container effects that arise in alternative methods, and high-frequency approaches are able to capture temporal dynamics that may be missed by discrete approaches (Stæhr and Sand-Jensen 2007).

Although the use of high-frequency free-water DO measurements to estimate whole-lake metabolism has advantages over alternative approaches, it presents researchers with its own challenges. One conceptual challenge results from the spatial heterogeneity of metabolic processes within a system. Most whole-lake metabolism studies using high-frequency free-water DO measurements have used a single sonde placed in the pelagic epilimnion of a lake and assumed that measurements made there were representative of biological processes occurring throughout the system, although this assumption is often problematic (Stæhr et al. 2010). Because the spatial variation in metabolic processes in an aquatic system may not be promptly and fully integrated into the DO dynamics at a given location, metabolism estimates can vary with the horizontal (Caraco and Cole 2002; Lauster et al. 2006; Van de Bogert et al. 2007) and

vertical (Gelda and Effler 2002; Coloso et al. 2008; Sadro et al. 2011) location of a sensor. Metabolism in the metalimnion of lakes is not measured by a sonde near the surface, yet metalimnetic production may be important in total ecosystem metabolism (Fee 1976; St. Amand and Carpenter 1993; Sadro et al. 2011), although this role has been questioned in some cases (Pick et al. 1984; Coloso et al. 2008). Although measuring metalimnetic in addition to epilimnetic metabolism may be desirable, placing a sonde in this layer to address the conceptual challenge of spatial heterogeneity may yield time series of metalimnetic DO with high variability relative to the diel metabolic signal. This noise has many potential causes, but is likely caused in part by surface and internal waves shifting the sensor between metalimnetic sublayers, which can lead to inaccurate metabolism estimates (Coloso et al. 2008). Thus, efforts to measure metalimnetic metabolism and address the conceptual challenge of spatial heterogeneity are confronted by the statistical challenge of noisy data.

Existing models used to estimate metabolism from sonde data either omit a term for error (Cole et al. 2000), or only include process error to represent lack of model fit (Hanson et al. 2008; Ciavatta et al. 2008). These types of models may be appropriate in some situations, but the nature of the noise present in metalimnetic data may require a different approach. A Kalman filter can be used to estimate metabolic parameters while accounting for not only process error, but also observation error, which represents variability in the DO measurements that is not related to metabolism (Harvey 1989). Kalman filtering has been applied to automated sensor data to estimate net ecosystem production (Soetaert and Gregoire 2011), but to our knowledge has not been used to estimate gross primary production (GPP) or respiration (R). If observation error better characterizes the high-frequency noise associated with metalimnetic data than process error, accounting for it in models should permit more accurate metabolism estimates. This paper

evaluates the ability of a Kalman filter to improve the accuracy of whole-lake metabolism estimates made from DO measurements exhibiting different varieties and magnitudes of noise.

Materials and procedures

This study employed both simulated and measured dissolved oxygen data, and in both cases estimated gross primary production (GPP), respiration (R), and net ecosystem production (NEP) using three distinct models. All models evaluated metabolism as it would occur in the metalimnion of a lake, where there is no diffusive exchange with the atmosphere, and diffusive exchange with nearby water layers can be assumed to be minimal (Cole and Pace 1998; Gelda and Effler 2002), leaving changes in DO concentration attributable to biological processes. The first two models are commonly used in whole-lake metabolism studies, while the third model is novel and served to estimate metabolism as well as to filter DO time series before use in conjunction with the first two models.

Models—The bookkeeping model (BK) is based on the model presented by Cole et al. (2000), and is implemented in numerous other studies calculating whole-lake metabolism from high-frequency DO data (Hanson et al. 2003; Coloso et al. 2008). The model is rooted in the Odum (1956) model,

$$\Delta DO = NEP + F = GPP + R + F \quad (1)$$

where the change in oxygen between each measured time step (ΔDO) results from diffusive exchange with the atmosphere and other water layers (F), plus net ecosystem production (NEP). NEP is the sum of gross primary production ($GPP \geq 0$) and total ecosystem respiration ($R \leq 0$) during that time interval. F was set equal to zero because changes in oxygen between time steps resulting from diffusive exchange with the atmosphere and adjacent water layers are assumed to be negligible in the metalimnion. While NEP can be measured directly, R and GPP need to be

determined algebraically because these two processes occur simultaneously during the day. However, total nighttime R is equal to nighttime NEP because GPP does not occur at night:

$$\sum \Delta DO_{night} = NEP_{night} = \sum R_{night} \quad (2)$$

Furthermore, by assuming that the respiration rate is constant over a 24-hour period (Carignan et al. 2000; Cole et al. 2000; Hanson et al. 2003), we were able to calculate the respiration rate during a given daylight period as the mean of the respiration rates from the nights (periods of darkness) preceding (*night[-1]*) and following (*night[+1]*) the daylight period of interest. Multiplying these daytime (calculated from $R_{night[-1]}$ and $R_{night[+1]}$) and nighttime (R_{night}) respiration rates by their respective durations (Δt_{day} and Δt_{night}) and subtracting them from NEP then yields GPP for a given day:

$$GPP = NEP - ([R_{night[-1]} + R_{night[+1]}]/2 \times \Delta t_{day}) - (R_{night} \times \Delta t_{night}) \quad (3)$$

GPP, R, and NEP are estimated by BK through the bookkeeping of diel changes in DO.

The second model is a linear model (LM) where change in DO between times *t* and *t-1* is a function of surface photosynthetically active radiation (PAR; *I*), the natural logarithm of water temperature (*T*), diffusive exchange with the atmosphere and other water layers (*F*), and unknown processes modeled as normally distributed error (ε) with a mean = *0* and variance = σ^2:

$$DO_t - DO_{t-1} = (\beta_1 \times I_{t-1} + \beta_2 \times ln(T_{t-1}) + F_{t-1}) \times \Delta t + \varepsilon_t \; ; \; \varepsilon \sim N(0, \sigma^2) \quad (4)$$

F is set equal to zero because diffusive exchange is assumed to be negligible in the metalimnion, β_1 and β_2 are parameters to be fit, and are factors in the terms that correspond to GPP and R, respectively:

$$GPP = \beta_1 \times I \; ; \; \beta_1 \geq 0 \quad (5)$$

$$R = \beta_2 \times ln(T); \; \beta_2 \leq 0 \quad (6)$$

In this model, change in GPP is driven by PAR, and change in R is driven by temperature. The Linear Model (LM) is similar to the simple model described in Hanson et al. (2008) in that it fits parameters to the DO time series and includes a term accounting for error in the modeled process. Models such as LM use fitted parameters, and are common in metabolism studies (Stæhr and Sand-Jensen 2006; Hanson et al. 2006; Van de Bogert et al. 2007; Langman et al. 2010), and contrast with the bookkeeping approach in that they include an error term, instead of subsuming the error in the estimates of the metabolism parameters.

The third model makes use of a Kalman filter, an approach that is well established in statistics (Kalman 1960; Harvey 1989). The process equation of the Kalman filter model (KF) is

$$DO_{[True]\,t} - DO_{[True]t-1} = (\beta_1 \times I_{t-1} + \beta_2 \times ln(T_{t-1}) + F_{t-1}) \times \Delta t + \varepsilon_t\,;\ \varepsilon \sim N(0, Q) \qquad (7)$$

where $DO_{[True]}$ is the true (but unknown) DO concentration, Q is the variance of the process error, and all other model parameters and terms are as described for LM. While models such as LM account for error in the predictions of DO (process error), they do not account for error in the observations of DO (observation error) that can occur if a sensor does not measure what it is intended to measure. Observation error occurs, for example, when surface waves shift a sensor into neighboring sublayers with DO concentrations distinct from the one intended for observation. Even though the sensor movement between layers is not related to metabolism, LM can only respond to this variability by adjusting estimates of biological parameters and process error variance. KF, in contrast, describes the relationship between true DO (DO in the sublayer of interest) and observed DO (the DO measured by the sensor) in a second equation, the observation equation,

$$DO_{[Observed]t} = DO_{[True]t} + v_t\,;\ v \sim N(0, H) \qquad (8)$$

where v is the error associated with the imperfect observation of DO, and H is the variance of the observation error.

The Kalman filter calculations (Harvey 1989, pp. 105-6) combine information about the data generating process (Eq. 7) with the manner in which the state variable is observed (Eq. 8). At each time step Eq. 7 gives an estimate of the true but unknown value of the state variable, DO. However, additional information concerning the true value of DO becomes available when a new observation of DO is made, and the Kalman filter routine updates the current estimate of DO to yield an estimate that is closer to the true value of DO than would be given by either Eq. 7 or 8. The update weights the two sources of information to yield a new estimate of DO that is somewhere between the predicted and observed value, but closer to the value that is more precise (1/Q for the prediction in Eq. 7, and 1/H for the observation in Eq. 8). Thus the Kalman filter recursion proceeds stepwise and unidirectionally through time, and given linear process and observation equations (Eqs. 7 and 8) with time-invariant model parameters (including the error variances Q and H) both the propagation of error variances through time and updating equations follow a standard algorithm (Harvey 1989, pp. 105-6, Eqs. 3.2.1-3). In Web Appendix A we have provided example code written in R (R Core Development Team 2011) that implements KF, and in Web Appendix B we have provided a sample data set that is used by the example code.

The parameters to be estimated in KF are β_1, β_2, Q, and H; however, values for Q and H cannot be fit simultaneously because a unique solution would not exist. β_1, β_2, and Q were fit using maximum likelihood estimation (Harvey 1989, p. 126, Eq. 3.4.5) after H was estimated independently and supplied to the model as a constant. H was estimated as the mean of a running variance of the DO time series with a window size of 10 samples (40 minutes). Window size was chosen to be small enough such that the effect of modeled and unknown processes on DO

variability would be minimal (leaving the majority of DO variability attributable to observation error), but large enough to acquire an accurate estimate of variance. The effects of our approach for estimating H on metabolism estimates and filtered DO are discussed later.

Because KF estimates of DO are dependent on temperature (Eq. 7), temperature data were filtered before being used to filter DO. The process equation for the temperature filter is

$$T_{[True]t} = (\beta_{1[T]} \times T_{[True]t-1} + \beta_{2[T]} \times (q_{[In]t} - q_{[Out]t})) \times \Delta t + \varepsilon_t \, ; \, \varepsilon \sim N(0, Q_{[T]}) \quad (9)$$

where $\beta_{1[T]}$ and $\beta_{2[T]}$ are parameters to be fit, $Q_{[T]}$ is the variance of the process error, q_{In} is the amount of energy entering the layer of interest in watts, and q_{Out} is energy exiting the layer. Energy values were estimated from PAR (400nm - 700nm) measurements, and energy (q) at a given depth (z) was calculated as

$$q_z = q_0 \times e^{\mu z} \quad (10)$$

where q_0 is the energy at the surface of the lake, e is the base of the natural logarithm, and μ is the attenuation coefficient of light in the lake. Light attenuation was calculated as

$$\mu = ln(0.01)/z_{0.01} \quad (11)$$

where $z_{0.01}$ is the depth at which 99% of light incident at the surface of the lake has been attenuated in the water column (measured with depth profiles of PAR). The observation equation for the temperature filter is

$$T_{[Observed]t} = T_{[True]t} + v_t \, ; \, v \sim N(0, H_{[T]}) \quad (12)$$

where v is the error associated with imperfect observation of temperature, and $H_{[T]}$ is its variance. The parameters and the error variance estimates for the temperature filter were calculated in the same fashion as they were for DO.

Measured data—Field data were collected from Ward Lake, a small (area = 1.9 ha, maximum depth = 8 m) mesotrophic lake at the University of Notre Dame Environmental

Research Center near Land O' Lakes, Wisconsin, USA. From May 26 through May 31, 2010 dissolved oxygen and temperature were measured every four minutes near the metalimnetic oxygen maximum (ca. 1% surface light and 4 m depth) using a YSI 600XLM sonde fitted with a rapid pulse oxygen probe (model 6562) and temperature probe. In the LM and KF models, the size of each time step (Δt) was set equal to the four-minute sampling frequency of DO and temperature as measured by the sonde. A vertical light profile was taken using LI-COR photosynthetically active radiation (PAR) sensors (models LI-190 and LI-193), and surface PAR was measured every 5 minutes with a LI-COR sensor on a buoy at nearby Peter Lake.

Simulated data—In order to assess the ability of the three models presented in this study to estimate metabolism accurately, DO time series with known underlying metabolic processes were simulated. DO time series were generated to fit the deployment duration and sampling frequency of measurements made by the sonde in Ward Lake. Eq. 7 and 8 were used to generate these data from field measurements of PAR, Kalman filtered temperature, and fixed values of β_1 and β_2. PAR data were linearly interpolated and resampled to match the 4-minute sampling frequency of sonde measurements. The deterministic portion of Eq. 7 was used to generate a noiseless DO time series, where the true values of GPP and R (Eq. 5 & 6, respectively) drove the changes in DO. Various magnitudes of process and observation error were then added to this deterministic skeleton (noiseless time series) to simulate the noisy DO time series used in sensitivity analyses. These stochastic components (noise) were independently generated for each combination of Q (n=6) and H (n=5), and for each replicate (n=30) of these combinations. Thus each time series was an independent realization of the same stochastic process.

Assessment

The ability of each model to accurately estimate true mean daily values for GPP (23.75 μmol O_2 L^{-1} d^{-1}) and R (-16.09 μmol O_2 L^{-1} d^{-1}) was examined for simulated time series collectively exhibiting a wide range of observation and process error. In addition to examining the accuracy of each model for noisy simulated data, we explored the potential for using the methods sequentially by first filtering noisy time series using KF, then implementing BK and LM. Simulations were also used to demonstrate the sensitivity of metabolism calculations to estimates of *H*. Having assessed their performance on simulated data, the models were then evaluated in a similar fashion using observational data from Ward Lake.

Simulation—When KF is applied to a DO time series, the resultant filtered time series contains substantially less variability than the noisy time series (Fig. 1). To test if such a reduction in variability would improve metabolism estimates generated by BK and LM, these models were run on thirty combinations of process error ($\varepsilon \sim N(0, Q)$; Q = 0.1, 0.5, 1, 5, 50, 100 (μmol O_2 L^{-1})^2) and observation error ($v \sim N(0, H)$; H = 1, 10, 50, 100, 500 (μmol O_2 L^{-1})^2) variance, both before and after filtering, replicated thirty times for each combination. Model estimates of GPP and R were calculated as the overall mean daily estimate for thirty replicate stochastic simulations of six-day deployments.

Estimates of GPP and R generated by BK rapidly departed from true values as the variance of process (Q) and observation error (H) increased (Fig. 2A,C). Increases in Q for a given value of H consistently resulted in greater absolute deviations of GPP and R from true values, and increases in H for a given value of Q resulted in greater absolute deviations for all but the highest value of Q. Overall, filtering DO time series with KF prior to estimating metabolism with BK reduced mean absolute deviations of estimates from true values (unfiltered data = 50.21 μmol O_2 L^{-1} d^{-1}, filtered data = 39.17 μmol O_2 L^{-1} d^{-1}). Specifically, filtering

substantially reduced the impact of observation error on the ability of BK to accurately estimate GPP and R (Fig. 2B,D). However, the ability of filtering to mitigate the effects of error on the accuracy of BK were largely limited to observation error, as increases in process error resulted in less accurate metabolism estimates even after filtering.

Metabolism estimated by BK and LM responded similarly to increased error variance in DO time series: increased process and observation error variances were accompanied by decreased accuracy (Fig. 3A,C). Furthermore, estimates from LM were more strongly influenced by process error than they were by observation error. Despite similarity in these trends, LM displayed a dampened sensitivity to increases in observation error variance relative to BK, and while filtering did serve to mitigate the effects of observation error, LM did not respond as strongly to filtering as BK (LM overall mean of GPP and R absolute differences for unfiltered and filtered data = 25.91 and 25.00 μmol O_2 L^{-1} d^{-1}, respectively). The overall mean accuracy of metabolism estimates was consistently greater in LM (25.45 μmol O_2 L^{-1} d^{-1}) than in BK (44.69 μmol O_2 L^{-1} d^{-1}), and estimates derived from time series filtered by KF were closer to true values than unfiltered estimates for both models.

Deviations of KF metabolism estimates from true values were driven almost exclusively by process error variance (Fig. 4), a pattern which is similar to that observed for the other two models when estimates were derived from filtered data. Estimates from KF (overall mean of GPP and R absolute differences = 24.99 μmol O_2 L^{-1} d^{-1}) were similar to those from LM on filtered data. This similarity between LM on filtered data and KF is reasonable because the main effect of filtering seems to be the removal of observation error, and the two models have an equivalent approach for estimating metabolism in the presence of the remaining process error. However, when values of H were high and values of Q low, the Kalman filter allowed LM to

yield metabolism estimates as accurate as those from KF. Among combinations of Q and H, KF tended to be equally or more accurate than LM.

The effects of over- and underestimating H on metabolism estimates were assessed for each model. Estimates of H were adjusted by factors of 0.1, 0.25, 0.5 (three underestimates), 1 (unadjusted), 2, 4, and 10 (three overestimates) for thirty stochastic simulations of DO time series (for each simulation Q and H = 0.5 and 100 (μmol O_2 L^{-1})^2, respectively). Mean model estimates of GPP, R, and NEP remained consistently near true values across all adjustments to the estimate of H (Fig. 5). Furthermore, variability was smallest near the unadjusted estimate of H for LM and KF estimates of GPP and R. However, variability in BK estimates of GPP and R declined as overestimates of H became more extreme. The variability in estimates of NEP was smallest for all models when H was adjusted by a factor of 0.5. Therefore metabolism estimates were robust to imperfect estimates of H, for their variability across adjustments to H was predictable and their mean never strongly biased.

Case study—The DO time series measured in the metalimnion of Ward Lake was characterized by substantial noise, but filtering the data with KF resulted in reduced noise and maintained diel cycles and overall trend (Fig. 6). However, the ability of KF to reduce noise was diminished in the case of measured data, relative to simulations. Filtering nonetheless reduced the metabolism estimates from the BK and LM models, causing estimates among models to become more similar (Fig. 7). Despite substantial noise remaining in the measured DO time series after filtering with KF, increased agreement among models after filtering suggests that filtering still increased model accuracy.

Estimates of H for measured data were adjusted to assess their influence on filter smoothing and metabolism estimates. Adjusting the estimate of H upward caused the DO time

series to be smoothed to a greater degree (Fig. 8), and also influenced metabolism estimates for all models (Fig. 9). As estimates of *H* were adjusted upward, estimates of GPP, R and NEP from all three models began to converge: estimates of GPP and R tended to decrease for the three models, and NEP tended to increase. These results are consistent with those for simulated data, where adjusting *H* had a minimal effect on the mean estimate but caused means among models to converge near true values as *H* was inflated (Fig. 5).

Overestimating *H* increased the smoothing effect of KF on DO time series (Fig. 8), reduced variability around mean metabolism estimates, and caused mean estimates to approach a true value or converge upon a value common to all models (Fig. 5,9). Furthermore, the ability of filtering to result in more similar estimates among models (Fig. 7) was enhanced by overestimating *H* to further smooth the DO time series supplied to BK and LM, as supplying a smoother time series resulted in more similar model estimates (Fig. 9). Thus KF performed consistently with both observed and simulated data, where it proved to be robust to estimates of *H*, and resulted in improved metabolism estimates—both independently and in conjunction with the BK and LM models.

Discussion

Application of a Kalman filter mitigated the adverse effects of observation error on metabolism estimates, and in simulation proved to be both necessary and sufficient to obtain the most accurate estimates among all models in this study. However, the advantage of the Kalman filter over the other models was confined to time series with high observation error and moderate to low process error. If substantial observation error was not present, or if process error was the main driver of inaccurate estimates, other models performed equally well. BK contained the simplest terms for processes (no error term or covariates), while LM and KF contained

equivalent process terms (temperature and PAR as covariates). KF performed better in simulation than the other models because it is the only model that included a term for observation error, giving it an advantage in the presence of observation error. Although the process equation used in KF was simple, other process error models can be incorporated into a Kalman filter framework, just as LM was incorporated into KF.

Although serially correlated process error caused DO time series smoothed by KF to depart from true values, smoothed time series were devoid of much of the noise caused by observation error, which is not serially correlated (Fig. 1,8). Furthermore, DO time series were smoother when estimates of the variance of observation error (H) were inflated (Fig. 8), a result consistent with other applications of the Kalman filter (Harvey 1989; Soetaert and Gregoire 2011). Thus KF not only improved the accuracy of metabolism estimates (Fig. 1,8), but it also provided a smoother time series that could then be used with the other models. While providing filtered DO time series to BK and LM did not yield estimates of metabolism that were more accurate than those provided by KF, filtering time series may still be useful. Specifically, filtering a time series with a Kalman filter may be useful when the filtered data is not used to estimate the same process that was used to filter that data (i.e., the process estimated by the Kalman filter, as was the case when filtered DO was supplied to BK and LM). For example, the temperature time series supplied to KF was first filtered with a Kalman filter that used a process equation that described change in temperature as the loss and gain of energy in the sublayer intended for measurement. This filtered temperature time series was then supplied to the KF to guide respiration dynamics (a process different from that used to filter the time series), thereby facilitating more accurate estimates of whole-lake metabolism.

Lakes play an important role in both regional and global carbon cycling (Cole et al. 2007; Buffam et al. 2010), and metalimnetic metabolism may be an important component of whole-lake metabolism (Fee 1976; St. Amand and Carpenter 1993; Coloso et al. 2008; Sadro et al. 2011), especially in oligotrophic and mesotrophic lakes which often exhibit a pronounced chlorophyll maximum (Moll and Stoermer 1982). Furthermore, the primary production in this habitat could be an important autochthonous food source for aquatic organisms (Winder et al. 2003; Francis et al. 2011), although the magnitude of metalimnetic autochthony has been debated (Winder et al. 2004; Cole et al. 2011). Stæhr et al. (2010) highlighted the need to obtain accurate estimates of metalimnetic metabolism, and recommend the use of vertically profiling instruments to obtain depth-integrated estimates. The sampling frequency of a vertical profile of DO recorded by one sensor would be substantially lower than the four minute frequency used in this study, which may affect the accuracy of estimates of H by reducing the sampling size from which the variance is calculated. However, KF was shown to be robust to estimates of H, especially if H is overestimated, suggesting that it may be successfully coupled with a profiling sampling regime to obtain accurate metalimnetic metabolism estimates.

Comments and recommendations

Although process error in the simulations and models of this study can be easily distinguished from observation error because the former is serially correlated, the two can become conceptually similar from certain perspectives. For example, observation error in time series collected from the metalimnion of Ward Lake may be caused by physical processes that could conceivably be modeled, such as waves that cause motion of the sensor relative to the water layer of interest. Our results show that improved metabolism estimates can be obtained by treating these errors, which have an unknown cause, as observation errors modeled by KF.

Nonetheless, physical modeling may show that alternate approaches based on alternate filtering methods, such as Gaussian-filtering at the periods of lower-frequency internal waves (MacIntyre et al. 2009), may also improve metabolism estimates. Lake size may provide an important clue for physically-based approaches. Such extensions of physical limnology modeling for metabolism studies are an important topic for further research.

KF was most useful when the dominant source of noise in simulated time series was observation error. The metalimnion of Ward Lake contained large amounts of noise that resembled the observation error in the DO time series simulated in this study, suggesting that future studies of metalimnetic metabolism may benefit greatly from the use of a Kalman filter. Most DO time series intended for use in lake metabolism studies are measured in the pelagic epilimnion, a habitat lacking the mechanisms believed to drive the high observation error present in metalimnetic time series. Although it was most advantageous to use KF when observation error was high, this study showed that under all simulated noise conditions a Kalman filter provides metabolism estimates that are similar to or better than those made by the other methods examined in this study, making it a useful approach to estimating metabolism in any aquatic habitat.

Acknowledgements

We thank the staff of the University of Notre Dame Environmental Research Center for facilitating our research, Jim Coloso for assistance in the field and technical advice; Tim Cline, Jason Kurtzweil, Laura Smith, and Lee Zinn for assistance in the field; Jordan Read for analytical advice; the Cascade team for instruments; Jon Cole and Mike Pace for discourse concerning analyses; and Jereme Gaeta, Paul Hanson, Sapna Sharma, Amanda Stone, Luke

Winslow and the referees for feedback on earlier versions of this manuscript. Financial support for this research was provided by the National Science Foundation.

Literature Cited in Chapter 1

Buffam, I., M. G. Turner, A. R. Desai, P. C. Hanson, J. A. Rusak, N. R. Lottig, E. H. Stanley, and S. R. Carpenter. 2010. Integrating aquatic and terrestrial components to construct a complete carbon budget for a north temperate lake district. Global Change Biology, doi:10.1111/j.1365-2486.2010.02313.x

Caraco, N. F., and J. J. Cole. 2002. Contrasting impacts of a native and alien macrophyte on dissolved oxygen in a large river. Ecological Applications **12**: 1496-1509, doi:10.1890/1051-0761(2002)012[1496:CIOANA]2.0.CO;2

Carignan, R., D. Planas, and C. Vis. 2000. Planktonic production and respiration in oligotrophic Shield lakes. Limnology and Oceanography **45**: 189-199.

Ciavatta, S., R. Pastres, C. Badetti, G. Ferrari, and M. B. Beck. 2008. Estimation of phytoplanktonic production and system respiration from data collected by a real-time monitoring network in the Lagoon of Venice. Ecological Modelling **212**: 28-36, doi:10.1016/j.ecolmodel.2007.10.025

Cole, J. J., S. R. Carpenter, J. F. Kitchell, M. L. Pace, C. T. Solomon, and B. Weidel. 2011. Strong evidence for terrestrial support of zooplankton in small lakes based on stable isotopes of carbon, nitrogen, and hydrogen. Proceedings of the National Academy of Sciences of the United States of America **108**: 1975-1980, doi:10.1073/pnas.1012807108

Cole, J. J., M. L. Pace, S. R. Carpenter, and J. F. Kitchell. 2000. Persistence of net heterotrophy in lakes during nutrient addition and food web manipulations. Limnology and Oceanography **45**: 1718–1730, doi:10.4319/lo.2000.45.8.1718

Cole, J. J., Y. T. Prairie, N. F. Caraco, W. H. McDowell, L. J. Tranvik, R. G. Striegl, C. M. Duarte, P. Kortelainen, J. A. Downing, J. J. Middelburg, and J. M. Melack. 2007. Plumbing

the global carbon cycle: Integrating inland waters into the terrestrial carbon budget. Ecosystems **10**: 171-184.

Cole, J. J., and M. L. Pace. 1998. Hydrologic variability of small, northern Michigan lakes measured by the addition of tracers. Ecosystems **1**: 310-320, doi:10.1007/s100219900024

Coloso, J. J., J. J. Cole, P. C. Hanson, and M. L. Pace. 2008. Depth-integrated, continuous estimates of metabolism in a clear-water lake. Canadian Journal of Fisheries and Aquatic Sciences **65**: 712-722, doi:10.1139/F08-006

Fee, E. J. 1976. The vertical and seasonal distribution of chlorophyll in lakes of the Experimental Lakes Area, northwestern Ontario: implications for primary production estimates. Limnology and Oceanography **21**: 767-783.

Francis, T. B., D. E. Schindler, G. W. Holtgrieve, E. R. Larson, M. D. Scheuerell, B. X. Semmens, and E. J. Ward. 2011. Habitat structure determines resource use by zooplankton in temperate lakes. Ecology Letters, doi:10.1111/j.1461-0248.2011.01597.x

Gelda, R. K., and S. W. Effler. 2002. Metabolic rate estimates for a eutrophic lake from diel dissolved oxygen signals. Hydrobiologia **485**: 51-66.

Hanson, P. C., D. L. Bade, S. R. Carpenter, and T. K. Kratz. 2003. Lake metabolism: relationships with dissolved organic carbon and phosphorus. Limnology and Oceanography **48**: 1112-1119, doi:10.4319/lo.2003.48.3.1112

Hanson, P. C., S. R. Carpenter, D. E. Armstrong, E. H. Stanley, and T. K. Kratz. 2006. Lake dissolved inorganic carbon and dissolved oxygen: changing drivers from days to decades. Ecological Monographs **76**: 343-363, doi:10.1890/0012-9615(2006)076[0343:LDICAD]2.0.CO;2

Hanson, P. C., S. R. Carpenter, N. Kimura, C. Wu, S. P. Cornelius, and T. K. Kratz. 2008. Evaluation of metabolism models for free-water dissolved oxygen methods in lakes. Limnology and Oceanography: Methods **6**: 454-465.

Harvey, A. C. 1989. Forecasting, Structural Time Series Models and the Kalman Filter, Cambridge University Press.

Kalman, R. E. 1960. A New Approach to Linear Filtering and Prediction Problems. Journal of Basic Engineering **82**: 35-45.

Langman, O. C., P. C. Hanson, S. R. Carpenter, and Y. H. Hu. 2010. Control of dissolved oxygen in northern temperate lakes over scales ranging from minutes to days. Aquatic Biology **9**: 193-202, doi:10.3354/ab00249

Lauster, G. H., P. C. Hanson, and T. K. Kratz. 2006. Gross primary production and respiration differences among littoral and pelagic habitats in northern Wisconsin lakes. Canadian Journal of Fisheries and Aquatic Sciences **63**: 1130-1141.

MacIntyre, S., J. P. Fram, P. J. Kushner, N. D. Bettez, W. J. O. Brien, J. E. Hobbie, and G. W. Kling. 2009. Climate-related variations in mixing dynamics in an Alaskan arctic lake. Limnology and Oceanography **54**: 2401-2417.

Moll, R. A., and E. F. Stoermer. 1982. A hypothesis relating trophic status and subsurface chlorophyll maxima of lakes. Archiv für Hydrobiologie **94**: 425-440.

Odum, H. T. 1956. Primary production in flowing waters. Limnology and Oceanography **1**: 102 - 117.

Pace, M. L., J. J. Cole, S. R. Carpenter, J. F. Kitchell, J. R. Hodgson, M. C. Van de Bogert, D. L. Bade, E. S. Kritzberg, and D. Bastviken. 2004. Whole-lake carbon-13 additions reveal terrestrial support of aquatic food webs. Nature **427**: 240-243, doi:10.1038/nature02215.1.

Pick, F. R., C. Nalewajko, and D. R. S. Lean. 1984. The Origin of a Metalimnetic Chrysophyte Peak. Limnology and Oceanography **29**: 125-134.

R Development Core Team. 2011. R: A Language and Environment for Statistical Computing. R Foundation for Statistical Computing, Vienna, Austria. ISBN 3-900051-07-0, URL http://www.r-project.org/.

Sadro, S., J. M. Melack, and S. MacIntyre. 2011. Depth-integrated estimates of ecosystem metabolism in a high-elevation lake (Emerald Lake, Sierra Nevada, California). Limnology and Oceanography **56**: 1764-1780, doi:10.4319/lo.2011.56.5.1764

Schindler, D. W., G. J. Brunskill, S. Emerson, W. S. Broecker, and T. Peng. 1972. Atmospheric carbon dioxide: Its role in maintaining phytoplankton standing crops. Science **177**: 1192-1194.

Soetaert, K., and M. Gregoire. 2011. Estimating marine biogeochemical rates of the carbonate pH system—A Kalman filter tested. Ecological Modelling **222**: 1929-1942, doi:10.1016/j.ecolmodel.2011.03.012

St. Amand, A. L., and S. R. Carpenter. 1993. Metalimnetic phytoplankton dynamics, p. 210-224. *In* S.R. Carpenter and J.F. Kitchell [eds.], The Trophic Cascade in Lakes. Cambridge University Press.

Stæhr, P. A., D. L. Bade, M. C. Van de Bogert, G. R. Koch, C. Williamson, P. C. Hanson, J. J. Cole, and T. K. Kratz. 2010. Lake metabolism and the diel oxygen technique: State of the science. Limnology and Oceanography: Methods **8**: 628-644.

Stæhr, P. A., and K. Sand-Jensen. 2006. Seasonal changes in temperature and nutrient control of photosynthesis, respiration and growth of natural phytoplankton communities. Freshwater Biology **51**: 249-262, doi:10.1111/j.1365-2427.2005.01490.x

Stæhr, P. A., and K. Sand-Jensen. 2007. Temporal dynamics and regulation of lake metabolism. Limnology and Oceanography **52**: 108-120.

Van de Bogert, M. C., S. R. Carpenter, J. J. Cole, and M. L. Pace. 2007. Assessing pelagic and benthic metabolism using free water measurements. Limnology and Oceanography: Methods **5**: 145-155.

Winder, M., H. R. Buergi, and P. Spaak. 2003. Seasonal vertical distribution of phytoplankton and copepod species in a high-mountain lake. Archiv für Hydrobiologie **158**: 197-213, doi:10.1127/0003-9136/2003/0158-0197

Winder, M., P. Spaak, and W. M. Mooij. 2004. Trade-offs in Daphnia habitat selection. Ecology **85**: 2027-2036, doi:10.1890/03-3108

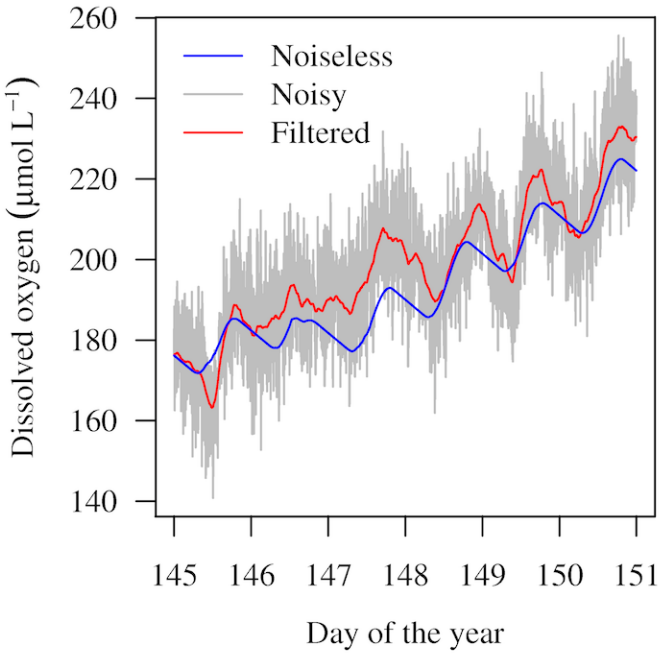

Fig. 1. Using the deterministic component of Eq. 4, the noiseless DO time series was simulated from field measurements of PAR and Kalman filtered water temperature. The noisy DO time series was generated by adding error to the noiseless time series (Observation Error σ^2 (H) = 100 (µmol O_2 L^{-1})^2; Process Error σ^2 (Q) = 0.5 (µmol O_2 L^{-1})^2). The filtered DO time series was created by applying the Kalman filter (KF) to the noisy time series.

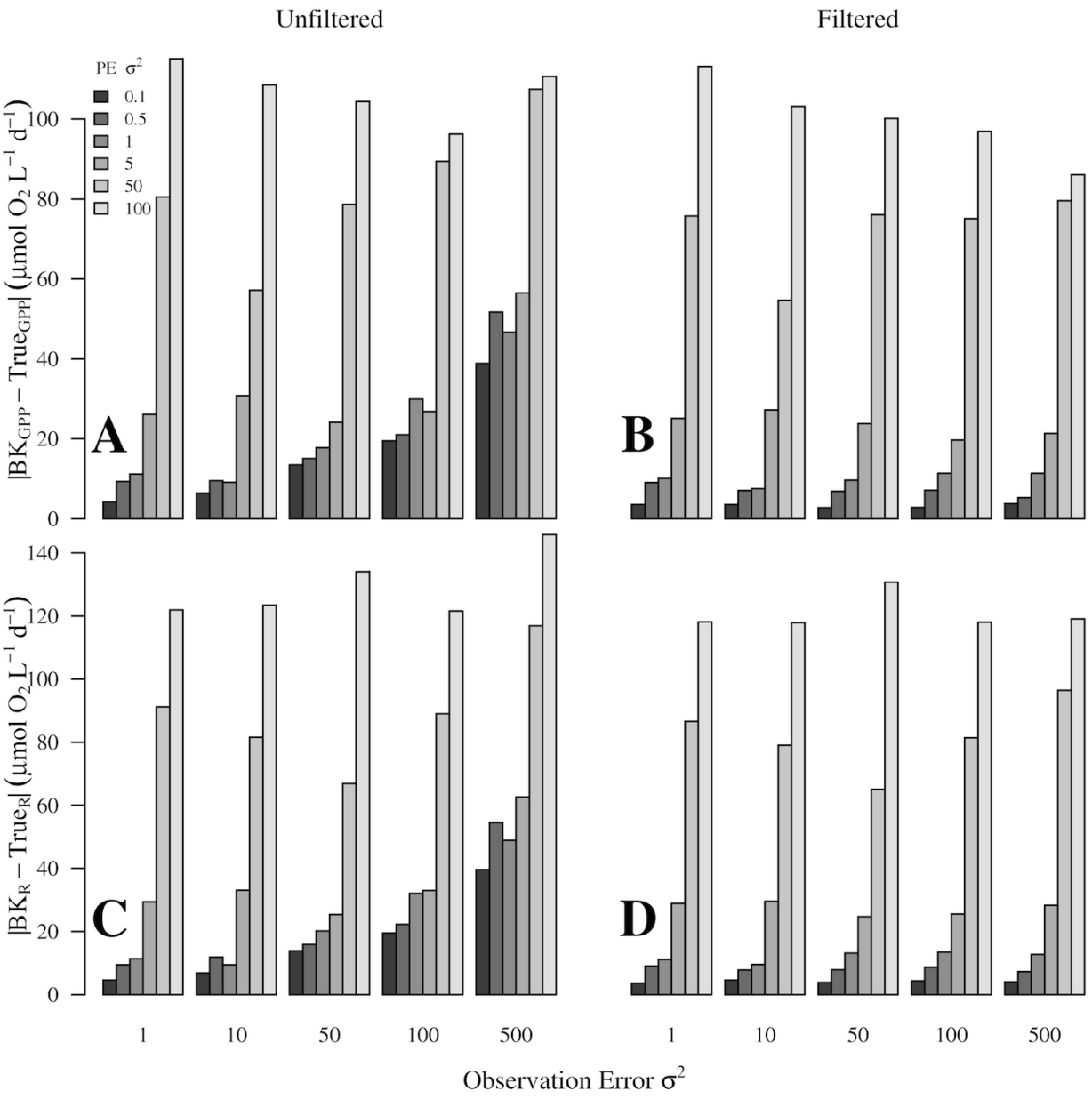

Fig. 2. The effects of filtering with KF on bookkeeping (BK) estimates of GPP and R. For each combination of *Q* (Process Error (PE) σ^2) and *H* (Observation Error σ^2), mean daily GPP and R were calculated for a 6-day simulation, and compared to the true values. Changes in the bar height for a given shading represents the effects of observation error on metabolism estimates; changes in bar height for a given observation error (the five bar groups in each panel) but among levels of shading represents the effects of process error on metabolism estimates. Differences in

bar height between the left (unfiltered) and right (filtered) column of panels indicates the effects of filtering on BK metabolism estimates. Bar heights are average absolute differences between calculated estimates and true values of GPP and R (23.75 μmol O_2 L^{-1} d^{-1} and -16.09 μmol O_2 L^{-1} d^{-1}, respectively) from 30 stochastic simulations.

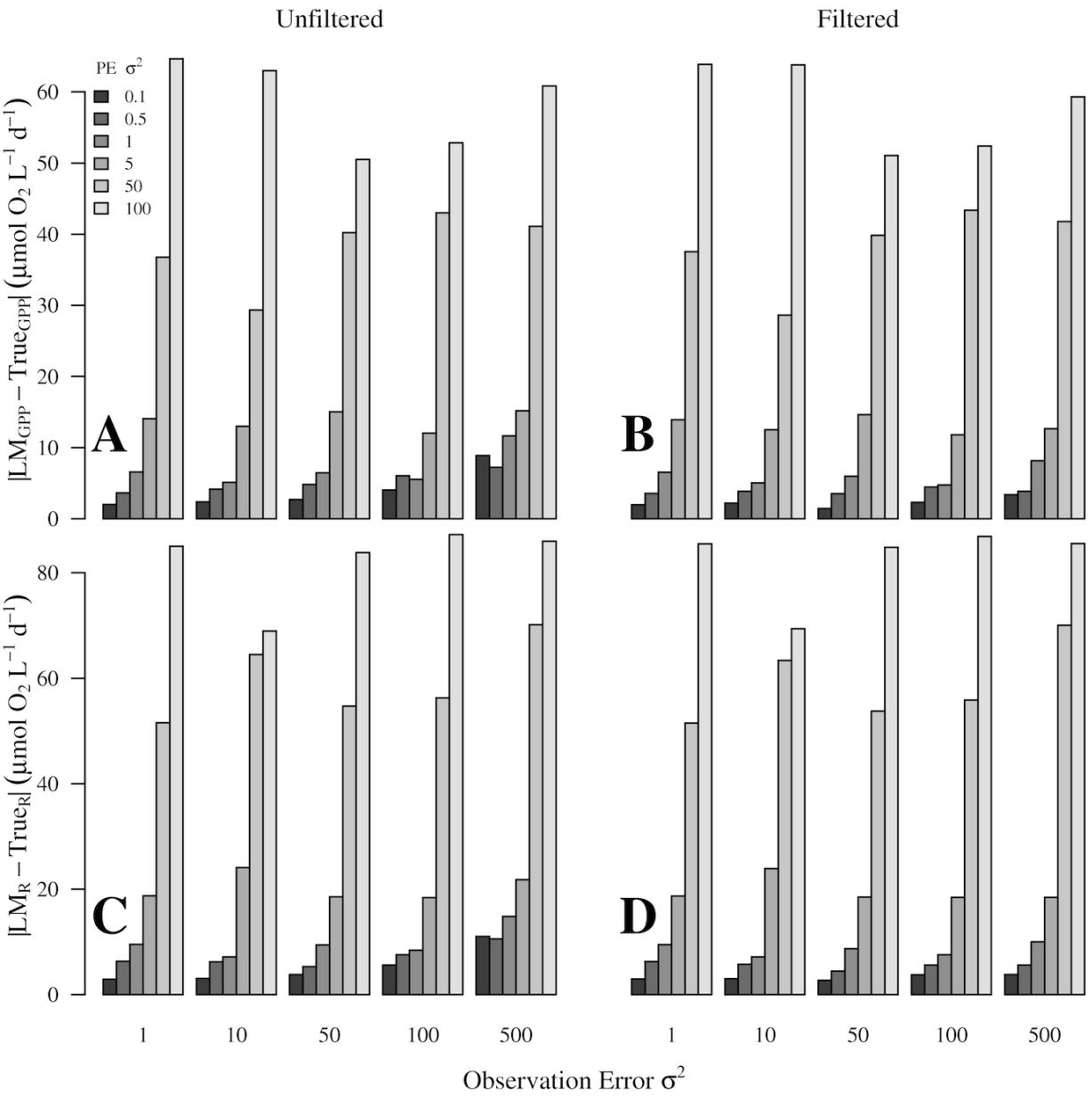

Fig. 3. The effects of filtering with KF on linear model (LM) estimates of GPP and R. For each combination of *Q* (Process Error (PE) σ^2) and *H* (Observation Error σ^2), mean daily GPP and R were calculated for a 6-day simulation, and compared to the true values. Changes in the bar height for a given shading represents the effects of observation error on metabolism estimates; changes in bar height for a given observation error (the five bar groups in each panel) but among levels of shading represents the effects of process error on metabolism estimates. Differences in

bar height between the left (unfiltered) and right (filtered) column of panels indicates the effects of filtering on LM metabolism estimates. Bar heights are average absolute differences between calculated estimates and true values of GPP and R (23.75 μmol O_2 L^{-1} d^{-1} and -16.09 μmol O_2 L^{-1} d^{-1}, respectively) from 30 stochastic simulations.

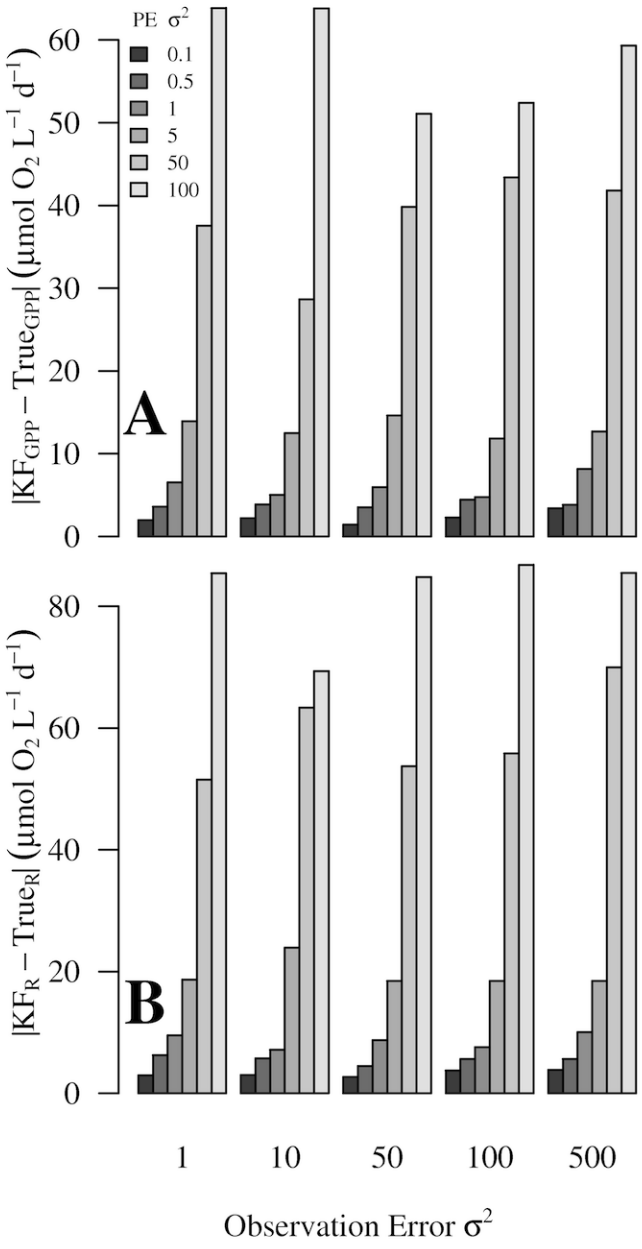

Fig. 4. Accuracy of GPP and R estimates derived from the Kalman filter (KF). For each combination of *Q* (Process Error (PE) σ^2) and *H* (Observation Error σ^2), mean daily GPP and R were calculated for a 6-day simulation, and compared to the true values. Changes in the bar height for a given shading represents the effects of observation error on metabolism estimates; changes in bar height for a given observation error (the five bar groups in each panel) but among

levels of shading represents the effects of process error on metabolism estimates. Bar heights are average absolute differences between calculated estimates and true values of GPP and R (23.75 μmol O_2 L^{-1} d^{-1} and -16.09 μmol O_2 L^{-1} d^{-1}, respectively) from 30 stochastic simulations.

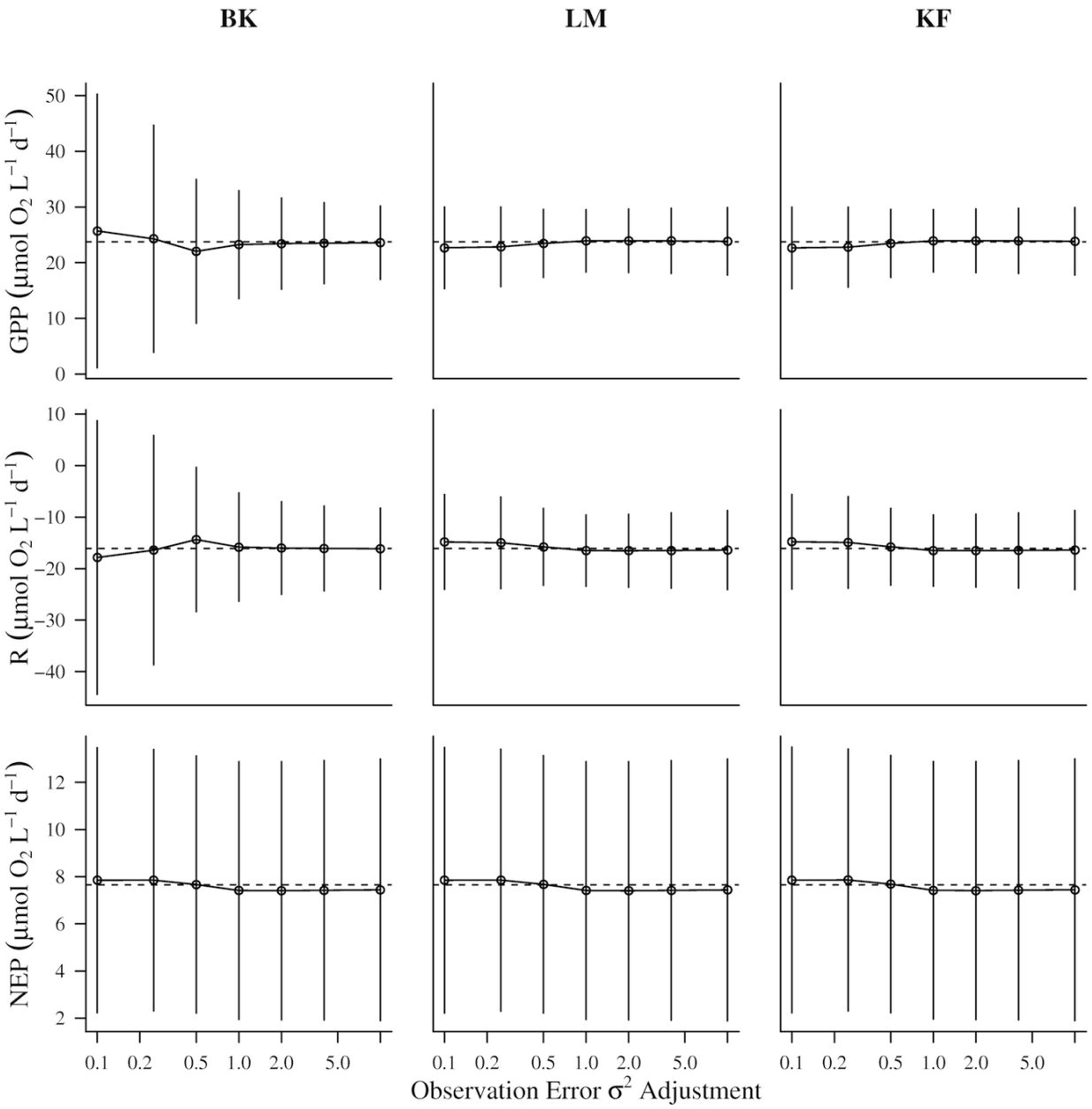

Fig. 5. Sensitivity of metabolic estimates to adjustments made to the variance of observation error (*H*). GPP, R, and NEP were estimated using the bookkeeping model (BK) on filtered data, the linear model (LM) on filtered data, and the Kalman filter (KF) on unfiltered data. Horizontal dashed lines represent the true values of the metabolic parameters. Vertical error bars are the standard deviations of metabolic estimates from 30 stochastic simulations of DO time series (Observation Error σ^2 (*H*) = 100 (µmol O_2 L^{-1})^2; Process Error σ^2 (*Q*) = 0.5 (µmol O_2 L^{-1})^2). Each

open circle is the mean model estimate of the metabolic parameter from those 30 stochastic simulations.

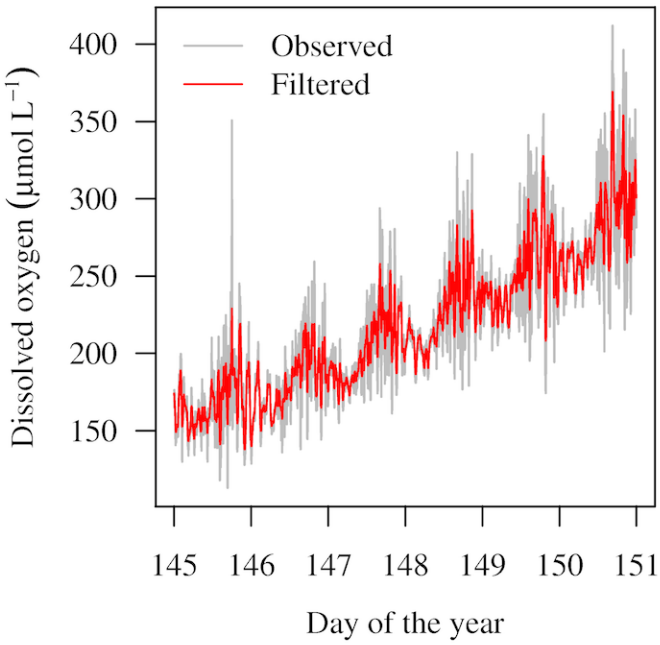

Fig. 6. Dissolved oxygen data collected from the metalimnion (4 m) of Ward Lake in 2010. The gray line represents unfiltered dissolved oxygen data, and the red line represents dissolved oxygen data after it was filtered with the Kalman filter (KF).

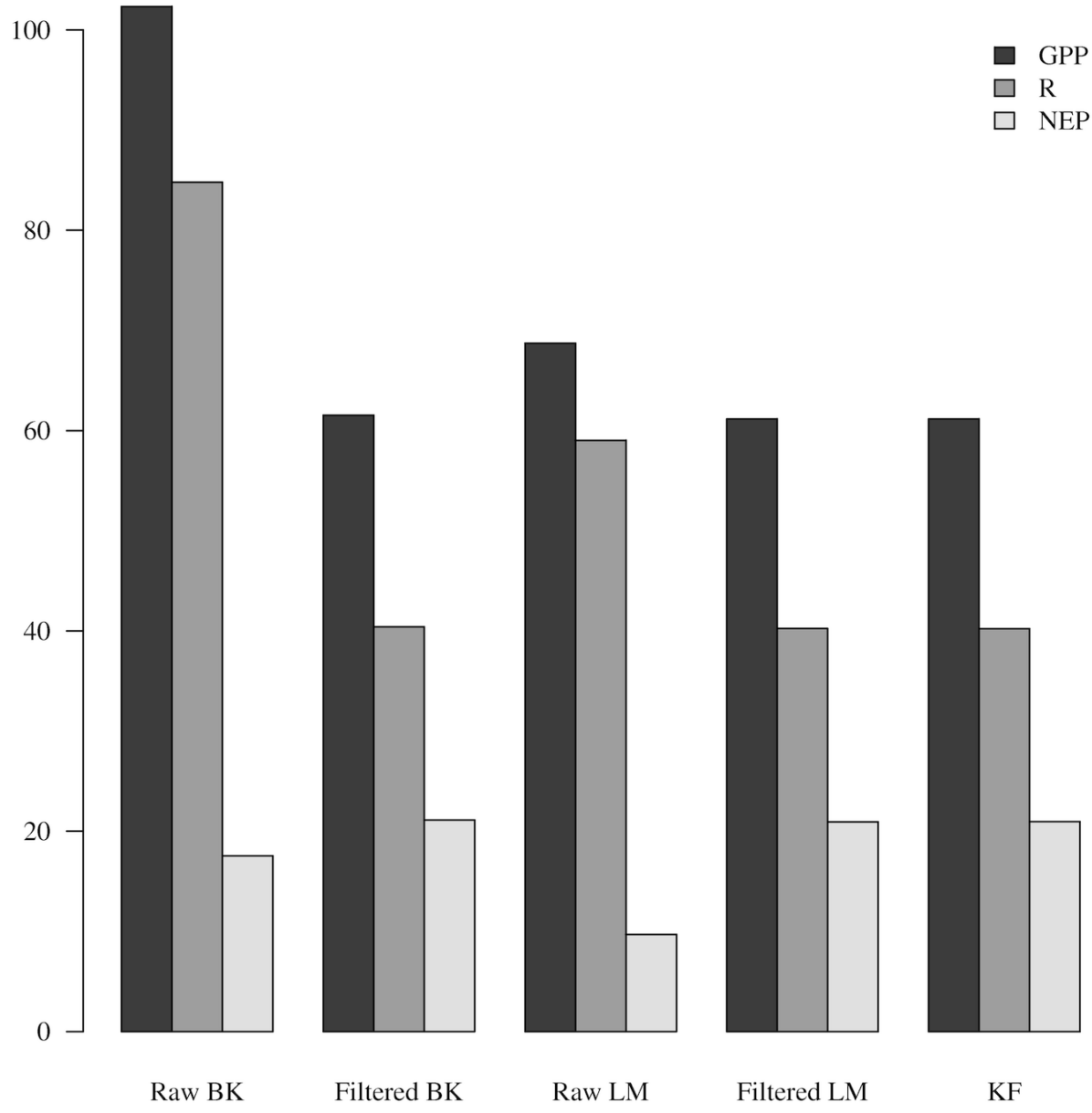

Fig. 7. Comparison of estimated metabolism for a 6-day deployment across models (data from Ward Lake). BK= bookkeeping, LM = linear model, KF = Kalman filter. R is represented by positive values for ease of comparison with GPP and NEP. Raw estimates are derived from the collected data before it was filtered with KF, whereas filtered estimates are derived from oxygen time series obtained by filtering the collected oxygen time series before using BK or LM to estimate metabolism.

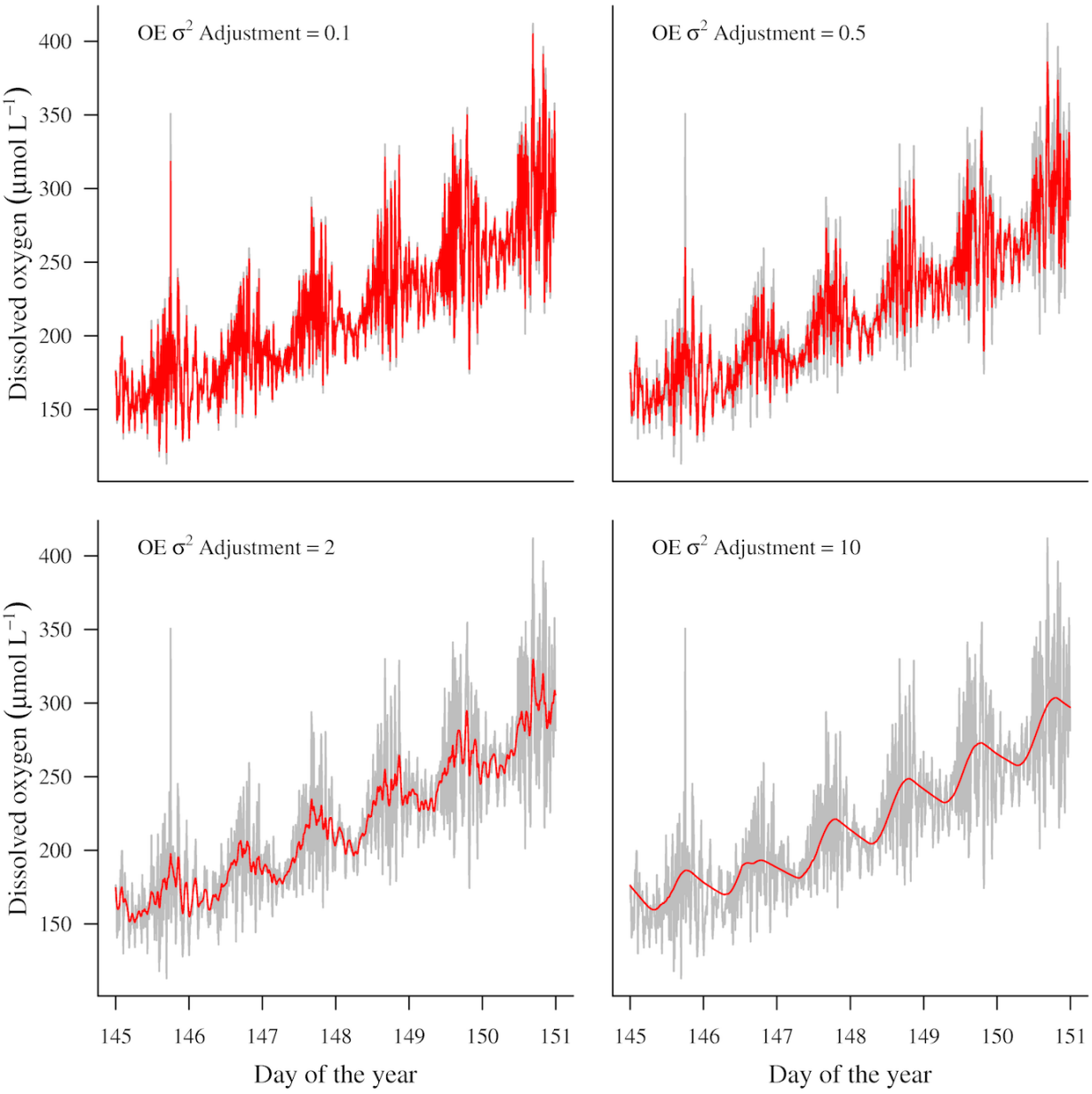

Fig. 8. The effect of adjusting the estimated variance of Observation Error (OE) σ^2 (*H*) on the filtered dissolved oxygen time series from Ward Lake when using the Kalman filter (KF). Gray lines are observed DO concentrations, red lines are filtered.

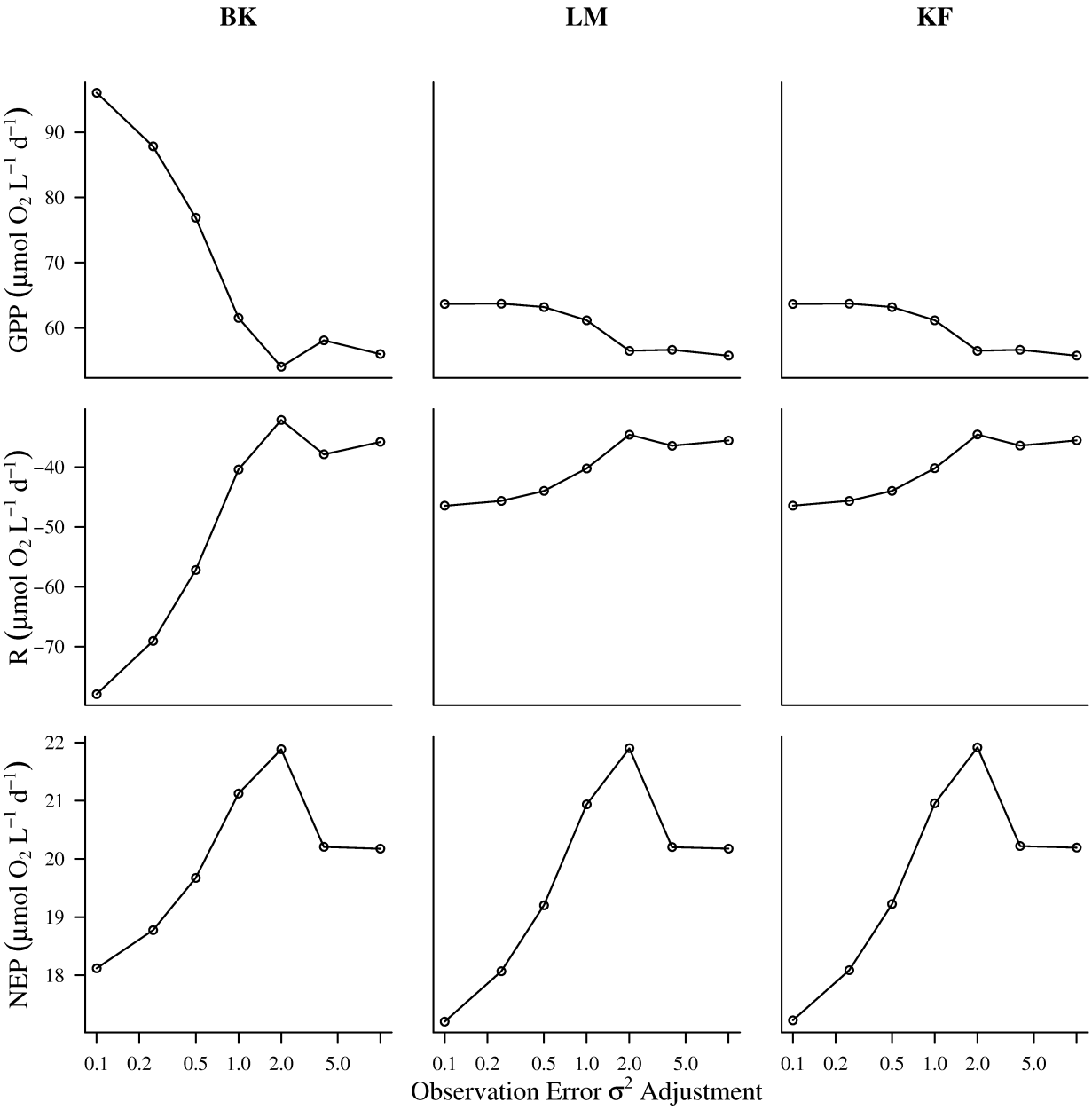

Fig. 9. Sensitivity of metabolic estimates to adjustments made to the variance of observation error (*H*). GPP, R, and NEP were estimated using the bookkeeping model (BK) on filtered data, the linear model (LM) on filtered data, and the Kalman filter (KF) on unfiltered data.

Chapter 2: Resources supporting the food web of a naturally productive lake*

Abstract

A Bayesian mixing model and stable isotopes of carbon, nitrogen, and hydrogen were used to evaluate the extent to which six consumers (three fishes, two zooplankton, and a snail) in a naturally productive lake used terrestrial resources, epilimnetic and metalimnetic phytoplankton, benthic algae, and macrophytes. Resource use varied with consumer habitat use and feeding ability, but allochthony was consistently low (averaging 15% among consumers). The pelagic invertebrates *Skistodiaptomus oregonensis* and *Chaoborus* spp. relied on phytoplankton from the epilimnion (59% and 49%, respectively), and to a lesser extent from the metalimnion (28% and 26%, respectively); terrestrial resources comprised 9% and 18% of the diet of these consumers, respectively. The snail *Helisoma trivolvis* relied mainly on littoral resources (floating-leafed macrophytes; 68% of diet), but terrestrial resources also constituted a substantial portion of its diet (21%). The fishes integrated among habitats more evenly than the other consumers, but pelagic resources formed the largest portion of their diets (*Pimephales promelas* = 64%, *Lepomis gibbosus* = 47%, and *Perca flavescens* = 47%). *L. gibbosus* was the fish with the most allochthonous diet (23%). The consumers of this productive lake were not highly dependent on allochthonous materials, and tended to rely most heavily on local resources, including macrophytes.

---

* Published as: Batt, R.D., S.R. Carpenter, J.J. Cole, M.L. Pace, T.J. Cline, D.A. Seekell. 2012. Resources supporting the food web of a naturally productive lake. *Limnology and Oceanography* **57**: 1443-1452, doi: 10.4319/lo.2012.57.5.1443

Introduction

The organic resources supporting a consumer often originate from a mix of habitats within an ecosystem, or even multiple ecosystems within a landscape. This spatial integration of organic resources by consumers is a long-recognized feature common to many food webs (Lindeman 1942; Polis et al. 1997) that influences ecosystem stability, dynamics, and metabolic balance (Cole et al. 1994; McCann and Rooney 2009). The importance of cross-habitat subsidies to a food web is influenced both by the relative availability of resources and by the extent to which its consumers use these subsidies (Marcarelli et al. 2011), making both availability and use relevant to ecosystem functioning.

The structure of resource subsidy and consumption is not constant among ecosystems, and is particularly interesting in lakes because their position in the surrounding landscape can cause them to receive large subsidies of terrestrial carbon (Kratz et al. 1997). Several studies have experimentally manipulated the $\delta^{13}C$ of aquatic primary producers and found that the use of terrestrially derived (allochthonous) resources by lake consumers can be substantial (Pace et al. 2004; Carpenter et al. 2005; Pace et al. 2007). However, the extent to which allochthonous resources are used by consumers changes with the types of resources available (Caraco et al. 2010; Marcarelli et al. 2011), the physiology and natural history of the consumers (Jansson et al. 2007), and qualities of the lake ecosystem and its constituent habitats (Francis et al. 2011). As a result, the importance of allochthonous resource use (hereafter allochthony) is contingent upon other resource use, which can vary widely both among lakes and among consumers within a given food web.

The use of terrestrial carbon by consumers is known to be variable among aquatic systems, and past studies have suggested that the magnitude of autotrophic production can

explain a portion of this variability in both lotic (Huryn 1996; Nakano and Murakami 2001) and lentic (Cole et al. 2002; Maguire and Grey 2006) systems. However, few studies have examined allochthony in the food webs of productive lakes (Cole In press). An important early effort by Bunn and Boon (1993) used ambient levels of the stable isotopes of carbon and nitrogen to examine the use of terrestrial carbon, phytoplankton, macrophytes, and epiphytes by consumers in several eutrophic billabongs. Although they found that many of the consumers in these productive systems relied primarily on aquatic resources, isotopic analysis was not able to resolve resource use for all consumers, in part due to isotopically indistinct end members.

Other studies of productive lentic systems have either used isotopic labeling experiments or natural abundances of ^{2}H to circumvent the issue of isotopically indistinct aquatic and terrestrial resources. Cole et al. (2002) and Carpenter et al. (2005) enriched aquatic primary producers with ^{13}C in two experimentally fertilized lakes and found that the zooplankton in these systems were highly autochthonous. Carpenter et al. (2005) also found that benthic consumers and fish relied heavily on algal resources. However, the fishes in this study had slow rates of biomass turnover, and because the nutrient fertilization only lasted one season, their long-term allochthony is unclear (Carpenter et al. 2005). Moreover, Babler et al. (2011) used ambient ^{2}H and found that gizzard shad (a detritivorous fish) exhibited a wide range of allochthony among several eutrophic and hypereutrophic impoundments. Together, these studies suggest that while fishes in eutrophic lakes rely heavily on phytoplankton, the extent of fish allochthony among eutrophic lakes can be highly variable.

Although the importance of allochthonous resources is measured relative to that of aquatic (autochthonous) resources, macrophytes represent a group of autochthonous resources whose contribution to lake food webs is poorly known. The ability of macrophytes to serve as

carbon sources to consumers has long been debated (Lodge 1991; Newman 1991), and in several systems their support of food webs appears negligible (Hecky and Hesslein 1995; France 1996). Other studies have found that macrophytes are likely a substantial source of carbon for consumers (Carpenter and Lodge 1986; Sheldon 1987), which suggests that macrophytes could support consumers in macrophyte-rich lakes. In lakes where macrophytes or other resources contribute substantially to a food web but are overlooked during analysis, consumer use of resources, allochthonous or otherwise, may not be accurately evaluated.

The present study uses ambient ^{13}C, ^{15}N, and ^{2}H isotopes to investigate the extent to which allochthonous organic matter supports the food web of a naturally productive lake. Due to the high abundance of aquatic resources in this productive system, we hypothesized that consumer allochthony would be low. With the expectation that resource use would vary among consumers, we assess the extent to which zooplankton, a benthic consumer, and fishes are supported by terrestrial, epilimnetic and metalimnetic phytoplankton, periphyton, and macrophytes. We hypothesized that both allochthony and the use of specific aquatic resources would vary among consumer taxa according to the degree to which consumers use multiple habitats (e.g., fish potentially feed in the littoral, benthic, and pelagic habitats), the availability of the autochthonous resources in those habitats, and consumer feeding capabilities.

Methods

Study site—This study was conducted on Ward Lake, located at the University of Notre Dame Environmental Research Center near the Wisconsin-Michigan border (46º15'N, 89º31'W) during the summer of 2010. Ward Lake is a small (0.019 km^2), shallow (max. depth = 8 m), dimictic and naturally productive lake. In 2010, the summer mean of surface total nitrogen and phosphorus concentrations were 491 $\mu g\ L^{-1}$ and 22.9 $\mu g\ L^{-1}$, respectively. The lake had relatively

high light absorbance (color) at 440 nm with a mean G440 of 2.49 m^{-1}, and was alkaline with a mean pH of 8.03. The lake also had high chlorophyll *a* concentrations, both at the surface (summer mean = 8.63 $\mu g\ L^{-1}$) and in the metalimnion (46.6 $\mu g\ L^{-1}$) where chlorophyll was at a maximum vertical concentration for most of the summer.

Ward Lake is located in a fen where speckled alder (*Alnus incana* subsp. *rugosa*) and sedges (*Carex* spp.) dominate the riparian plant community. Macrophytes are abundant, with 18% of lake surface area being covered (6% volume infested; percent cover estimated visually from the surface). The macrophyte community is comprised of a number of species, the most abundant of which include a macroalga (*Chara* sp.), fragrant water lily (*Nymphaea odorata*), yellow water lily (*Nuphar variegata*), watershield (*Brasenia schreberi*), and small pondweed (*Potamogeton pusillus*). The calanoid copepod *Skistodiaptomus oregonensis* is abundant, as is the invertebrate predator *Chaoborus* spp. The fish community is dominated by a number of small fishes, including the pumpkinseed sunfish (*Lepomis gibbosus*) and the fathead minnow (*Pimephales promelas*). The top predator in Ward Lake is the yellow perch (*Perca flavescens*).

Sample collection and isotope analysis—In order to trace the basal resources supporting the lake food web, autotrophic end members and aquatic consumers were collected between May and August of 2010 and subsequently analyzed for their $\delta^{13}C$, $\delta^{15}N$, and $\delta^{2}H$ (deuterium) signatures. Between June and August, lake water was collected once a month from three sites near the center of the lake in the epilimnion (0.5 m) and in the metalimnion (at the depth of the chlorophyll maximum, which ranged from 2.5 m to 4 m), filtered through a 25 mm glass fiber filter (Whatman GF/F), and the filtrate stored for $\delta^{2}H_2O$ analysis (sample size of $n = 12$). Particulate organic matter (POM) was collected in June and August from lake water taken from three pelagic epilimnion sites ($n = 6$) and two pelagic metalimnion sites ($n = 4$). In June, the

liquid portion of the POM filtrate from the epilimnion and metalimnion was evaporated, and the dried residue sampled as dissolved organic matter (DOM; $n = 2$). For POM δ^2H, the lake water was screened through a 153 μm mesh, and POM collected on a MicronSep Cellulosic filter, back-rinsed with a small amount of water, and dried at 60ºC. For δ^{13}C and δ^{15}N, the POM was collected on a previously ashed 25 mm GF/F filter and dried.

Terrestrial, benthic, and littoral end members were sampled from around and within Ward Lake in June and August. The terrestrial end members were represented by *A. incana* subsp. *rugosa* ($n = 5$) leaves, *Carex* spp. ($n = 5$), and DOM ($n = 2$). Lake DOM in this region is predominantly allochthonous (Bade et al. 2007). By sampling key tree species in the area and using a Bayesian mixing model, we determined that the DOM in Ward Lake is also largely terrestrial (*see* below). Therefore, the terrestrial source in this analysis is comprised of shoreline plants and DOM, with DOM being a composite of shoreline and upgradient end members. The littoral end members were characterized by samples of five of the most prevalent macrophyte species in Ward Lake, collected from different locations in the littoral zone on several dates between June and August. The spatial and temporal extent of sampling was constrained by seasonal changes in the presence and relative abundance of each species. Leaves from *N. variegata* ($n = 5$), *N. odorata* ($n = 5$), and *B. schreberi* ($n = 4$) were collected on each date and cleaned of any debris and epiphytic growth. The leaves and stalk of *P. pusillus* ($n = 5$) and *Chara* sp. ($n = 5$) were also collected and rinsed several times to remove debris. Periphyton ($n = 6$) served as the benthic end member, and was grown on a series of ceramic tiles suspended throughout the littoral zone of the lake at a depth of 0.5 m and collected after four weeks of growth in June and in August. Periphyton samples were grown on tiles to facilitate separation of the algae from their substrate in order to obtain samples dominated by algal material. These

samples serve as generic physiological and isotopic surrogates for attached algae that may be available to consumers in Ward Lake.

All consumers were sampled in June and again in August, except *P. promelas*, which was sampled in May and June. Zooplankton samples (n = 12) were taken from three pelagic epilimnion and three pelagic metalimnion sites by lowering the inlet hose of an open diaphragm bilge pump to the desired depth (0.5 m in the epilimnion, and the depth of the chlorophyll maximum in the metalimnion) and pumping water from the outlet hose into a 153 μm mesh net. *S. oregonensis* was the most abundant zooplankton species (by biomass), and enough *S. oregonensis* individuals were picked from each sample to reach a pooled biomass sufficient for isotopic analysis. *Chaoborus* spp. (n = 6) were collected at night using an oblique net tow through the water column, and pooled to reach sufficient biomass for a sample. The snail, *H. trivolvis* (n = 6), was sampled from across the littoral zone, and the foot of several individuals was dissected and pooled as a single sample. Fishes (n = 6 for each species) were also sampled from the littoral zone, with adult *P. promelas* and juvenile *L. gibbosus* being caught by minnow trap, and *P. flavescens* by hoop net. The intestinal tracts were excised from each fish, and the remainder of an individual treated as one sample.

All solid samples were dried at 60ºC, ground to a powder, and stored in a desiccator pending analysis. Samples were sent to the Colorado Plateau Stable Isotope Laboratory (CPSIL) at Northern Arizona University where they were analyzed with isotope ratio mass spectrometers (IRMS). Analysis of δ^2H followed the methods of Doucett et al. (2007), and we report non-exchangeable H in this paper.

Model and food web analysis—This study employed a Bayesian mixing model adapted from Solomon et al. (2011) to describe lake consumers as a mixture of autotrophic resources

originating from terrestrial, pelagic epilimnion, pelagic metalimnion, benthic, and littoral habitats. We characterized consumers and end members by their isotopic signatures ($\delta^{13}C$, $\delta^{15}N$, and $\delta^{2}H$), and calculated the end-member composition of consumers using the following system of equations:

$$\delta^{13}C_{C[i]} = \sum_{j=1}^{4} (\varphi_{S[j]} \times \delta^{13}C_{S[j]}) + \varepsilon_{C[i]} \quad (1)$$

$$\delta^{15}N_{C[i]} = \sum_{j=1}^{4} (\varphi_{S[j]} \times \delta^{15}N_{S[j]}) + \Delta_{tot} + \varepsilon_{N[i]} \quad (2)$$

$$\delta^{2}H_{C[i]} = (1 - \omega_{tot[C]}) \times \sum_{j=1}^{4} (\varphi_{S[j]} \times \delta^{2}H_{S[j]}) + \omega_{tot[C]} \times \delta^{2}H_{W} + \varepsilon_{H[i]} \quad (3)$$

$$1 = \sum_{j=1}^{4} \varphi_{S[j]} \quad (4)$$

where $\delta^{13}C_{C[i]}$, $\delta^{15}N_{C[i]}$, and $\delta^{2}H_{C[i]}$ are the isotopic ratios of sample i of consumer species C, $\delta^{13}C_{S[j]}$, $\delta^{15}N_{S[j]}$, and $\delta^{2}H_{S[j]}$ are the isotopic ratios of the j^{th} source (S), $\varepsilon_{C[i]}$, $\varepsilon_{N[i]}$, and $\varepsilon_{H[i]}$ are residual errors (normally and independently distributed with mean = 0 and variance = σ^2) for each isotope and consumer sample $C_{[i]}$, and $\varphi_{S[j]}$ is the fraction φ that source S[j] contributes to the diet of consumer C. The total trophic fraction of $\delta^{15}N$ (Δ_{tot}) was calculated as

$$\Delta_{tot} = \Delta_{Herb} + \Delta_{Carn} \times (\tau - 1) \quad (5)$$

where Δ_{Herb} is the $\delta^{15}N$ fractionation of an herbivorous link (mean (μ) = 2.52‰, standard deviation (σ) = 2.5‰), Δ_{Carn} is the $\delta^{15}N$ fractionation of a carnivorous link (μ = 3.4‰, σ = 0.4‰), and τ is the trophic level of the consumer as levels above primary producers when primary production equals trophic level 0 (Vander Zanden and Rasmussen 2001). The total proportion of tissue H derived from water (W) in a given consumer species ($\omega_{tot[C]}$) was calculated as

$$\omega_{tot[C]} = 1 - (1 - \omega)^{\tau} \quad (6)$$

where ω is the fraction of tissue H derived from water by a particular consumer (as opposed to $\omega_{tot[C]}$, which also includes water assimilated by the prey of the consumer). For each consumer, the mean and variance of ω were selected from the literature values of the most similar taxa available: *S. oregonensis* = 0.20, 0.0016; *Chaoborus* spp. = 0.14, 0.0036; *H. trivolvis* = 0, 0; fishes = 0.12, 0.0004 (Estep and Dabrowski 1980; Solomon et al. 2009). Based on presumed feeding habits, consumers were assigned a trophic level with a variance of 0.1 and the following means: *S. oregonensis* and *H. trivolvis* were assigned trophic level 1 (primary consumers); *Chaoborus* spp., *L. gibbosus,* and *P. promelas* trophic level 2; *P. flavescens* trophic level 3.

The isotopic signatures of phytoplankton end members were estimated in the framework of a Bayesian mixing model by treating POM as a mixture of phytoplankton and terrestrial matter:

$$\delta X_{POM[L]} = \theta_{P[L]} \times \delta X_{P[L]} + \theta_{T[L]} \times \delta X_T + \varepsilon_{X[L]} \quad (7)$$

$$1 = \theta_{T[L]} + \theta_{P[L]} \quad (8)$$

where $\delta X_{POM[L]}$ and $\delta X_{P[L]}$ are the respective isotopic signatures for isotope X of POM and phytoplankton in layer L (either the epilimnion or metalimnion), δX_T is the isotopic signature of terrestrial matter, $\theta_{P[L]}$ and $\theta_{T[L]}$ are the fractions that phytoplankton and terrestrial matter contribute to POM in layer L, and $\varepsilon_{X[L]}$ the residual error (independently and normally distributed, $\mu = 0$, variance = σ^2). The values of $\delta X_{POM[L]}$ and δX_T are known from sampling, whereas $\delta X_{P[L]}$, $\theta_{T[L]}$, and $\theta_{P[L]}$ were not directly measured. However, phytoplankton δ^2H was calculated from the known ^2H_2O photosynthetic fractionation of phytoplankton and from the δ^2H_2O taken from the appropriate layer (Solomon et al. 2009; Cole et al. 2011) and supplied to the model (Eqs. 7,8) as an informative prior, permitting the mixing model to estimate the remaining unknown values.

A challenge common among studies employing mixing models is the excess of end members relative to the number equations. In this study there are eleven end members, and each model has four equations afforded by the three isotopes. The two models described by Eqs. 7,8 (one model for each value of L) can estimate the contribution of two sources to the POM mixture from layer L. By assuming that POM was comprised only of terrestrial matter and phytoplankton, the number of end members was limited to three. Some end members were grouped into aggregate sources in order to restrict the number of sources to two. Such grouping is commonly achieved by grouping the end members according to their proximity in isotopic space, or by their ecological similarity (Phillips et al. 2005). While the two approaches are not necessarily mutually exclusive, this study employed the latter, and in the case of Eqs. 7,8 the terrestrial end members were grouped into one source, while the phytoplankton end member remained a separate source.

In the case of the consumer mixing models (Eqs. 1–4), the number of end members was first limited by excluding *Chara* sp. and *P. pusillus* from analysis because their isotopic signatures suggested that they were unlikely to contribute to the diets of any of the consumers (*see* Results and Discussion). The remaining end members were grouped into sources representing the terrestrial (*A. incana* subsp. *rugosa, Carex* spp., and DOM), pelagic epilimnion (phytoplankton), pelagic metalimnion (phytoplankton), benthic (periphyton), and littoral (floating-leafed macrophytes) habitats. Because there are five sources, two mixing models were run for each consumer: the first model grouped the benthic and littoral habitats into a single benthic-littoral source, and the second grouped the pelagic epilimnion and pelagic metalimnion into a single pelagic source while assessing the benthic and littoral habitats separately. Thus each

model examined the contribution of four sources to the diet of a consumer by grouping two similar habitats into a single source.

The composition of DOM was assessed using a Bayesian mixing model similar to that used for the consumers of Ward Lake. In this model DOM was the mixture, Δ_{tot} and ω_{tot} were set equal to zero, and the sources contributing to DOM were pelagic (pooled phytoplankton), benthic (periphyton), littoral (floating-leafed macrophytes), and terrestrial. For this analysis, the terrestrial end member included *A. incana* subsp. *rugosa* and *Carex* spp., as well as several upgradient tree end members. The leaves of these trees were sampled, and their isotopic signatures have been used in previous studies that investigated allochthony in lakes near Ward Lake (Solomon et al. 2011; Cole et al. 2011). The tree species include black spruce (*Picea mariana*), balsam fir (*Abies balsamea*), red maple (*Acer rubrum*), sugar maple (*Acer saccharum*), white cedar (*Thuja occidentalis*), and yellow birch (*Betula alleghaniensis*). For the purposes of this analysis, the isotopic signatures of these tree species were averaged for each species, and the mean of these averages taken to form a single 'Tree' end member. This Tree end member was analyzed as a part of the terrestrial source to the DOM mixture. The mode of the posterior distribution of the terrestrial contribution to DOM was 90%, while the modes of the other sources were near 0%. These results suggest that DOM in Ward Lake is predominantly terrestrial. As a result, we treated DOM as a terrestrial end member for the other analyses in this study.

Grouping end members into a single source for use with the Bayesian mixing models required that a composite mean and variance be calculated for each source. The mean of a source comprised of multiple end members was calculated separately for each isotope as the equally weighted average of the isotopic ratios of the end members comprising the source. The variance of each source was calculated by one-way analysis of variance, using the ratio of a given isotope

as the response variable and end members as categorical treatments. If the treatment was not significant ($p > 0.1$), the variance of the source was set equal to the residual mean squared error (MSE). If the treatment was significant ($p < 0.1$), the variance of the source was calculated as the sum of the residual MSE and the treatment MSE.

All calculations were performed in R (R Development Core Team 2012) and WinBUGS (Lunn et al. 2000) using the contributed R package R2WinBUGS (Sturtz et al. 2005), programs written by the authors, and programs adapted from Solomon et al. (2011). Unless otherwise stated, all parameters were given uninformative priors, and models were fit by running 8 Markov chains for 10,000 iterations with a 5000-iteration burn-in period and thinned so as to sample 1000 iterations of the posterior distribution.

Results

Bayesian mixing models were used to estimate the contribution of phytoplankton and terrestrial end members to POM, the isotopic signature of the phytoplankton end member, as well as the reliance of consumers on basal resources. All estimates are presented here as the mean of the modeled posterior distribution. POM in the epilimnion of Ward Lake was comprised of 43% terrestrial matter and 57% phytoplankton (Fig. 1A,B). Epilimnetic phytoplankton $\delta^{13}C$ was estimated as −33.5‰, $\delta^{15}N$ as −0.14‰ (Fig. 1C,D), and $\delta^{2}H$ as −230‰. Metalimnetic POM was comprised of slightly less terrestrial matter (38%) and more phytoplankton (62%) than epilimnetic POM (Fig. 2A,B). Metalimnetic phytoplankton $\delta^{13}C$, $\delta^{15}N$, and $\delta^{2}H$ signatures were −36.2‰, 0.16‰ (Fig. 2C,D), and −232‰, respectively. Phytoplankton $\delta^{2}H$ signatures in both habitats were similar to the priors supplied to the model, indicating that additional data had little effect on these distributions.

The isotopic signatures of end members varied between terrestrial, pelagic, benthic, and littoral habitats, as well as between consumers (Fig. 3). Phytoplankton were substantially more depleted in $\delta^{13}C$ and $\delta^{2}H$ than the other end members, while *P. pusillus* was the most enriched in $\delta^{13}C$ (−14.1‰) followed by *Chara* sp. ($\delta^{13}C$ = −16.7‰), and *Chara* sp. had the highest $\delta^{2}H$ signature (−119‰) (Fig. 3A). The separation of end-member $\delta^{15}N$ was not as strong as for the other isotopes, but phytoplankton were the most enriched and *P. pusillus* the most depleted (Fig. 3B). Pelagic and terrestrial end members were isotopically similar to other end members within the same habitat, but there was more variability within the benthic-littoral habitat as *Chara* sp. and *P. pusillus* were far more enriched in $\delta^{13}C$ than other macrophytes and periphyton, and periphyton was more depleted in $\delta^{2}H$ than the macrophytes.

The signatures of the consumers also varied, but less so than the end members (Fig. 3). Among consumers, *S. oregonensis* was the most depleted in $\delta^{13}C$ (−33.5‰) and $\delta^{2}H$ (−188‰), and *H. trivolvis* was the most depleted in $\delta^{15}N$ (0.17‰). *H. trivolvis* had the most enriched signatures for $\delta^{13}C$ (−25.3‰) and $\delta^{2}H$ (−151‰), and *L. gibbosus* was the most enriched in $\delta^{15}N$ (5.62‰).

Pelagic consumers relied heavily upon pelagic resources, with the pelagic resource constituting 82% of the diet for *S. oregonensis* and 71% for *Chaoborus* spp. (Fig. 4). Separating the pelagic resource into its constituent end members revealed that epilimnetic phytoplankton contributed more than metalimnetic phytoplankton to the diets of *S. oregonensis (*59% and 28%, respectively) and *Chaoborus* spp. (49% and 26%, respectively) (Fig. 4B,C). Terrestrial and benthic-littoral resources contributed minimally to the diets of these pelagic consumers in both groupings of model sources (Fig. 4).

The benthic consumer *H. trivolvis* was supported almost exclusively by benthic-littoral and terrestrial resources (Fig. 4), although the terrestrial component shifted from 43% when the benthic-littoral end members were pooled, to 21% when periphyton was modeled as a source separate from the macrophytes (Fig. 4A,E). As a pooled source, the benthic-littoral end members were estimated to comprise 54% of the diet (Fig. 4D). As a separate benthic source, periphyton constituted 8% of the diet (Fig. 4G), whereas the littoral source (floating-leafed macrophytes) was estimated to be 68% of the diet (Fig. 4H). Thus the estimated diet composition of *H. trivolvis* was sensitive to how end members were grouped into sources, with the exception that the importance of pelagic resources remained low.

Fishes were similar to one another in diet composition, consuming mostly terrestrial and pelagic resources, although benthic-littoral resources constituted a non-trivial component of their diet as well (Fig. 4). *P. promelas* relied more heavily on the pooled pelagic resource (64%) than either *L. gibbosus* or *P. flavescens* (47% for both species) (Fig. 4F). The terrestrial source was of greatest importance to *L. gibbosus* (27% for the first grouping, 23% for the second) relative to *P. promelas* (11% and 8%) and *P. flavescens* (12% for both groupings) (Fig. 4A,E), and the respective benthic-littoral resource use was 20%, 25%, and 38% for these fishes (Fig. 4D). Metalimnetic resources comprised less of fish diets than epilimnetic resources, a difference that was larger for *P. promelas* (epilimnetic = 53%, metalimnetic = 17%) than it was for *P. flavescens* (34% and 17%) or *L. gibbosus* (31% and 17%) (Fig 4B,C). Although the estimate of resource use from the terrestrial, pelagic, and benthic-littoral habitats varied between the two groupings, the relative importance of these three habitats to fish diets generally remained the same.

Discussion

Ward Lake presents a large number of potential carbon sources to its consumers. Some of these sources appeared to be unimportant for all consumers—namely *Chara* sp. and *P. pusillus*. The position of these end members in isotopic space suggested that they were unlikely to be a major carbon source to consumers. These submersed macrophytes had an average $\delta^{13}C$ of −15.4‰, and their lack of contribution to consumer diets is consistent with France (1996), who found that macrophytes with a $\delta^{13}C$ signature near −16‰ did not support littoral consumers. Consequently, these end members were omitted from mixing models. Despite this initial screening, the number of end members still necessitated their grouping into aggregate sources, and this grouping influenced model estimates. The sensitivity of mixing model estimates to the grouping of end members is a common problem in food web studies that increases the uncertainty surrounding estimates of resource use (Phillips et al. 2005). However, the qualitative importance of resource use was less sensitive to grouping than were the quantitative estimates, and the role of these resources in supporting lake consumers was elucidated.

The pelagic consumers of Ward Lake relied heavily on pelagic resources, which is consistent with the findings of previous studies conducted in experimentally fertilized lakes (Cole et al. 2002; Carpenter et al. 2005). The contrasting terrestrial-phytoplankton composition of pelagic consumers vs. POM is indicative of selective feeding by pelagic herbivores, and is consistent with the ability of *S. oregonensis* to feed selectively among phytoplankton (Kerfoot and Kirk 1991). The ratio of color to chlorophyll in a lake can serve as an index of the relative availability of terrestrial and phytoplankton resources, respectively. Past studies of pelagic consumers that were conducted in lakes over a range of color : chlorophyll found that allochthony tends to increase as color : chlorophyll increases (Carpenter et al. 2005; Pace et al. 2007; Cole et al. 2011). The allochthony of *S. oregonensis* relative to the color : chlorophyll in

Ward Lake is consistent with the trend found in these past studies, and the relationship suggests that resource use is influenced by the relative availability of resources (Fig. 5). Nonetheless, there is substantial variability around this relationship, and additional data are needed to assess the pattern among systems.

Estimates of resource use suggest that phytoplankton from both the epilimnion and metalimnion were important to pelagic consumers. However, the overlap in the isotopic signatures of the two types of phytoplankton (Fig. 3) adds uncertainty to estimates that parse consumer use of epilimnetic and metalimnetic phytoplankton. Nonetheless, *S. oregonensis* feeds efficiently at high algal concentrations, and it would encounter especially high algal concentrations in the metalimnion of Ward Lake during diel vertical migration (Torke 2001). Also, algal production in the low-light, high-nutrient environment of the metalimnion could produce a high-quality food source for *S. oregonensis* and other zooplankton (Fee 1976; Sterner et al. 1997). Although the metalimnion may offer high-quality food and refuge from predators, the benefits of metalimnetic feeding may be offset by enhanced growth rates facilitated by the warmer temperatures in the epilimnion (Winder et al. 2004). Francis et al. (2011) also argue that metalimnetic phytoplankton may be an important part of zooplankton diets in lakes such as Ward Lake where the euphotic zone extends beyond the mixing depth. Thus, the characteristics of Ward Lake and the feeding abilities and habitat usage of *S. oregonensis* support the finding that both epilimnetic and metalimnetic phytoplankton were important food sources for pelagic consumers. Ward Lake may be an extreme case in this regard. It is highly productive, strongly stratified, and has metalimnetic chlorophyll concentrations that are exceedingly high. In two other lakes in this region that are less productive and have less-pronounced metalimnetic chlorophyll peaks, Cole et al. (2011) demonstrated that zooplankton were supported by a

combination of phytoplanktonic and terrestrial sources, with only minor contributions from the metalimnion. Our results point to the need for studying lakes over a broad range of conditions to determine the importance of terrestrial resources to zooplankton and the conditions that enhance or diminish this support.

The benthic consumer *H. trivolvis* fed primarily on a combination of floating-leafed macrophytes and terrestrial matter, but fed minimally on periphyton and phytoplankton. While the absence of phytoplankton from the diet of a snail is not surprising, the minimal use of periphyton is more conspicuous because many snails feed heavily on periphyton. However, *H. trivolvis* is known to preferentially consume terrestrial detritus and living macrophytes over periphyton (Lombardo and Cooke 2002). The species of submersed macrophyte consumed by *H. trivolvis* in Lombardo and Cooke (2002) has a far lower phenolic concentration than the floating-leafed macrophytes of this study (specifically, *N. variegata*), making the floating-leafed macrophytes a lower-quality diet item (Smolders et al. 2000). The presence of secondary chemicals such as phenolics is one reason the consumption of living macrophytes is thought uncommon (Lodge 1991; Newman 1991). However, when macrophytes decompose, their phenolic concentrations quickly decrease, and the alkaline water of Ward Lake accelerates this process (Kok et al. 1992). Furthermore, relatively modest variability surrounded the estimated contribution of littoral (epiphyte-free macrophytes) and terrestrial resources to the diet of the benthic consumer, *H. trivolvis*. Therefore, it is likely that *H. trivolvis* was mainly supported by terrestrial and macrophyte (living and/or detrital) resources, rather than by periphyton.

The fishes in this study relied on a greater variety of resources than the benthic or pelagic consumers. While all fishes relied on pelagic production for a large portion of their diet, resource use was more evenly distributed among habitats for *L. gibbosus* and *P. flavescens* than it was for

other consumers. Although adult *L. gibbosus* are known to feed on mollusks, the individuals sampled in this study were unlikely to feed on mollusks because they were juveniles (mean length = 59.5 mm), permitting the difference in resource use between *L. gibbosus* and *H. trivolvis*. Fishes relied on resources from multiple habitats, a pattern consistent with that observed in other lakes (Vander Zanden and Vadeboncoeur 2002). Resource use by fishes also followed the more generalized expectation that consumers occupying higher trophic levels and with greater mobility will integrate among a greater number of habitats (Lindeman 1942; McCann and Rooney 2009). In this sense, resource use by *P. flavescens* represents the best single-consumer proxy for resource use at the ecosystem level, indicating that resources from all habitats contributed to the lake food web.

The consumers of Ward Lake had consistently low allochthony, but their use of specific autochthonous resources was more variable. Furthermore, just as the food web of Ward Lake tended to use local (autochthonous) resources, consumer resource use tended to reflect their habitat use. For example, consumer use of pelagic resources was inversely proportional to littoral resource use, with zooplankton relying heavily on epilimnetic and metalimnetic phytoplankton, the snail primarily consuming macrophytes, and the mobile fishes exhibiting intermediate use of pelagic and littoral resources. Although frequently abundant in lakes and important resources in this study, metalimnetic phytoplankton and macrophytes are not commonly considered in the context of the allochthony of lake food webs. We suggest that these resources contributed to the food web because they were abundant, present in habitats used by consumers, and that the physiology of the consumers interacted with the characteristics of the resources (e.g., stoichiometry) and the ecosystem (e.g., alkalinity, temperature) in a way that made these resources available and of high quality. Future studies may gain further insight into patterns in

resource use by accounting for additional resource characteristics, such as the taxonomic composition of periphyton and phytoplankton. Our findings emphasize the variability in resource use among the consumers of a lake, and the importance of considering end members from multiple habitats when assessing which resources support lake food webs.

Resource use is variable among consumers and food webs. However, our findings contribute to a growing body of literature that highlights resource quantity and quality as an important driver of this variability (Brett et al. 2009; Francis et al. 2011; Marcarelli et al. 2011). This literature also suggests that lake trophic status can serve as a measure of the quantity of high-quality autochthonous resources in lakes (Carpenter et al. 2005; Cole et al. 2006; Pace et al. 2007), which is consistent with the high autochthony of Ward Lake consumers. Our study demonstrates that resources such as metalimnetic phytoplankton and macrophytes can be important to lake food webs, and should be included in future studies of resource use and allochthony. Furthermore, the use of deuterium in this study and others (Babler et al. 2011; Cole et al. 2011; Solomon et al. 2011) suggests that considering more end members in allochthony studies is more tractable now than in the past. In conclusion, we encourage future research to build upon an emerging understanding of which factors shape patterns in resource use across organisms and ecosystems.

Acknowledgements

We thank Chase Brosseau, Jim Coloso, Emily Kara, Jason Kurtzweil, Laura Smith, and Lee Zinn for assistance in the field and laboratory, Jereme Gaeta for dialogue on study design, Chris Solomon for analytical advice, Gary Belovsky, Michael Cramer, and the University of Notre Dame Environmental Research Center staff for their assistance, and two anonymous referees for their constructive feedback. We are grateful for financial support from the National

Science Foundation (Division of Environmental Biology (DEB)-0917696, DEB-0917719, DEB-0917858) and a fellowship from the Wisconsin Alumni Research Foundation.

Literature Cited in Chapter 2

Babler, A. L., A. Pilati, and M. J. Vanni. 2011. Terrestrial support of detritivorous fish populations decreases with watershed size. Ecosphere **2**: art76, doi:10.1890/ES11-00043.1

Bade, D. L., S. R. Carpenter, J. J. Cole, M. L. Pace, E. Kritzberg, M. C. Bogert, R. M. Cory, and D. M. McKnight. 2007. Sources and fates of dissolved organic carbon in lakes as determined by whole-lake carbon isotope additions. Biogeochemistry **84**: 115-129, doi:10.1007/s10533-006-9013-y

Brett, M. T., M. J. Kainz, S. J. Taipale, and H. Seshan. 2009. Phytoplankton, not allochthonous carbon, sustains herbivorous zooplankton production. Proc. Natl. Acad. Sci. USA **106**: 21197-21201, doi:10.1073/pnas.0904129106

Bunn, S. E., and P. I. Boon. 1993. What sources of organic carbon drive food webs in billabongs? A study based on stable isotope analysis. Oecologia **96**: 85-94.

Caraco, N., J. E. Bauer, J. J. Cole, S. Petsch, and P. Raymond. 2010. Millennial-aged organic carbon subsidies to a modern river food web. Ecology **91**: 2385-2393.

Carpenter, S. R., J. J. Cole, M. L. Pace, M. Van de Bogert, D. L. Bade, D. Bastviken, C. M. Gille, J. R. Hodgson, J. F. Kitchell, and E. S. Kritzberg. 2005. Ecosystem subsidies: Terrestrial support of aquatic food webs from ^{13}C addition to contrasting lakes. Ecology **86**: 2737-2750, doi:10.1890/04-1282

Carpenter, S. R., and D. M. Lodge. 1986. Effects of submersed macrophytes on ecosystem processes. Aquat. Bot. **26**: 341–370.

Cole, J. J. In press. Are fish made of trees: Magnitude and patterns of allochthony in lakes, *In* Kinne, O. [ed.], Multiple roles of freshwater ecosystems in the carbon cycle. Inter Research.

Cole, J. J., N. F. Caraco, G. W. Kling, and T. K. Kratz. 1994. Carbon dioxide supersaturation in the surface waters of lakes. Science **265**: 1568-1570, doi:10.1126/science.265.5178.1568

Cole, J. J., S. R. Carpenter, J. F. Kitchell, and M. L. Pace. 2002. Pathways of organic carbon utilization in small lakes: Results from a whole-lake ^{13}C addition and coupled model. Limnol. Oceanogr. **47**: 1664-1675, doi:10.4319/lo.2002.47.6.1664

Cole, J. J., S. R. Carpenter, J. F. Kitchell, M. L. Pace, C. T. Solomon, and B. Weidel. 2011. Strong evidence for terrestrial support of zooplankton in small lakes based on stable isotopes of carbon, nitrogen, and hydrogen. Proc. Natl. Acad. Sci. USA **108**: 1975-1980, doi:10.1073/pnas.1012807108

Doucett, R. R., J. C. Marks, D. W. Blinn, M. Caron, and B. A. Hungate. 2007. Measuring terrestrial subsidies to aquatic food webs using stable isotopes of hydrogen. Ecology **88**: 1587-1592.

Estep, M. F., and H. Dabrowski. 1980. Tracing food webs with stable hydrogen isotopes. Science **209**: 1537-1538, doi:10.1126/science.209.4464.1537

Fee, E. J. 1976. The vertical and seasonal distribution of chlorophyll in lakes of the Experimental Lakes Area, northwestern Ontario: Implications for primary production estimates. Limnol. Oceanogr. **21**: 767-783.

France, R. L. 1996. Stable isotopic survey of the role of macrophytes in the carbon flow of aquatic foodwebs. Vegetatio **124**: 67-72, doi:10.1007/BF00045145

Francis, T. B., D. E. Schindler, G. W. Holtgrieve, E. R. Larson, M. D. Scheuerell, B. X. Semmens, and E. J. Ward. 2011. Habitat structure determines resource use by zooplankton in temperate lakes. Ecol. Lett. **14**: 364-372, doi:10.1111/j.1461-0248.2011.01597.x

Hecky, R. E., and R. H. Hesslein. 1995. Contributions of benthic algae to lake food webs as revealed by stable isotope analysis. J. North Am. Benthol. Soc. **14**: 631, doi:10.2307/1467546

Huryn, A. D. 1996. An appraisal of the Allen paradox in a New Zealand trout stream. Limnol. Oceanogr. **41**: 243–252.

Jansson, M., L. Persson, A. M. De Roos, R. I. Jones, and L. J. Tranvik. 2007. Terrestrial carbon and intraspecific size-variation shape lake ecosystems. Trends Ecol. Evol. **22**: 316-322, doi:10.1016/j.tree.2007.02.015

Kerfoot, W. C., and K. L. Kirk. 1991. Degree of taste discrimination among suspension-feeding cladocerans and copepods: Implications for detritivory and herbivory. Limnol. Oceanogr. **36**: 1107-1123, doi:10.4319/lo.1991.36.6.1107

Kok, C. J., C. H. J. Hof, J. P. M. Lenssen, and G. van der Velde. 1992. The influence of pH on concentrations of protein and phenolics and resource quality of decomposing floating leaf material of *Nymphaea alba* L. (Nymphaeaceae) for the detritivore *Asellus aquaticus* (L.). Oecologia **91**: 229-234.

Kratz, T. K., K. E. Webster, C. J. Bowser, J. J. Magnuson, and B. J. Benson. 1997. The influence of landscape position on lakes in northern Wisconsin. Freshw. Biol. **37**: 209-217.

Lindeman, R. L. 1942. The trophic-dynamic aspect of ecology. Ecology **23**: 399-417.

Lodge, D. M. 1991. Herbivory on freshwater macrophytes. Aquat. Bot. **41**: 195-224, doi:10.1016/0304-3770(91)90044-6

Lombardo, P., and G. D. Cooke. 2002. Consumption and preference of selected food types by two freshwater gastropod species. Arch. Hydrobiol. **155**: 667-685.

Lunn, D. J., A. Thomas, N. Best, and D. Spiegelhalter. 2000. WinBUGS - A Bayesian modeling framework: Concepts, structure, and extensibility. Stat. Comput. **10**: 325-337, doi:10.1023/A:1008929526011

Maguire, C. M., and J. Grey. 2006. Determination of zooplankton dietary shift following a zebra mussel invasion, as indicated by stable isotope analysis. Fresw. Biol. **51**: 1310-1319, doi:10.1111/j.1365-2427.2006.01568.x

Marcarelli, A. M., C. V. Baxter, M. M. Mineau, and R. O. Hall. 2011. Quantity and quality: Unifying food web and ecosystem perspectives on the role of resource subsidies in freshwaters. Ecology **92**: 1215-1225, doi:10.1890/10-2240.1

McCann, K. S., and N. Rooney. 2009. The more food webs change, the more they stay the same. Philos. Trans. R. Soc. Lond. B Biol. Sci. **364**: 1789-1801, doi:10.1098/rstb.2008.0273

Nakano, S., and M. Murakami. 2001. Reciprocal subsidies: Dynamic interdependence between terrestrial and aquatic food webs. Proc. Natl. Acad. Sci. USA **98**: 166-170, doi:10.1073/pnas.98.1.166

Newman, R. M. 1991. Herbivory and detritivory on freshwater macrophytes by invertebrates: A review. J. North Am. Benthol. Soc. **10**: 89, doi:10.2307/1467571

Pace, M. L., S. R. Carpenter, J. J. Cole, J. J. Coloso, J. F. Kitchell, J. R. Hodgson, J. J. Middelburg, N. D. Preston, C. T. Solomon, and B. C. Weidel. 2007. Does terrestrial

organic carbon subsidize the planktonic food web in a clear-water lake? Limnol. Oceanogr. **52**: 2177-2189.

Pace, M. L., J. J. Cole, S. R. Carpenter, J. F. Kitchell, J. R. Hodgson, M. C. Van de Bogert, D. L. Bade, E. S. Kritzberg, and D. Bastviken. 2004. Whole-lake carbon-13 additions reveal terrestrial support of aquatic food webs. Nature **427**: 240-243, doi:10.1038/nature02215.1.

Phillips, D. L., S. D. Newsome, and J. W. Gregg. 2005. Combining sources in stable isotope mixing models: Alternative methods. Oecologia **144**: 520–527.

Polis, G. A., W. B. Anderson, and R. D. Holt. 1997. Toward an integration of landscape and food web ecology: The dynamics of spatially subsidized food webs. Annu. Rev. Ecol. Syst. **28**: 289-316, doi:10.1146/annurev.ecolsys.28.1.289

R Development Core Team. 2011. R: A Language and Environment for Statistical Computing. R Foundation for Statistical Computing. URL: http://www.r-project.org/

Sheldon, S. P. 1987. The effects of herbivorous snails on submerged macrophyte communities in Minnesota lakes. Ecology **68**: 1920–1931.

Smolders, A. J. P., L. H. T. Vergeer, G. van der Velde, and J. G. M. Roelofs. 2000. Phenolic contents of submerged, emergent and floating leaves of aquatic and semi-aquatic macrophyte species: Why do they differ? Oikos **91**: 307-310, doi:10.1034/j.1600-0706.2000.910211.x

Solomon, C. T., S. R. Carpenter, M. K. Clayton, J. J. Cole, J. J. Coloso, M. L. Pace, M. J. Vander Zanden, and B. C. Weidel. 2011. Terrestrial, benthic, and pelagic resource use in lakes: Results from a three-isotope Bayesian mixing model. Ecology **92**: 1115-1125.

Solomon, C. T., J. J. Cole, R. R. Doucett, M. L. Pace, N. D. Preston, L. E. Smith, and B. C. Weidel. 2009. The influence of environmental water on the hydrogen stable isotope ratio in aquatic consumers. Oecologia **161**: 313-324, doi:10.1007/s00442-009-1370-5

Sterner, R. W., J. J. Elser, E. J. Fee, S. J. Guildford, and T. H. Chrzanowski. 1997. The light: nutrient ratio in lakes: The balance of energy and materials affects ecosystem structure and process. Am. Nat. **150**: 663-684.

Sturtz, S., U. Ligges, and A. Gelman. 2005. R2WinBUGS: A package for running WinBUGS from R. J. Stat. Softw. **12**: 1-16.

Torke, B. 2001. The distribution of calanoid copepods in the plankton of Wisconsin lakes. Hydrobiologia **453**: 351–365, doi:10.1023/A:1013185916287

Vander Zanden, M. J., and J. B. Rasmussen. 2001. Variation in δ^{15}N and δ^{13}C trophic fractionation: Implications for aquatic food web studies. Limnol. Oceanogr. **46**: 2061-2066, doi:10.4319/lo.2001.46.8.2061

Vander Zanden, M. J., and Y. Vadeboncoeur. 2002. Fishes as integrators of benthic and pelagic food webs in lakes. Ecology **83**: 2152, doi:10.2307/3072047

Winder, M., P. Spaak, and W. M. Mooij. 2004. Trade-offs in *Daphnia* habitat selection. Ecology **85**: 2027-2036, doi:10.1890/03-3108

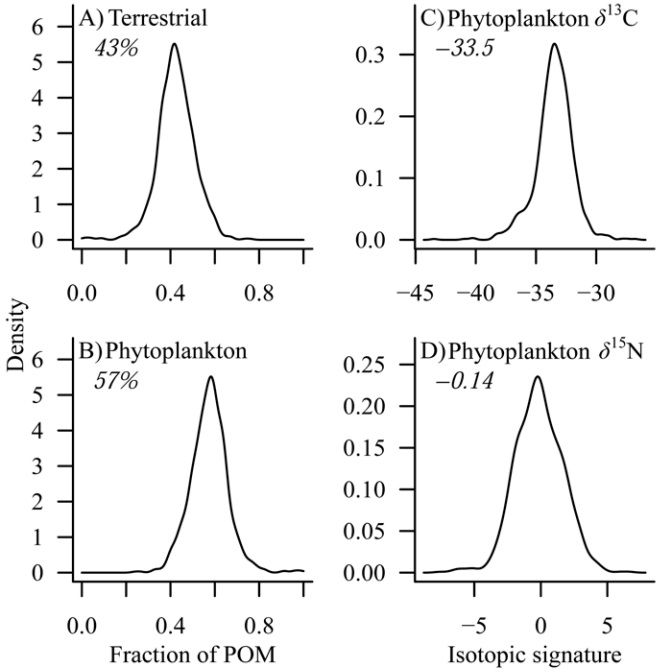

Figure 1. Epilimnetic posterior estimates of particulate organic matter (POM) composition as fractions of (A) terrestrial matter and (B) phytoplankton; italicized values are mean percent contributions of terrestrial matter and phytoplankton to POM. Posterior estimates of phytoplankton (C) δ^{13}C and (D) δ^{15}N signatures; italicized values are mean isotopic signatures (‰).

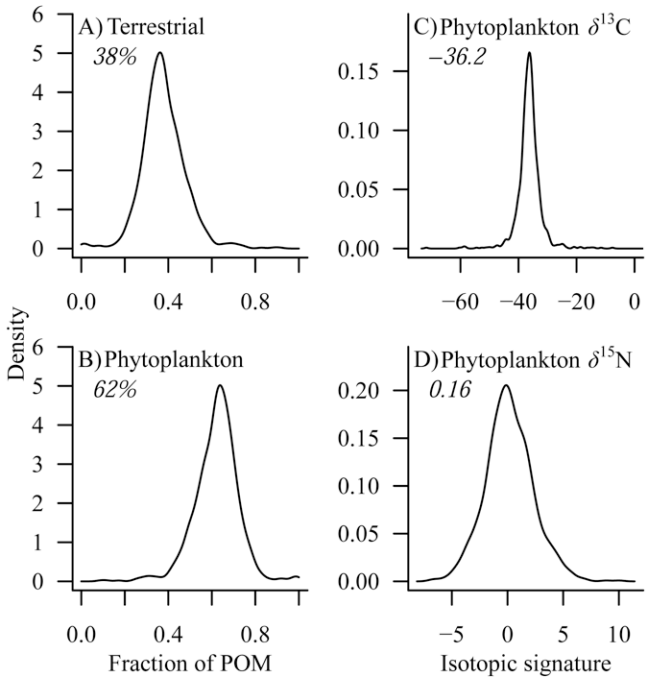

Figure 2. Metalimnetic posterior estimates of particulate organic matter (POM) composition as fractions of (A) terrestrial matter and (B) phytoplankton; italicized values are mean percent contributions of terrestrial matter and phytoplankton to POM. Posterior estimates of phytoplankton (C) δ^{13}C and (D) δ^{15}N signatures; italicized values are mean isotopic signatures (‰).

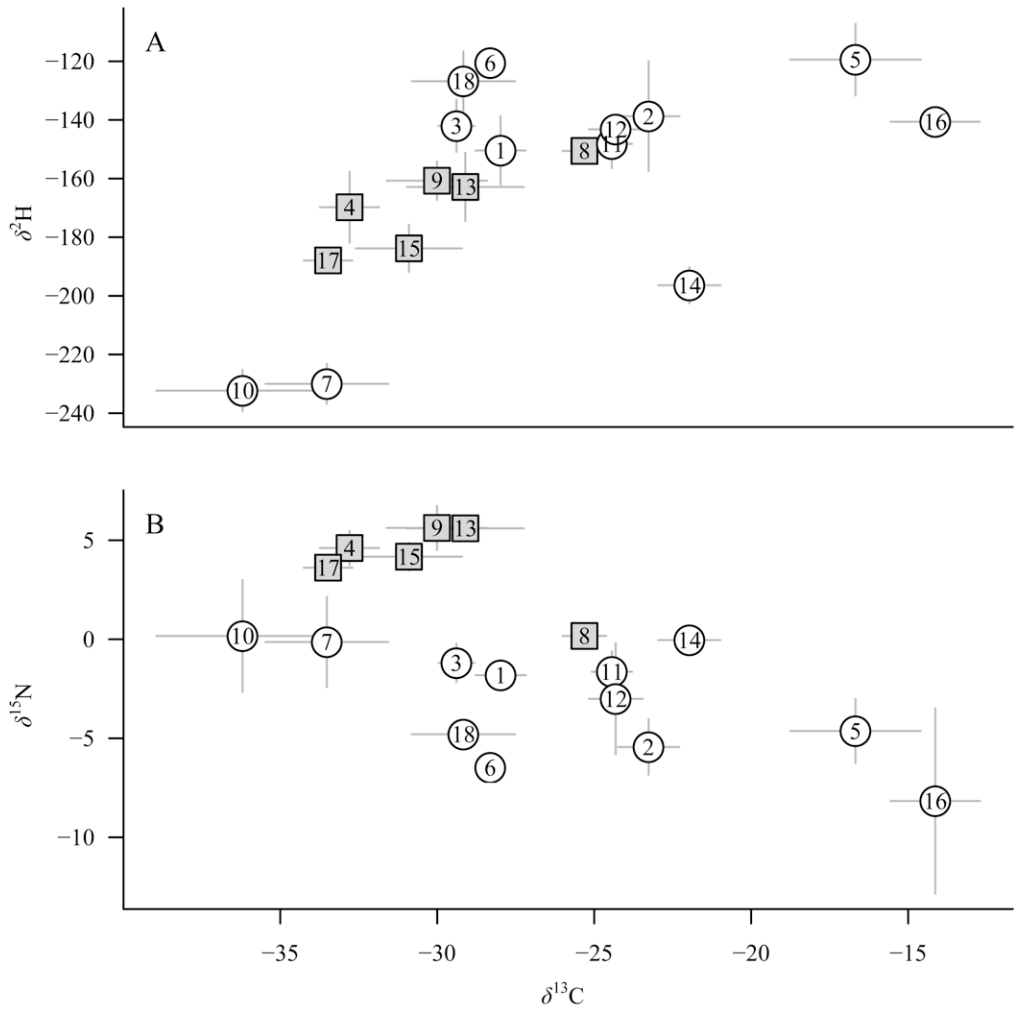

Figure 3. The location of end members (circles) and consumers (gray squares) in isotopic space for (A) δ^2H and δ^{13}C, and for (B) δ^{15}N and δ^{13}C; all values are given in parts per mil (‰) relative to a standard. Circumscribed numbers designate particular end members and consumers: 1 = speckled alder (*Alnus incana* subsp. *rugosa*); 2 = watershield (*Brasenia schreberi*); 3 = sedge *(Carex* spp.); 4 = *Chaoborus* spp.; 5 = *Chara* sp.*; 6* = dissolved organic matter; 7 = epilimnetic phytoplankton; 8 = ramshorn snail (*Helisoma trivolvis*); 9 = pumpkinseed sunfish (*Lepomis gibbosus*); 10 = metalimnetic phytoplankton; 11 = yellow water lily (*Nuphar variegata*); 12 = fragrant water lily (*Nymphaea odorata*); 13 = yellow perch (*Perca flavescens*); 14 = periphyton; 15 = fathead minnow (*Pimephales promelas*); 16 = small pondweed (*Potamogeton pusillus*); 17

= calanoid copepod (*Skistodiaptomus oregonensis*); 18 = nearby tree species. Error bars represent ± 1 standard deviation; error bars not extending beyond the symbol perimeter are not shown.

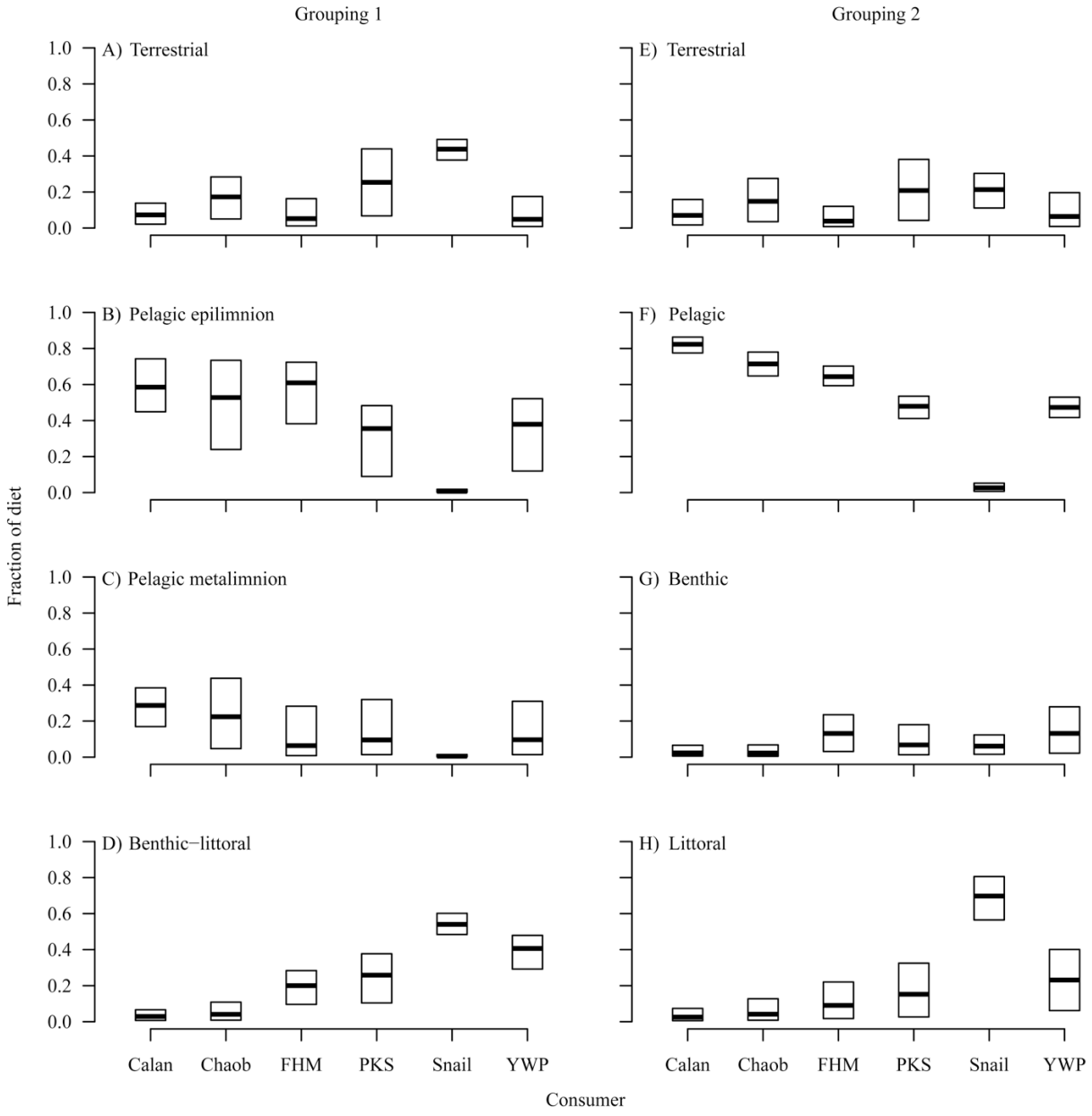

Figure 4. Box plots of mixing model posterior distributions showing the fraction that each source contributed to the diet of a given consumer. The bottom of the box is the 25th percentile of the posterior, the thick line inside the box is the median, and the top of the box is the 75th percentile. (A-D) Grouping 1 shows the results of a model that pooled benthic and littoral end members into a single source, and separated pelagic end members into two sources. (E-H) Grouping 2 pooled pelagic end members and separated benthic and littoral end members. Each

source is comprised of one or more end members: Terrestrial = *A. incana* subsp. *rugosa*, *Carex* spp., and dissolved organic matter; Pelagic epilimnion = epilimnetic phytoplankton; Pelagic metalimnion = metalimnetic phytoplankton; Benthic = periphyton; Littoral = *B. schreberi*, *N. variegata*, and *N. odorata*. Consumer abbreviations are as follows: Calan = Calanoid (*S. oregonensis*); Chaob = *Chaoborus* spp.; FHM = fathead minnow (*P. promelas*); PKS = pumpkinseed sunfish (*L. gibbosus*); YWP = yellow perch (*P. flavescens*).

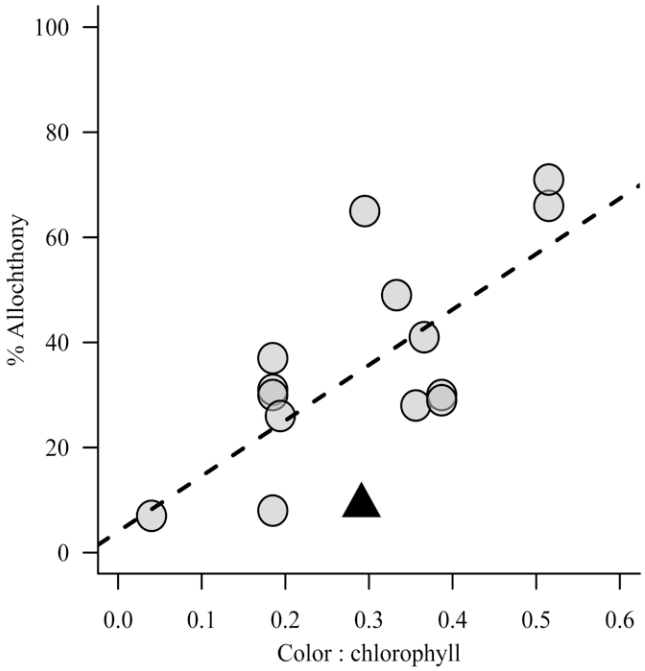

Figure 5. The relationship between mean allochthony of crustacean zooplankton and the color : chlorophyll ratio. The blackened triangle represents *S. oregonensis* from this study, and gray circles represent zooplankton taxa from past studies of other lakes (Pace et al. 2007; Solomon et al. 2011; Cole et al. 2011). The dotted line represents the predicted values of a linear regression of percent allochthony against the ratio of color : chlorophyll ($R^2 = 0.48$; slope = 106, $p < 0.01$).

Chapter 3: Altered energy flow in the food web of an experimentally darkened lake*

Abstract

Theory suggests that alternative energy sources may stabilize a food web when important resources become depleted. To test the potential for alternative resources to support consumers, we experimentally darkened a lake whose consumers had relied heavily on algal resources. Between a prior year and the darkened year phytoplankton biomass diminished by 50%, and net ecosystem production and pCO_2 indicated a shift from autotrophy to heterotrophy. Although a specialist copepod maintained a high reliance on phytoplankton, a generalist zooplankton predator (*Chaborus* spp.) derived more support from terrestrial sources. Benthic algae contributed less to fish biomass after darkening, while phytoplankton support of fish converged towards its support of zooplankton. Overall, most consumers received more support from resource alternatives like terrestrial material (snail, *Chaoborus*, spp., some fishes) or from floating-leafed macrophytes (some fishes). These shifts highlight the potential for increased support by alternative resources, which may provide a mechanism that stabilizes ecosystems.

* To be submitted for publication with the following coauthors: Stephen R. Carpenter, Jonathan J. Cole, Michael L. Pace, Robert A. Johnson, Jason T. Kurtzweil, Grace M. Wilkinson

Introduction

Ecosystems across the globe are experiencing rapid shifts in environmental conditions that will alter the availability of the basal sources of carbon that support their food webs. Carbon fixation by primary producers is the ultimate source of the organic carbon in a food web, and most primary production requires light. In freshwater systems, light availability is closely linked to the concentration of dissolved organic matter (DOM). Lake color and DOM vary around a baseline condition (Pace and Cole 2002), but sustained trends of increasing DOM and color (which reduces clarity) have recently been documented in some freshwaters at northern latitudes (Monteith et al. 2007, Köhler et al. 2013). Furthermore, DOM in many northern lakes is predominantly terrestrial in origin (Karlsson et al. 2003, Wilkinson et al. 2013b), and an influx of DOM could increase the availability of terrestrial carbon resources while decreasing aquatic primary production via light limitation (Jones *et al.* 2012). Thus changes in DOM can differentially affect the availability of basal resources to lake food webs.

Darkening water could greatly impact consumers that rely on resources that are susceptible to light limitation. Fish carbon is ultimately derived from a variety of habitats, but in many cases benthic algae (periphyton) contribute to a larger portion of fish biomass than would be suggested by its relative availability (Vadeboncoeur et al. 2002, Vander Zanden and Vadeboncoeur 2002, Vander Zanden et al. 2011). Periphyton production tends to be higher in clear lakes than in dark lakes (Vadeboncoeur et al. 2008, Ask et al. 2009), and is positively associated with fish biomass per area (Karlsson et al. 2009, Finstad et al. 2014). Furthermore, periphyton support of fish is proportionally lower in darker lakes, where a larger portion of fish biomass is derived from alternative resources (Karlsson *et al.* 2009). If this pattern in lakes

spanning a gradient of water clarity were echoed in a lake darkening over time, we would expect alternative resources to increasingly support its food web.

Fish can rely on a variety of other basal resources to complement the decreased support by periphyton. Compared to periphyton, phytoplankton and floating-leafed macrophytes are less prone to light limitation. Evidence for increased fish reliance on phytoplankton in darker lakes stems from isotope studies indicating that fish become more isotopically similar to zooplankton (Karlsson *et al.* 2009), the primary grazers of phytoplankton. However, terrestrially derived (allochthonous) carbon can support a substantial portion of zooplankton biomass, particularly in dark lakes (Wilkinson *et al.* 2013a). As a result, fish can derive terrestrial resources directly through terrestrial prey, or indirectly through allochthonous aquatic prey (Weidel et al. 2008, Tanentzap et al. 2014). Floating-leafed macrophytes can also contribute substantially to the biomasses of snails and fish (Batt et al. 2012, Mendonça et al. 2012, Kovalenko and Dibble 2013), although little is known about the controls on the strength of this connection. Therefore, terrestrial material, macrophytes, or phytoplankton could serve as alternative basal resources for fish and other consumers in dark lakes with reduced periphyton.

Theory suggests that allochthonous subsidies and alternative energy sources can confer stability on food webs (Huxel et al. 2002, Leroux and Loreau 2008, Rooney and McCann 2012, Tunney et al. 2012). However, few field studies have tracked changes in the relative contributions of carbon sources to consumer biomass as primary producers decline. In one experiment, the contribution of terrestrial resources to fish and invertebrates decreased when a lake was eutrophied (Carpenter *et al.* 2005), and subsequently increased upon cessation of the experimental fertilization (Solomon et al. 2011, Cole et al. 2011). In another system, a zebra mussel invasion led to decreased phytoplankton abundance, and was coincident with enriched

zooplankton $\delta^{13}C$, possibly indicating an increase in zooplankton allochthony (Maguire and Grey 2006). By contrast, when phytoplankton production in San Francisco Bay decreased, zooplankton biomass decreased due to dietary recalcitrance of the terrestrial resource in that system (Sobczak *et al.* 2002). These studies suggest that if local resources are depleted and labile alternatives exist, carbon resources that previously did not contribute to consumer biomass could begin to support the food web.

We tested this idea with a whole-ecosystem experiment, where we greatly reduced light availability by adding a dye to Ward Lake. The goal was to test if reducing light transmission in a naturally productive lake would alter ecosystem metabolism and change the basal resources supporting the food web. Prior to manipulation, consumers in Ward Lake were supported by a variety of basal resources, including algae and floating-leafed macrophytes, and to a lesser extent, terrestrial subsidies (Batt *et al.* 2012). We expected the relative availability of resources in a dyed (henceforth darkened) lake to be different than in the natural state, and that consumer support by terrestrial and floating-leafed macrophyte resources would increase relative to algal resources.

Methods

Study Site

We measured resource support of consumers in Ward and Paul lakes in 2010 and 2012. In 2012 we added a blue dye, Aquashade (Applied Biochemists, Germantown, WI), to Ward Lake while using Paul Lake as an unmanipulated reference. Ward and Paul are small (1.9 ha and 1.6 ha, respectively), shallow (maximum depth = 8 m and 12 m, respectively) lakes at the University of Notre Dame Environmental Research Center in northern Wisconsin, USA (46º 15'N, 89º 31'W). These lakes are located less than a kilometer apart and experience similar

environmental conditions. Ward Lake is productive (summer surface means in 2010; chlorophyll-*a* [Chl] = 8.6 ug L^{-1}, total phosphorus [TP] = 22.9 μg L^{-1}, total nitrogen [TN] = 491 ug L^{-1}), has high alkalinity compared to other lakes in the region (pH = 8.03, dissolved inorganic carbon [DIC] = 1739 μmol L^{-1}), and is colored with a water absorbance measured at 440 nm (color) of 2.49 m^{-1}. Paul Lake is less productive (Chl = 6.3 μg L^{-1}, TP = 3.8 μg L^{-1}, TN = 224 μg L^{-1}), has low alkalinity (pH = 6.6, DIC = 113 μmol L^{-1}), and color of 1.34 m^{-1}.

Aquashade Manipulation

Aquashade is a commercially available dye marketed for controlling the growth of aquatic plants. It contains the dyes acid blue 9 and acid yellow 23, and is blue in appearance. Our target concentration for Aquashade in Ward Lake was 1.5 ppm (volume fraction), which was within the range recommended by the manufacturer (0.5 ppm to 2.0 ppm). We used spectrophotometry to monitor Aquashade concentrations throughout the season because we anticipated that vertical mixing of the water column and surface flow into or out of the lake could dilute concentrations after the initial addition. To reach our target concentration of 1.5 ppm at the start of the season, we added 90.8 L of Aquashade to Ward Lake over three days starting April 23, 2012 (day of year 114) to initiate the experiment. Further additions on days 145 (3.8 L), 163 (15.1 L), and 195 (22.7 L) were made to maintain the depth of the photic zone (depth of 1% surface light) and similar Aquashade concentration. In total we added 132.5 L of dye to Ward Lake.

Physical, Chemical, and Biological Sampling

Physical, chemical, and biological characteristics of the lakes were measured weekly in both years (Appendix). These included vertical profiles of light, oxygen and temperature (from the surface into the hypolimnion), profiles of chlorophyll concentration throughout the photic

zone (100% to 1% surface light), and surface measurements of pCO_2. *Chaoborus* spp. and crustacean zooplankton community compositions were estimated from weekly vertical net tows, and their biomasses were estimated by applying standard mass–length regressions to lengths measured under a microscope (Appendix).

The ecosystem metabolism of the lakes was estimated from data gathered by automated sensors. We made high-frequency surface measurements of dissolved oxygen (DO) and vertically distributed measurements of temperature, as well as measurements of the meteorological parameters of air temperature, relative humidity, photosynthetically active radiation, and wind speed. It is common in limnological research to estimate metabolism from models involving diel changes in dissolved oxygen and atmospheric gas exchange (Cole et al. 2000, Stæhr et al. 2010, Hoellein et al. 2013). We used the R package rLakeAnalyzer to calculate high-frequency estimates of mixing depth, which in turn were supplied to models calculating atmospheric gas exchange (Read et al. 2011, 2012). To aid in mitigating potential bias introduced by noisy oxygen time series, we estimated net ecosystem production (NEP), gross primary production (GPP), and respiration (R) using a metabolism model that fits parameters in the framework of a Kalman filter (Batt and Carpenter 2012; Appendix).

Isotope Methods

Resource support of Ward Lake consumers was assessed using stable isotopes of carbon, nitrogen, and hydrogen and a Bayesian mixing model. Our methods follow those of Batt et al. (2012), who measured resource support of consumers in Ward Lake in 2010. Isotope samples were collected in 2010 and 2012, and our 2010 data partially supplement those data analyzed by Batt et al. (2012). Samples were collected monthly between May and August in 2010, and

between June and August in 2012. Samples for both consumers and end members were horizontally distributed among 5 sites in 2010, and 3 sites in 2012.

Water samples taken from the epilimnion and metalimnion were analyzed for the δ^2H of H_2O, and δ^{13}C, δ^{15}N, and δ^2H of particulate and dissolved organic matter (POM and DOM). In accordance with the methods of previous studies, POM samples formed the basis for calculating the isotope value of the phytoplankton end member (Solomon et al. 2009, Cole et al. 2011, Batt et al. 2012). Terrestrial end members included *Larix laricina*, *Carex* sp., and *Alnus incana* subsp. *rugosa*, and an aggregate "tree" end member taken from previously measured values of *Picea mariana*, *Abies balsamea*, *Acer rubrum*, *Acer saccharum*, *Thuja occidentalis*, and *Betula alleghaniensis* sampled in the watershed surrounding Ward Lake (Solomon et al. 2011, Cole et al. 2011). Macrophytes included floating-leafed morphologies (*Nymphaea odorata*, *Nuphar variegata*, *Brasenia schreberi*, *Potamogeton nodosus*), and submersed morphologies (*Chara* sp., *Najas flexilis*, *Potamogeton pusillus*, *Potamogeton amplifolius*). Benthic algae were sampled from ceramic tiles, submerged at a depth of 0.5 m in 2010 and 0.25 m in 2012. The zooplankton primary consumer *Skistodiaptomus oregonensis* was sampled by bilge pump from the epilimnion and metalimnion, and the zooplankton predator *Chaoborus* spp. was sampled at night using oblique net tows. The snail *Helisoma trivolvis* was collected from the perimeter of the lake, where hoop nets and minnow traps were set to collect the fishes *Pimephales promelas* (fathead minnow), *Phoxinus* spp. (dace), *Umbra limi* (central mud minnow), and young-of-the-year *Ameiurus melas* (black bullhead). The foot of each snail and the non-gut biomass of fishes were analyzed for isotopes. All solid samples were dried at 60 ºC and sent to Colorado Plateau Stable Isotope Laboratory for analysis (Doucett *et al.* 2007).

Isotope Mixing Model

Resource contributions to consumer biomass were estimated by analyzing consumer isotope values as a mixture of primary producer isotope values. We used a Bayesian mixing model similar to that used by Solomon et al. (2011) and identical to the model presented by Batt et al. (2012). The general form of the mixing model is $Y_i = X\Phi + D + E_i$. Y is a 3x1 vector containing the isotope values of sample i of the mixture. X is a 3xS matrix of end member isotope values, Φ is an Sx1 vector of the proportional contribution of each source to the organic matter of the consumer, and S is the number of organic matter sources. D contains discrimination factors, and E is a matrix of error terms. Furthermore, the sum of Φ was constrained to equal 1 (sources in X fully comprise the mixture, Y). Written in long form, the model is

$$Y = \begin{bmatrix} \delta^{13}C \\ \delta^{15}N \\ \delta^{2}H \end{bmatrix} = \begin{bmatrix} \delta^{13}C_1 & \cdots & \delta^{13}C_S \\ \delta^{15}N_1 & \cdots & \delta^{15}N_S \\ \delta^{2}H_1(1-\omega) & \cdots & \delta^{2}H_S(1-\omega) \end{bmatrix} \begin{bmatrix} \varphi_1 \\ \vdots \\ \varphi_S \end{bmatrix} + \begin{bmatrix} 0 \\ \Delta \\ (\delta^{2}H_2O)\omega \end{bmatrix} + \begin{bmatrix} \varepsilon_C \\ \varepsilon_N \\ \varepsilon_H \end{bmatrix}$$

The parameters estimated from data are the φ's for each source (S), and the variances of the ε's, which are normally distributed with means of 0 and variances σ_ε^2. All Φ were given uninformative priors drawn from a uniform distribution in a centered log-ratio space. The total proportion of consumer ^2H derived from ^2H_2O is $\omega=1-(1-\omega_0)^\tau$. The fractional contribution of dietary water (ω_0) is amplified with increasing trophic level, τ, because predators ingest ^2H_2O directly as well as indirectly through their prey, which incorporate dietary water themselves. The trophic enrichment of $\delta^{15}N$ is $\Delta=\Delta_{herb}+(\tau-1)\Delta_{carn}$. We used literature values for $\delta^{15}N$ enrichment across herbivorous (Δ_{herb}; mean (μ) = 2.52‰, standard deviation (σ) = 2.5‰) and carnivorous (Δ_{carn}; μ= 3.4‰, σ= 0.4‰) linkages, and for taxon-specific values for dietary water (respective means and standard deviations: *S. oregonensis* = 0.20, 0.04; *Chaoborus* spp. = 0.14, 0.06; *H.*

trivolvis = 0.21, 0.03; fishes = 0.12, 0.02) (Estep and Dabrowski 1980, Vander Zanden and Rasmussen 2001, Solomon et al. 2009, Bortolotti et al. 2013).

S. oregonensis and *H. trivolvis* (the primary consumers) were assigned trophic level 1 (levels above primary producers), and all other consumers were assigned trophic level 2. All trophic levels were assigned a variance of 0.1. Our data do not permit the estimation of isotope turnover rates in consumer tissue, and we assume that the isotopic composition of consumer tissue reflects recently incorporated organic matter. This assumption is met for the consumers born post-manipulation (*S. oregonensis*, *Chaoborus* spp., and young-of-the-year *A. melas*), but is violated if a consumer sampled in 2012 bore the isotopic signature of resources incorporated in 2010. However, not accounting for isotopic disequilibrium in older consumers would result in a conservative bias that underestimates between-year changes in the isotope values of consumers (Y) and in the contributions of resources to those consumers (Φ).

In the isotope mixing model, the number of sources (S) was limited to four (one plus the number of isotopes measured) because Φ was unknown. To reduce source number, end members can be pooled into ecologically similar groups (Phillips *et al.* 2005). We pooled end members into the following groups: terrestrial resources, phytoplankton (both depths), floating-leafed macrophytes, submersed macrophytes, all macrophytes, and benthic algae. The isotope values of each resource were taken from the average of its constituent end members. The variances of the resource signatures were determined by performing a one-way analysis of variance for each isotope-resource combination: the variance was set equal to the total mean squared error if the taxa had significantly different signatures ($p < 0.1$), or to the residual mean squared error if they were not significantly different. For each consumer we used known feeding habits and deviance information criterion to select two, three, or four sources from the 7 possible groups of pooled

end members. Our estimates of source contribution (Φ) were robust to source selection (Appendix).

Source contributions to POM and DOM were estimated using Eq. 1. In the case of POM, two Φ values (terrestrial and phytoplankton) were estimated along with the isotope values of the phytoplankton source. Phytoplankton δ^2H was given an informative prior based on δ^2H_2O, and δ^{13}C and δ^{15}N of phytoplankton were given uninformative priors (Solomon et al. 2009, Batt et al. 2012). The estimated isotope values for phytoplankton were subsequently used for the phytoplankton end member when estimating the composition of consumers and DOM. The composition of DOM was estimated after algebraically correcting for the influence of Aquashade on the isotope values of DOM by using measured concentrations, isotope values, and the C:N:H stoichiometry of the dye and of DOM (Appendix). The number of sources (S) was 4 for DOM, with the model containing terrestrial, macrophyte (both morphologies), phytoplankton, and periphyton sources. For both POM and DOM, trophic fractionation (Δ) and dietary water use (ω) were 0.

The compositions of mixtures (consumers, DOM, POM) from 2010 and 2012 were estimated from independent model runs. Benthic algal and phytoplankton samples used as sources in X were restricted to the sampling year of the mixture, whereas this distinction was not made for macrophyte or terrestrial sources. The same restriction was applied to POM and δ^2H_2O when modeling phytoplankton isotope values. Analyses were performed in R and JAGS, using the packages R2WinBUGS, rjags, R2jags, and programs written by the authors (Plummer 2003, Sturtz et al. 2005, R Core Team 2014). Each JAGS model run generated 6000 iterations of 8 Markov chains, thinned to 1000 samples of the posterior.

Results

Light attenuation

Aquashade was first added to Ward Lake in the spring of 2012, after which it remained near a concentration of 1.5 ppm. After Aquashade was added, the photic depth of Ward Lake was 2 m – half of the 4 m average in 2010 (Fig. 1). Similarly, the depth of the mixed layer was reduced from 1.8 m in 2010 to 0.9 m in 2012. Meanwhile, Paul Lake, a nearby unmanipulated lake, experienced a slight increase in mixed layer depth (2.4 m in 2010 to 2.8 m in 2012) and in photic zone depth (5.5 m in 2010 to 6.5 m in 2012).

Chlorophyll, dissolved gases, zooplankton biomass

The areal density of chlorophyll in the photic zone is a measure of the biomass of phytoplankton that could be photosynthesizing. In Paul Lake, areal chlorophyll was similar between years (seasonal average; 54.6 μg m^{-2} in 2010 and 53.6 μg m^{-2} in 2012), but Ward Lake areal chlorophyll decreased from 86.9 μg m^{-2} in 2010 to 34.9 μg m^{-2} in 2012 (Fig. 2). Mean epilimnetic GPP increased in both lakes, although the change in Paul Lake GPP was relatively small (13.2 to 16.4 mmol O_2 m^{-3} d^{-1}) compared to that in Ward Lake (32.6 to 44.8 mmol O_2 m^{-3} d^{-1}). In Paul Lake mean epilimnetic R was -18.1 mmol O_2 m^{-3} d^{-1} in 2010 and -21.7 mmol O_2 m^{-3} d^{-1} in 2012, and in Ward Lake there was a strong increase in the magnitude of R, shifting from -30.8 in 2010 to -66.6 mmol O_2 m^{-3} d^{-1} in 2012. The epilimnion of Paul Lake was slightly net heterotrophic in both years (NEP = -5.0 mmol O_2 m^{-3} d^{-1} in 2010, -5.3 mmol O_2 m^{-3} d^{-1} in 2012), while the epiliminon of Ward Lake shifted from slightly net autotrophic in 2010 (NEP = 1.7 mmol O_2 m^{-3} d^{-1}) to net heterotrophic in 2012 (NEP = -21.8 mmol O_2 m^{-3} d^{-1}) (Fig. 2). This pattern in metabolic balance was also reflected in high-frequency measurements of dissolved oxygen saturation (DO; saturation relative to 1 atm pressure) and in weekly measurements of the partial pressure of CO_2 (pCO_2). Paul Lake DO and pCO_2 were similar between years (DO = 99%

and pCO_2 = 987 μatm in 2010, 98% and 941 μatm in 2012), but Ward Lake DO decreased from 101% to 87% and pCO_2 increased from 976 μatm to 2134 μatm (Fig. 2). Summer means of weekly measurements of metalimnetic DO increased slightly in Paul Lake (90% in 2010, 99% in 2012), but decreased drastically in Ward Lake (86% in 2010, 30% in 2012).

In Ward Lake the zooplankton and *Chaoborus* spp. biomass declined between years (zooplankton = 0.9 g/m^2 in 2010 and 0.5 g/m^2 in 2012; *Chaoborus* spp. = 2.1 g/m^2 in 2010 and 0.4 g/m^2 in 2012) (Fig. 2). In Paul Lake, the biomasses of zooplankton (annual mean was 0.6 g/m^2 in 2010 and 0.7 g/m^2 in 2012) and *Chaoborus* spp. (6.8 g/m^2 in 2010 and 9.0 g/m^2 in 2012) were similar between years. The large change in zooplankton biomass in Ward Lake was not attributable to adult *S. oregonensis*, but to decreases in the adults of other copepod taxa and to a large decrease in the biomass of copepod larvae (Appendix).

Isotope values and mixing model results

We summarize mixing model estimates of the composition (Φ) of consumers and other pools of organic matter in Ward Lake as means of the posterior distributions of Φ, reported as percentages. We refer to changes between years that were less than 10% as not being ecologically important.

The sizes of the particulate and dissolved organic matter (POM and DOM) pools were similar between years (Appendix), but their compositions changed. POM in 2010 was 67% algal and 33% terrestrial, and in 2012 each of these end members comprised 50% of the POM pool. The DOM analysis included terrestrial material, macrophytes, phytoplankton, and periphyton as potential sources. In the baseline year terrestrial material comprised 89% of the DOM pool, but in 2012 macrophytes (pooled source of floating-leafed and submersed morphologies) were 56%

of the DOM pool and terrestrial material was only 20%. In 2012, phytoplankton comprised 6% and periphyton 18% of DOM.

Groups of end members (phytoplankton, periphyton, terrestrial, floating macrophytes, submersed macrophytes) occupied distinct regions of the three-dimensional (axes of $\delta^{13}C$, $\delta^{15}N$, $\delta^{2}H$) isotope space (Fig. 3A,B). Phytoplankton end members had the lowest $\delta^{2}H$ and $\delta^{13}C$ values, and also the highest $\delta^{15}N$ values. By contrast, submersed macrophytes had the highest $\delta^{2}H$ and $\delta^{13}C$ isotope values, and also the lowest $\delta^{15}N$ values. The $\delta^{13}C$ values of the algal end members (periphyton, epilimnetic and metalimnetic phytoplankton) decreased between years; similarly, consumer $\delta^{13}C$ tended to either decrease or be similar between years (Fig. 3 C-F). In 2010, $\delta^{2}H$ values for *S. oregonensis* and *Chaoborus* spp. were similar, but in 2012 the $\delta^{2}H$ values for these consumer became more distinct, with mean $\delta^{2}H$ increasing in *Chaoborus* spp. but decreasing in *S. oregonensis* (Fig. 3C). In 2010 the isotope value of the snail *H. trivolvis* was similar to that of the floating leafed macrophytes, but in 2012 its isotope values became similar to the terrestrial end members (Fig. 3C,D). Little change was seen in the isotope values of *U. limi*, but for the three other fishes the largest changes in isotope values involved increases in $\delta^{2}H$ and decreases $\delta^{13}C$ (Fig. 3E,F). These changes in fish isotope values amount to fish shifting away from the location of isotopic space occupied by periphyton.

Periphyton support of fish was lower in 2012 than in 2010, but phytoplankton support remained similar between years (Fig. 4). The periphyton end member was a potential source for three of the four fishes (not a source for *U. limi*), and support by this end member declined for each – from a mean posterior of 26% and standard deviation (σ) of 14% (2010) to 4% (σ =6%; 2012) for *P. promelas*, 44% (σ =14%) to 32% ± (σ=19%) for *Phoxinus spp.*, and 36% ± (σ =14%) to 10% ± (σ =11%) for *A. melas*. However, phytoplankton contribution to fish did not

decline, and for two of the fishes, phytoplankton support increased (*U. limi* = 31% [σ =9%] in 2010 and 46% [σ =6%] in 2012; *A. melas* = 16% [σ =10%] in 2010 and 31% [σ =7%] in 2012). Support by terrestrial and macrophyte resources tended to be similar or increase between years, with the exception that *U. limi* allochthony was lower in 2012 (56% [σ =19%] down to 31% [σ =19%]).

Allochthony increased for two of the three invertebrate consumers. Allochthony increased for both the snail *H. trivolvis* (from 36% [σ =12%] in 2010 to 62% [σ =14%] in 2012) and the predatory zooplankton *Chaoborus* spp. (from 19% [σ =11%] to 39% [σ =10%]). Increased *Chaoborus* spp. allochthony was complemented by decreased phytoplankton support (from 81% [σ =11%] to 67% [σ =10%]), whereas the snail received similar support from periphyton (34% [σ =18%] in 2010, 34% [σ =15%] in 2012) but derived less support from floating-leafed macrophytes (30% [σ =27%] to 4% [σ =6%]). In 2010, the zooplankton primary consumer *S. oregeonensis* was 15% (σ =7%) allochthonous, similar to *Chaoborus* spp. allochthony in the same year. However, unlike *H. trivolvis* and *Chaoborus* spp., *S. oregonensis* did not become more allochthonous in 2012, maintaining a high reliance on phytoplankton in both years (85% [σ =7%] in 2010, 93% [σ =5%] in 2012).

Between years, relative resource support (Φ) changed for most consumers. The sources (S) present in mixing models varied among consumers, and the terrestrial resource was the only source present in all consumer models. Of the seven consumers, five of them were more allochthonous in 2012 than in 2010 (Fig. 5). At least one of the algal end members (phytoplankton or periphyton) was present in each model, and the sum of the change in algal support was negative for four of the consumers. Note that for the three consumers whose models only contained algal and terrestrial resources, model structure necessitated that any change in

support by these resources be complementary. However, the changes in algal and terrestrial support were not perfectly complementary for the four consumers supported by macrophyte resources, and *H. trivolvis* was the only consumer to receive less macrophyte support in 2012 relative to 2010.

In 2010, all fishes derived less support from the phytoplankton resource than *Chaoborus* spp. (Fig. 4). Phytoplankton support of *Chaoborus* spp. decreased between years but remained higher than that of the fishes, for which phytoplankton support either increased or was similar between years (Figs. 4, 5). Therefore, compared to 2010, in 2012 the phytoplankton contribution to all fishes was more similar to its contribution to *Chaoborus* spp. (Fig. 6).

Discussion

Darkening Ward Lake reduced net ecosystem production (NEP), altering the relative availability of resources. NEP provides a broad perspective on food web energy flow because it integrates across processes and habitats. Consistent with patterns of increasingly negative NEP across lakes with increasing DOC concentration, Ward Lake shifted toward net heterotrophy after the manipulation. Loss of benthic algal production likely contributed to this shift because benthic algae are consistently less productive in shaded lakes (Vadeboncoeur et al. 2001, Ask et al. 2012). Phytoplankton have a more complicated response to increased DOC and water color (Hanson et al. 2003, Ask et al. 2012), but in Ward Lake, both chlorophyll measurements and the abundance and composition of POM indicate that phytoplankton were less abundant in 2012. Particularly, metalimnetic phytoplankton tend to make a greater contribution to zooplankton biomass in clearer systems (Francis *et al.* 2011), and the drastically decreased DO in the metalimnion of Ward Lake after it was darkened suggests that this algal resource was less available in 2012. Therefore, decreased production by both phytoplankton and periphyton likely

contributed to heterotrophic NEP in 2012, which suggests that they were less available to consumers in 2012 relative to 2010.

Changes in NEP can result from decreased gross primary production (GPP), increased respiration (R), or both. Both GPP and R increased in Ward Lake (37% increase in GPP, 116% increase in R) and in Paul Lake (25% increase in GPP, 20% increase in R). The increase in Ward Lake GPP was unexpected. Increased nutrient concentrations can stimulate both GPP and R, and relative to 2012, 2010 concentrations of total nitrogen (TN) and total phosphorus (TP) were much higher in both Paul Lake (TN = 223.6 μg/L in 2010, 427.8 μg/L in 2012; TP = 3.9 μg/L in 2010, 14 μg/L in 2012) as well as in Ward Lake (TN = 491 μg/L in 2010, 726 μg/L in 2012; TP = 23 μg/L in 2010, 58 μg/L in 2012). Thus, it may be that amplified rates of GPP and R in both lakes were driven by increased nutrient availability, and that the proportional increase in GPP and R in Paul Lake but not Ward Lake was due to the massive reduction in light availability in Ward Lake.

Estimates of decreased floating-leafed macrophyte support and unchanged periphyton support of *H. trivolvis* were surprising because decreased water clarity was expected to impact periphyton more than floating-leafed macrophytes. Although posterior estimates of resource support of *H. trivolvis* reveal a large degree of uncertainty for floating-leafed macrophyte support in both years, visual surface surveys indicated that the cover of floating-leafed macrophytes in the littoral zone (within 30 m of shore) of Ward Lake decreased from 27% in 2011 to 16% in 2012. Furthermore, between 2010 and 2012, macrophytes (combined morphologies) supplanted allochthonous material as the dominant constituent of DOM. Thus, the change in *H. trivolvis* resource use may be tied to a shift of macrophyte organic matter from living to dissolved forms.

In contrast with previous studies, our hypotheses, and other Ward Lake consumers, the calanoid copepod *S. oregonensis* did not become more allochthonous after light transmission declined and phytoplankton became less abundant. Several studies have documented that zooplankton can use terrestrial resources, especially in high DOC lakes with allochthonous particulate matter, including many lakes that are in the same watershed as Ward Lake (Carpenter et al. 2005, Marcarelli et al. 2011, Wilkinson et al. 2013a, Taipale et al. 2014). Rather than increasing in allochthony, *S. oregonensis* maintained high use of phytoplankton, even as the biomasses of other zooplankton and copepod larvae declined considerably. However, because *Chaoborus* spp. is a predator that integrates across the zooplankton community, its moderate increase in allochthony suggests that other taxa of zooplankton in Ward Lake increased their allochthony in 2012, and that the zooplankton consumers exhibited a variety of feeding habits. Indeed, *S. oregonensis* is a highly selective feeder (Kerfoot and Kirk 1991), and calanoids tend to be less allochthonous than either cyclopoids or cladocerans (Karlsson et al. 2012, Cole 2013, Wilkinson et al. 2013a). Therefore, our results and those of previous studies suggest that zooplankton may become increasingly allochthonous as phytoplankton become less available, but taxon-specific feeding habits may impose a limit on the extent of change.

The decreased contribution of periphyton to fishes in a darkened Ward Lake is consistent with patterns seen for fish and periphyton across lakes with increasing DOC concentration and decreased benthic primary productivity (Karlsson et al. 2009, Vander Zanden et al. 2011, Ask et al. 2012). Fish in darker lakes tend to be more isotopically similar to zooplankton, but we did not observe consistent complementarity between periphyton and phytoplankton support of fish. However, phytoplankton support of all fishes (including *U. limi*, which did not use periphyton) did become more similar to that of *Chaoborus* spp. In other words, the fishes showed an

increased connection to pelagic prey without necessarily relying more on pelagic primary producers, a pattern that was possible because some zooplankton relied less on phytoplankton in 2012. Floating-leafed macrophytes were another alternative resource that increased its support of some fishes after Ward was darkened. This response contrasts with the change in macrophyte use observed for *H. trivolvis*, and highlights the diversity of consumer responses to the manipulation and the variety of pathways connecting consumers to basal resources. In fact, the high mobility and trophic position of fishes is thought to facilitate both breadth and flexibility in resource use, which in turn stabilize food web dynamics (Rooney and McCann 2012). Overall, while fish support by periphyton was partially exchanged for support by phytoplankton, their repertoire of compensatory resources was diverse and integrated several habitats and the terrestrial ecosystem.

Future environmental changes may alter the base of food webs, removing preferred resources and forcing consumers to eat less or turn to alternative energy sources. When Ward Lake was darkened, algal resources became less abundant and a higher proportion of consumer biomass was supported by energetic alternatives like terrestrial material. This dynamic highlights that the strength of the energetic connection between consumer and source can change with resource availability and the environment. Given the global prevalence of rapid environmental change, further effort is needed to understand how resource support can change under other conditions and at other time scales. Our study challenges a perspective that holds resources as unimportant if they currently support a small fraction of consumer biomass, and embraces a view of such resources serving food webs as insurance, mitigating constricted energy flow and consumer starvation.

Acknowledgements

We thank Emily Read, Jordan Read, Tim Cline, Carol Yang, Cal Buelo, Megan Tomamichel, and Max Kleinhans for help in the field and lab, Tyler Tunney, Tony Ives and Jake Vander Zanden for helpful comments, the Notre Dame Environmental Research Center staff, and the National Science Foundation (Division of Environmental Biology [DEB]-0917858, DEB-1144683) and a Bunde Graduate Research Grant from the UW-Madison Department of Zoology for funding.

Literature Cited in Chapter 3

Ask, J., J. Karlsson, and M. Jansson. 2012. Net ecosystem production in clear-water and brown-water lakes. Global Biogeochemical Cycles 26:1–7.

Ask, J., J. Karlsson, L. Persson, and P. Ask. 2009. Whole-lake estimates of carbon flux through algae and bacteria in benthic and pelagic habitats of clear-water lakes. Ecology 90:1923–1932.

Batt, R. D., and S. R. Carpenter. 2012. Free-water lake metabolism: Addressing noisy time series with a Kalman filter. Limnology and Oceanography: Methods 10:20–30.

Batt, R. D., S. R. Carpenter, J. J. Cole, M. L. Pace, T. J. Cline, R. A. Johnson, and D. a. Seekell. 2012. Resources supporting the food web of a naturally productive lake. Limnology and Oceanography 57:1443–1452.

Bortolotti, L. E., R. G. Clark, and L. I. Wassenaar. 2013. Hydrogen isotope variability in prairie wetland systems: implications for studies of migratory connectivity. Ecological applications : a publication of the Ecological Society of America 23:110–21.

Carpenter, S. R., J. J. Cole, M. L. Pace, M. Van de Bogert, D. L. Bade, D. Bastviken, C. M. Gille, J. R. Hodgson, J. F. Kitchell, and E. S. Kritzberg. 2005. Ecosystem subsidies: Terrestrial support of aquatic food webs from 13C addition to contrasting lakes. Ecology 86:2737–2750.

Cole, J. J. 2013. Freshwater ecosystems and the carbon cycle. Page 146 (K. O, Ed.) Volume 18 in the Excellence in Ecology. Inter Research, Oldendorf/ Luhe.

Cole, J. J., S. R. Carpenter, J. Kitchell, M. L. Pace, C. T. Solomon, and B. Weidel. 2011. Strong evidence for terrestrial support of zooplankton in small lakes based on stable isotopes of

carbon, nitrogen, and hydrogen. Proceedings of the National Academy of Sciences of the United States of America 108:1975–1980.

Cole, J. J., M. L. Pace, S. R. Carpenter, and J. F. Kitchell. 2000. Persistence of net heterotrophy in lakes during nutrient addition and food web manipulations. Limnology and Oceanography 45:1718–1730.

Doucett, R. R., J. C. Marks, D. W. Blinn, M. Caron, and B. A. Hungate. 2007. Measuring terrestrial subsidies to aquatic food webs using stable isotopes of hydrogen. Ecology 88:1587–1592.

Estep, M. F., and H. Dabrowski. 1980. Tracing food webs with stable hydrogen isotopes. Science 209:1537–1538.

Finstad, A. G., I. P. Helland, O. Ugedal, T. Hesthagen, and D. O. Hessen. 2014. Unimodal response of fish yield to dissolved organic carbon. Ecology letters 17:36–43.

Francis, T. B., D. E. Schindler, G. W. Holtgrieve, E. R. Larson, M. D. Scheuerell, B. X. Semmens, and E. J. Ward. 2011. Habitat structure determines resource use by zooplankton in temperate lakes. Ecology Letters 14:364–72.

Hanson, P. C., D. L. Bade, S. R. Carpenter, and T. K. Kratz. 2003. Lake metabolism: relationships with dissolved organic carbon and phosphorus. Limnology and Oceanography 48:1112–1119.

Hoellein, T. J., D. a. Bruesewitz, and D. C. Richardson. 2013. Revisiting Odum (1956): A synthesis of aquatic ecosystem metabolism. Limnology and Oceanography 58:2089–2100.

Huxel, G. R., K. McCann, and G. A. Polis. 2002. Effects of partitioning allochthonous and autochthonous resources on food web stability. Ecological Research 17:419–432.

Jones, S., C. Solomon, and B. Weidel. 2012. Subsidy or subtraction: how do terrestrial inputs influence consumer production in lakes? Freshwater Reviews:37–49.

Karlsson, J., M. Berggren, J. Ask, P. Byström, A. Jonsson, H. Laudon, and M. Jansson. 2012. Terrestrial organic matter support of lake food webs: Evidence from lake metabolism and stable hydrogen isotopes of consumers. Limnology and Oceanography 57:1042–1048.

Karlsson, J., P. Byström, J. Ask, P. Ask, L. Persson, and M. Jansson. 2009. Light limitation of nutrient-poor lake ecosystems. Nature 460:506–509.

Karlsson, J., A. Jonsson, M. Meili, and M. Jansson. 2003. Control of zooplankton dependence on allochthonous organic carbon in humic and clear-water lakes in northern Sweden. Limnology and Oceanography 48:269–276.

Kerfoot, W. C., and K. L. Kirk. 1991. Degree of taste discrimination among suspension-feeding cladocerans and copepods: Implications for detritivory and herbivory. Limnology and Oceanography 36:1107–1123.

Köhler, S. J., D. Kothawala, M. N. Futter, O. Liungman, and L. Tranvik. 2013. In-lake processes offset increased terrestrial inputs of dissolved organic carbon and color to lakes. PloS One 8:e70598.

Kovalenko, K. E., and E. D. Dibble. 2013. Invasive macrophyte effects on littoral trophic structure and carbon sources. Hydrobiologia 721:23–34.

Leroux, S. J., and M. Loreau. 2008. Subsidy hypothesis and strength of trophic cascades across ecosystems. Ecology Letters 11:1147–56.

Maguire, C. M., and J. Grey. 2006. Determination of zooplankton dietary shift following a zebra mussel invasion, as indicated by stable isotope analysis. Freshwater Biology 51:1310–1319.

Marcarelli, A. M., C. V. Baxter, M. M. Mineau, and R. O. Hall. 2011. Quantity and quality: Unifying food web and ecosystem perspectives on the role of resource subsidies in freshwaters. Ecology 92:1215–1225.

Mendonça, R., S. Kosten, G. Lacerot, N. Mazzeo, F. Roland, J. P. Ometto, E. A. Paz, C. P. Bove, N. C. Bueno, J. H. C. Gomes, and M. Scheffer. 2012. Bimodality in stable isotope composition facilitates the tracing of carbon transfer from macrophytes to higher trophic levels. Hydrobiologia 710:205–218.

Monteith, D. T., J. L. Stoddard, C. D. Evans, H. A. de Wit, M. Forsius, T. Høgåsen, A. Wilander, B. L. Skjelkvåle, D. S. Jeffries, J. Vuorenmaa, B. Keller, J. Kopácek, and J. Vesely. 2007. Dissolved organic carbon trends resulting from changes in atmospheric deposition chemistry. Nature 450:537–540.

Pace, M. L., and J. J. Cole. 2002. Synchronous variation of dissolved organic carbon and color in lakes. Limnology and Oceanography 47:333–342.

Phillips, D. L., S. D. Newsome, and J. W. Gregg. 2005. Combining sources in stable isotope mixing models: alternative methods. Oecologia 144:520–527.

Plummer, M. 2003. JAGS: A program for analysis of Bayesian graphical models using Gibbs sampling. Proceedings of the 3rd International Workshop on Distributed Statistical Computing.

R Core Team. 2014. R: A Language and Environment for Statistical Computing. R Foundation for Statistical Computing, Vienna, Austria.

Read, J. S., D. P. Hamilton, A. R. Desai, K. C. Rose, S. MacIntyre, J. D. Lenters, R. L. Smyth, P. C. Hanson, J. J. Cole, P. a. Staehr, J. a. Rusak, D. C. Pierson, J. D. Brookes, A. Laas, and C.

H. Wu. 2012. Lake-size dependency of wind shear and convection as controls on gas exchange. Geophysical Research Letters 39.

Read, J. S., D. P. Hamilton, I. D. Jones, K. Muraoka, L. a. Winslow, R. Kroiss, C. H. Wu, and E. Gaiser. 2011. Derivation of lake mixing and stratification indices from high-resolution lake buoy data. Environmental Modelling & Software 26:1325–1336.

Rooney, N., and K. S. McCann. 2012. Integrating food web diversity, structure and stability. Trends in ecology & evolution 27:40–46.

Sobczak, W. V, J. E. Cloern, A. D. Jassby, and A. B. Müller-Solger. 2002. Bioavailability of organic matter in a highly disturbed estuary: the role of detrital and algal resources. Proceedings of the National Academy of Sciences of the United States of America 99:8101–8105.

Solomon, C. T., S. R. Carpenter, M. K. Clayton, J. J. Cole, J. J. Coloso, M. L. Pace, M. J. Vander Zanden, and B. C. Weidel. 2011. Terrestrial, benthic, and pelagic resource use in lakes: results from a three-isotope Bayesian mixing model. Ecology 92:1115–1125.

Solomon, C. T., J. J. Cole, R. R. Doucett, M. L. Pace, N. D. Preston, L. E. Smith, and B. C. Weidel. 2009. The influence of environmental water on the hydrogen stable isotope ratio in aquatic consumers. Oecologia 161:313–324.

Stæhr, P. A., D. L. Bade, M. C. Van de Bogert, G. R. Koch, C. Williamson, P. C. Hanson, J. J. Cole, and T. K. Kratz. 2010. Lake metabolism and the diel oxygen technique: State of the science. Limnology and Oceanography: Methods 8:628–644.

Sturtz, S., U. Ligges, and A. Gelman. 2005. R2WinBUGS: A package for running WinBUGS from R. Journal of Statistical Software 12:1–16.

Taipale, S. J., M. T. Brett, M. W. Hahn, D. Martin-Creuzburg, S. Yeung, M. Hiltunen, U. Strandberg, and P. Kankaala. 2014. Differing Daphnia magna assimilation efficiencies for terrestrial, bacterial and algal carbon and fatty acids. Ecology 95:563–576.

Tanentzap, A. J., E. J. Szkokan-Emilson, B. W. Kielstra, M. T. Arts, N. D. Yan, and J. M. Gunn. 2014. Forests fuel fish growth in freshwater deltas. Nature Communications 5:1–9.

Tunney, T. D., K. S. McCann, N. P. Lester, and B. J. Shuter. 2012. Food web expansion and contraction in response to changing environmental conditions. Nature communications 3:1–9.

Vadeboncoeur, Y., D. M. Lodge, and S. R. Carpenter. 2001. Whole-lake fertilization effects on distribution of primary production between benthic and pelagic habitats. Ecology 82:1065–1077.

Vadeboncoeur, Y., G. Peterson, M. J. Vander Zanden, and J. Kalff. 2008. Benthic algal production across lake size gradients: interactions among morphometry, nutrients, and light. Ecology 89:2542–2552.

Vadeboncoeur, Y., J. M. Vander Zanden, and D. M. Lodge. 2002. Putting the lake back together: Reintegrating pathways into lake food web models. BioScience 52:44–54.

Weidel, B., S. Carpenter, J. Cole, J. Hodgson, J. Kitchell, M. Pace, and C. Solomon. 2008. Carbon sources supporting fish growth in a north temperate lake. Aquatic Sciences 70:446–458.

Wilkinson, G. M., S. R. Carpenter, J. J. Cole, M. L. Pace, and C. Yang. 2013a. Terrestrial support of pelagic consumers: patterns and variability revealed by a multilake study. Freshwater Biology 58:2037–2049.

Wilkinson, G. M., M. Pace, and J. J. Cole. 2013b. Terrestrial dominance of organic matter in north temperate lakes. Global Biogeochemical Cycles 27:43–51.

Vander Zanden, M. J., and J. B. Rasmussen. 2001. Variation in δ15N and δ13C trophic fractionation: implications for aquatic food web studies. Limnology and Oceanography 46:2061–2066.

Vander Zanden, M. J., and Y. Vadeboncoeur. 2002. Fishes as integrators of benthic and pelagic food webs in lakes. Ecology 83:2152–2161.

Vander Zanden, M. J., Y. Vadeboncoeur, and S. Chandra. 2011. Fish reliance on littoral–benthic resources and the distribution of primary production in lakes. Ecosystems 14:894–903.

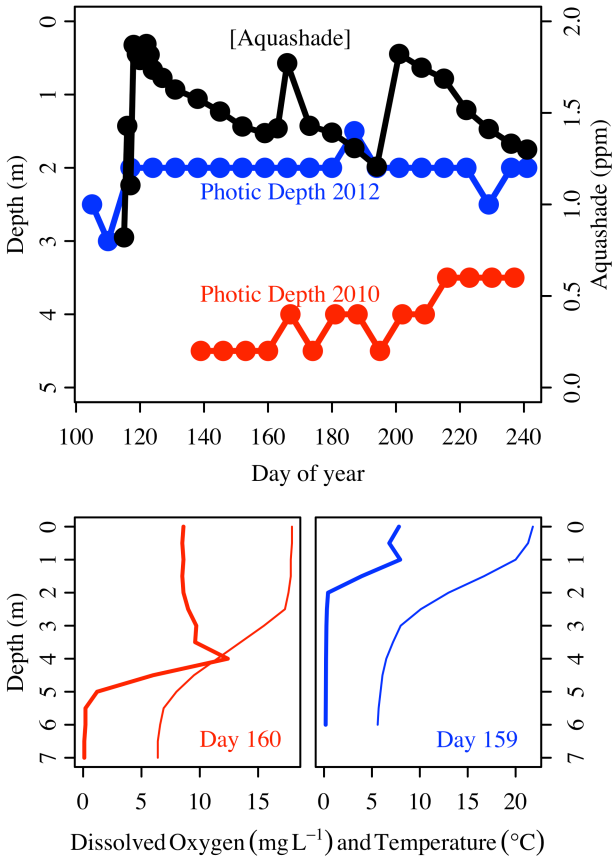

Figure 1. The top panel shows time series of Aquashade concentration in 2012 (black), photic depth in 2010 (red), and photic depth in 2012 (blue). Photic depth was defined as the depth where photosynthetically active radiation (PAR) was equal to 1% of PAR at 0 m. The bottom panels show temperature (thin lines) and dissolved oxygen (thick lines) profiles on a single representative day in each year (day 160 in 2010 and day 159 in 2012).

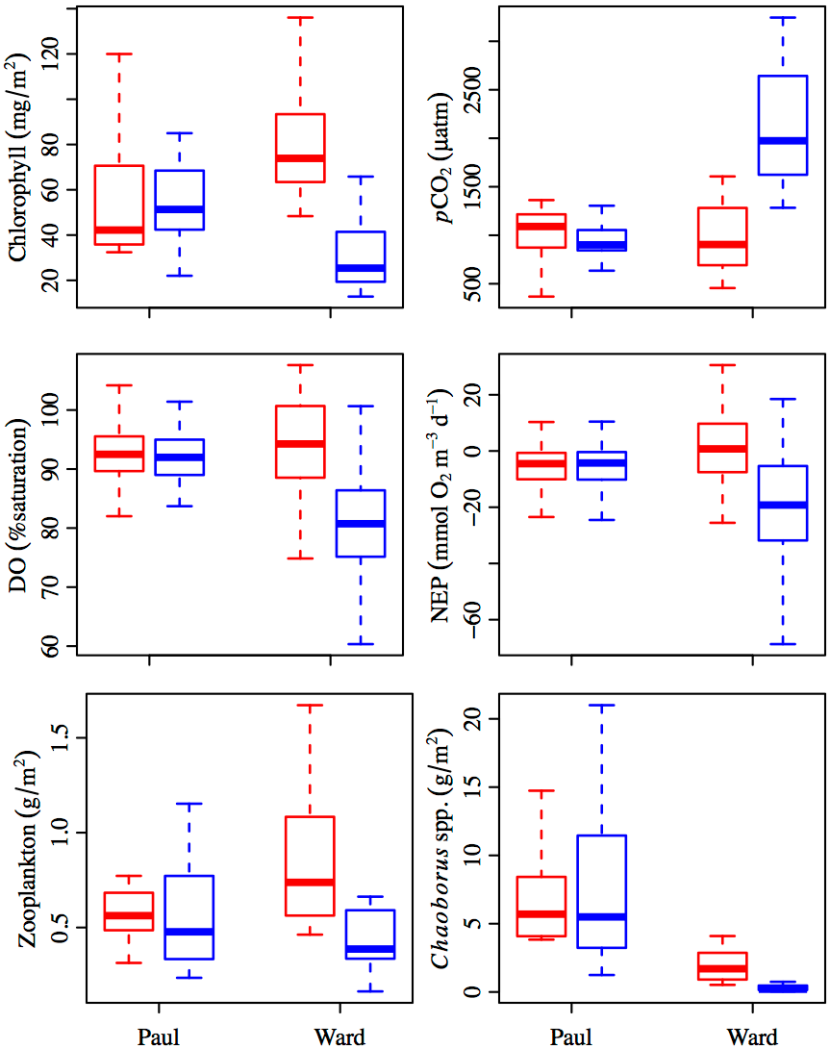

Figure 2. Box and whisker plots of areal chlorophyll (measured weekly), pCO_2 (measured weekly), dissolved oxygen (DO, percent saturation; daily average of 5-min observations), net ecosystem production (NEP; daily), crustacean zooplankton biomass (weekly), and *Chaoborus* spp. biomass (weekly) in the manipulated lake (Ward Lake) and a nearby reference lake (Paul Lake) in 2010 (red) and in 2012 (blue). Each box bounds the 25-75th percentile of data, with each whisker extending to the most extreme datum that is no more than 1.5 * (interquartile range) beyond the box. The thick line in the center of a box is the median. All data were included in statistical calculations, but to preserve the scaling of axes, outliers are not displayed.

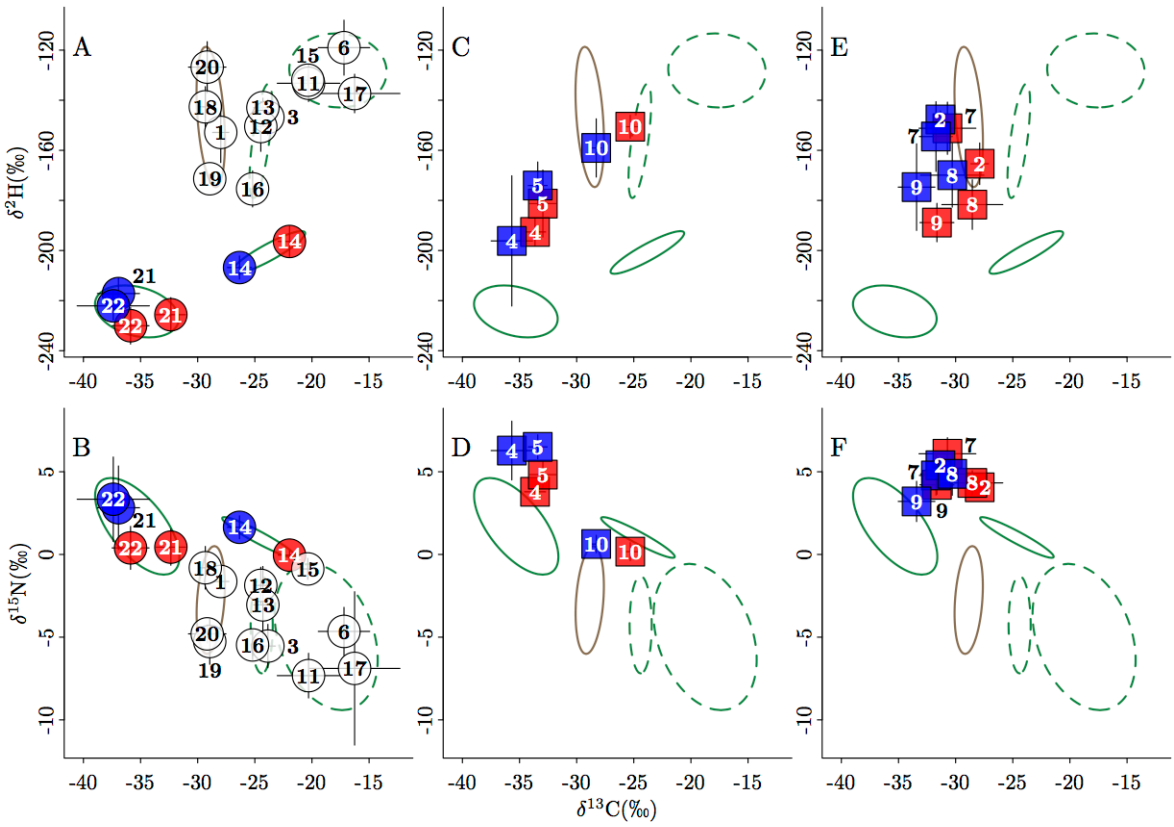

Figure 3. Biplots of mean end member (circles) and consumer (squares) $\delta^{13}C$, $\delta^{15}N$, and $\delta^{2}H$ isotope values and their standard deviations (black error bars). (A, B) End members; brown ellipse indicates terrestrial end members (1= *A. incana* subsp. *rugosa*, 18 = Carex sp., 19 = *L. laricina*, 20 = tree species), dashed green ellipses indicate macrophytes of floating (3 = *B. schreberi*, 12 = *N. variegata*, 13 = *N. odorata*, 16 = *P. pusillus*) and submersed morphologies (6 = *Chara* sp., 11 = *N. flexilis*, 15 = *P. amplifolius*, 17 = *P. pusillus*), solid green ellipses indicate algal end members (14 = periphyton, 21 = epilimnetic phytoplankton, 22 = metalimnetic phytoplankton). (C, D) Invertebrate consumers; 4 = *S. oregonensis*, 5 = *Chaoborus* spp., 10 = *H. trivolvis*. (E, F) Fish consumers; 2 = *A. melas*, 7 = *U. limi*, 8 = *Phoxinus* spp., 9 = *P. promelas*. Red symbols correspond to 2010 values, blue to 2012, and white symbols correspond to end member values that were pooled between years.

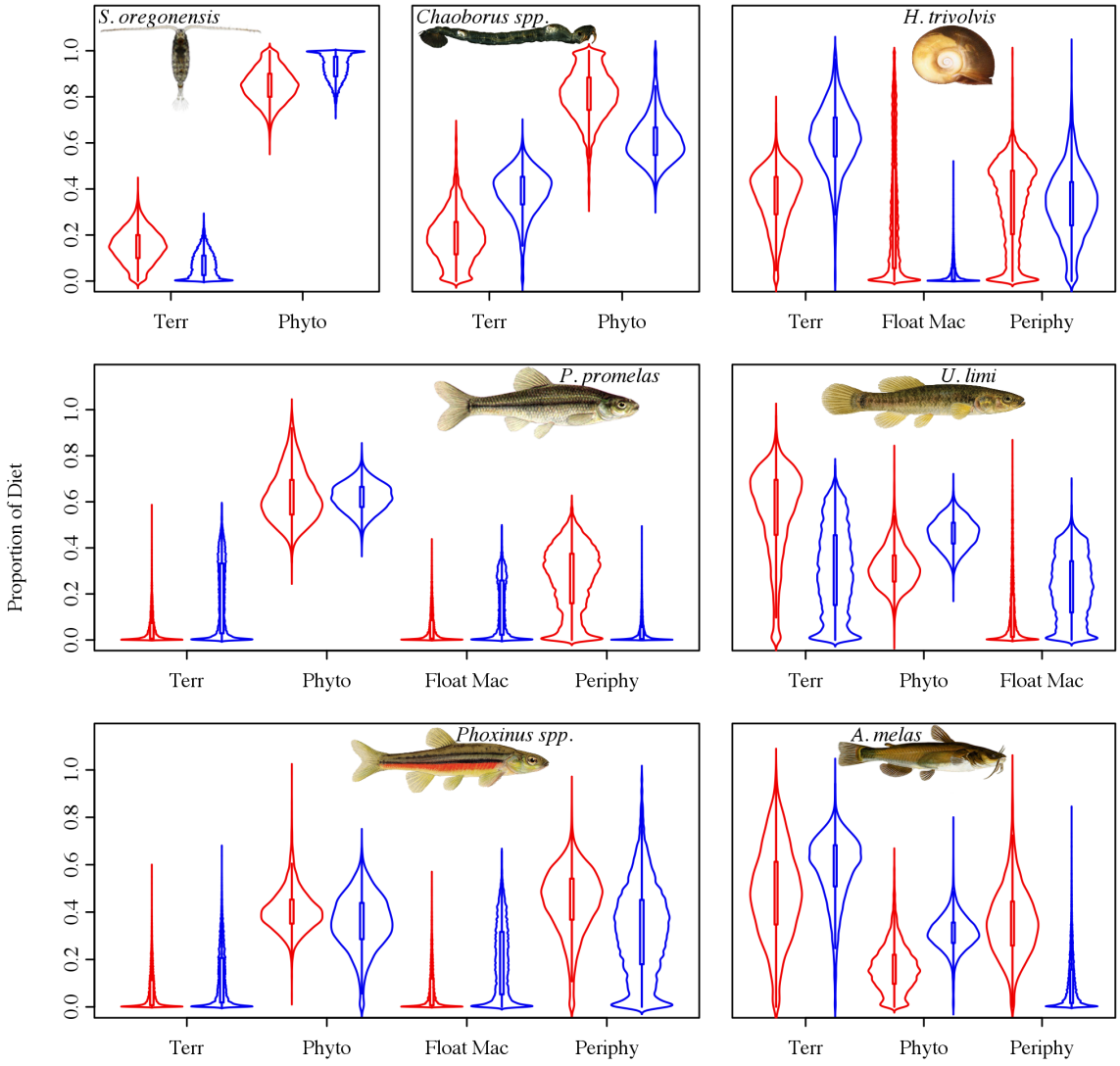

Figure 4. Violin plots of the proportional contributions of resources to consumers (posterior of Φ) in Ward Lake in 2010 (red) and 2012 (blue). Each violin is a mirror image of a nonparametric density estimate of a posterior (violins are wider at higher densities), and in the center of the violins are boxplots. Consumers include *S. oregonensis* (a zooplankton primary consumer), *Chaoborus* spp. (predatory zooplankton), *H. trivolvis* (a snail), *P. promelas* (fathead minnow), *U. limi* (central mud minnow), *Phoxinus* spp. (dace), and young-of-year *A. melas* (black bullhead). Terr = terrestrial (*A. incana* subsp. *rugosa*, *Carex* sp., *L. laricina,* and other nearby tree species);

Phyto = phytoplankton; Float Mac = floating-leafed macrophytes (*B. schreberi*, *N. variegata*, *N. odorata*, and *P. nodosus*); Periphy = periphyton.

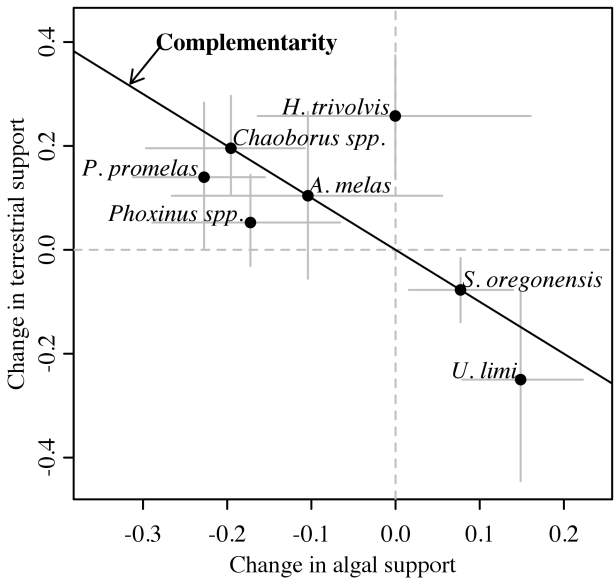

Figure 5. Changes in resource support between 2010 and 2012. The solid black line indicates where the changes in support by algal and terrestrial resources were perfectly complementary, which was necessitated by model structure for the three consumers that were not supported by macrophytes. Consumers below this line received more support from macrophytes in the second year, and the consumer above the line received less support from macrophytes. Positive values indicate an increase in the median support by the resource in 2012 relative to 2010. Error bars are 25^{th} and 75^{th} percentiles of the differences. The change in the algal resource is the sum of the changes in the phytoplankton and periphyton resources.

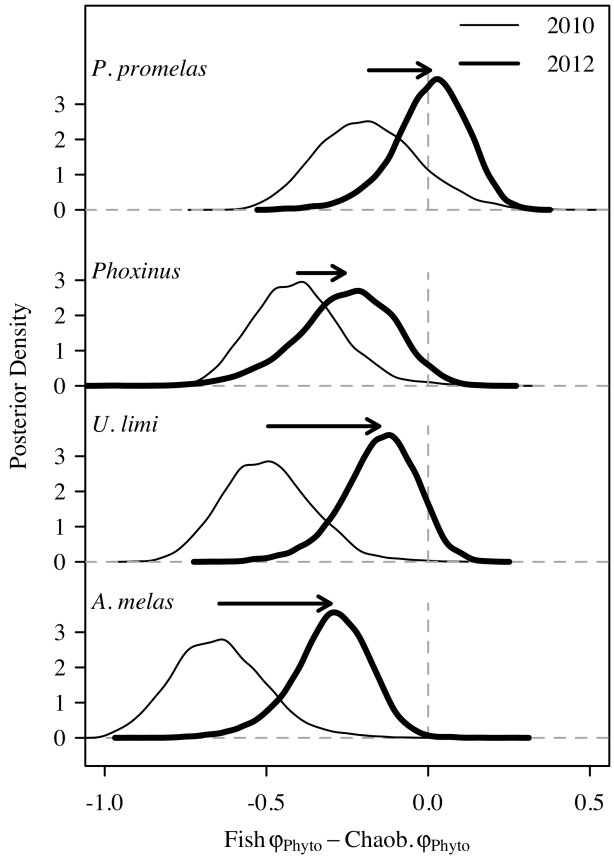

Figure 6. Phytoplankton support (φ_{Phyto}) of the four fishes, expressed as a deviation from φ_{Phyto} of *Chaoborus* spp. The vertical axis is the density of the difference between the posterior distributions of φ_{Phyto} for the two consumers. Thin lines are the posterior densities in 2010, and thick lines are from 2012. Negative values on the horizontal axis (to the left of the vertical dashed line) indicate that phytoplankton comprised a greater proportion of *Chaoborus* spp. than of the fish. The horizontal arrows show the direction and magnitude of the change in Fish φ_{Phyto} − Chaob φ_{Phyto} between years, with the arrow starting at the mean difference in 2010, and ending at the mean difference in 2012. In all cases, phytoplankton support of fish was more similar to support of *Chaoborus* spp. in 2012 than in 2010.

Appendix to Chapter 3

Limnological measurements

During the ice-free periods of 2010 and 2012 we took weekly measurements of a suite of limnological variables in Paul and Ward Lakes using standard methods, which are described briefly below. Detailed descriptions of these methods can be found in previous publications (Carpenter and Kitchell 1993, Carpenter et al. 2001) and in an online repository (http://c13.valuemembers.net/Documents/CascadeManual1998.pdf).

Depth profiles of temperature and dissolved oxygen (DO) were taken from the surface (0 m) to the hypolimnion at 0.5 m intervals. DO and temperature were measured using a YSI Professional Plus handheld meter. Profiles of photosynthetically active radiation (PAR, 400 nm to 700 nm) were taken at 0.25 m intervals from 0 m to 1 m, and at 0.5 m intervals from 1 m until 1% of surface light was reached. PAR was measured with a LI-COR LI-193 underwater sensor for the depth profiles, and with a LI-COR LI-190 Quantum Sensor for surface readings. Depths corresponding to 100%, 50%, 25%, 10%, 5%, and 1% of surface light were obtained in the field by linearly interpolating the ratio of underwater PAR to surface PAR between consecutive depths.

Measurements of chlorophyll (Chl), and dissolved inorganic carbon (DIC) were taken from water samples at depths corresponding to the aforementioned light gradient (100% to 1% surface light), while partial pressure of CO_2 (pCO_2), total nitrogen (TN), total phosphorus (TP) were measured from a pooled sample of three epilimnetic depths. Chl was measured from water samples filtered through a Whatman GF/F glass fiber filter, frozen, extracted in methanol, and analyzed using a fluorometer (Sequoia Turner Model 450). TN and TP were measured from unfiltered water samples (100 mL) that had been preserved using 1 mL of 1N Optima sulfuric

acid. DIC was measured on a Shimadzu gas chromatograph (GC-8A) by the syringe gas stripping method of Stainton (1973). *p*CO2 was measured using the large volume equilibration method of Cole *et al.* (1994).

Weekly daytime vertical net tows were made with a conical net to measure the abundance and composition of the zooplankton biomass and community composition in each lake, and the same was done for *Chaoborus* spp., a zooplankton predator, using nighttime tows. Crustacean zooplankton were sampled using a net with a mesh size of 80 μm, and for *Chaoborus* spp. we sampled with a mesh of 153 μm. Both sets of samples were taken at a central location that was near the deepest point of the lake. In Paul Lake tows were taken from a depth of 8 m, and in Ward Lake from a depth of 6 m. Crustaceans and *Chaoborus* spp. were preserved in a 1% Lugol's solution, subsampled and enumerated. The length of 15 individuals were measured and lengths converted to biomasses following the equations of Downing & Rigler (1984).

Sensor and Metabolism Methods

We used automated *in situ* sensors (sondes) to measure dissolved oxygen (DO), which was used to estimate metabolism, which includes gross primary production (GPP), respiration (R), and net ecosystem production (NEP). The sonde models were YSI 600XLM (rapid pulse DO probe model 6562) for Ward in 2010, and YSI 6600 V2 (optical DO probe model 6150) for Ward in 2012 and Paul in 2010 and 2012. We used thermistor chains to measure temperature in both lakes. In Paul Lake we used NexSens T-node sensors with thermistors placed every 0.5 m from 0.5 m to 4 m, and an additional thermistor at 5.0 m. In Ward Lake we used HOBO thermistors, which in 2010 were placed every 0.5 m between 0.5 m and 5.5 m, and in 2012 were placed every 0.25 m between 0 m and 2 m, and at 2.5 m and 3.0 m. Before June of 2010 high

frequency thermal profiles were not available for Ward Lake, and estimates of mixed layer depth were instead made from manual weekly profiles. We measured photosynthetically active radiation (PAR; W m^{-2} s^{-1}) and wind speed (m s^{-1}) at 2 m above the lake surface with an anemometer on a buoy on nearby Peter Lake (adjacent to Paul Lake, similar in size to both lakes in this study). Hourly measurements of air temperature, relative humidity, barometric pressure were made by a nearby weather station on the UNDEC property, and linearly interpolated to a 5-minute frequency. This weather station also provided supplemental measurements of PAR and wind speed which were used to fill in missing portions of those time series collected by the Peter Lake buoy. Automated sensors for DO and temperature in Ward in 2010 sampled at a 4-minute frequency while sensors in other lakes or years sampled at a 5-minute frequency.

Metabolism was calculated from automated high-frequency measurements of DO using a model that was fit in the framework of a Kalman filter (Batt and Carpenter 2012). This metabolism model includes process error and observation error, and fits parameters relating PAR to GPP and temperature to R using maximum likelihood. Process errors propagate throughout a time series but observation errors do not, and can be thought of as noise added to the oxygen data after they are generated. A model that makes this distinction between error types must explicitly consider both the true state of the system (which is unknown) and the observed state of the system (which we measure). Given such a model, the likelihood of the data given a set of parameter estimates can be computed using a Kalman filter (Kalman 1960, Harvey 1989).

The negative log likelihood function involves two key sets of equations that describe the process and observation components of the model:

$$y_t = \alpha_t + \eta_t;\ \eta \sim N(0,H) \qquad [1]$$

$$\alpha_{t|t-1} = \alpha_{t-1} + \iota * I_{t-1} + \rho * \log_e T_{t-1} + F_{t-1} + \varepsilon_t;\ \varepsilon \sim N(0,Q) \qquad [2]$$

Where y is the observed concentration of oxygen (mmol O_2 m^{-3}), α is the true value of oxygen, η are observation errors, H is the variance of η, ι and ρ are a parameter to be estimated, T is water temperature (ºC), F is discrete atmospheric gas exchange (m per 5-minutes) (Read *et al.* 2012), ε are process errors, and Q is the variance of ε. Written in a form that expands F and solves for gas exchange in continuous time, the process equation becomes:

$$\alpha_{t|t-1} = a_t * k_{t-1}^{-1} * z_{t-1} + -\exp\{-k_{t-1} * z_{t-1}^{-1}\} * a_t * k_{t-1}^{-1} * z_{t-1} + \alpha_{t-1} \quad [3]$$

$$a_t = \iota * I_{t-1} + \rho * \log_e T_{t-1} + k_{t-1} * z_{t-1}^{-1} * O_{s,t-1} \quad [4]$$

where z is the depth of the mixed layer in meters (Read *et al.* 2011), and O_s is the concentration of oxygen at saturation given water temperature and atmospheric pressure. In addition to making predictions for the system state at each time step, the Kalman filter also makes predictions of the error covariance matrix, P:

$$P_{t|t-1} = P_{t-1} * (k_{t-1} * z_{t-1}^{-1})^2 \quad [5]$$

The subscript t|t-1 indicates that the estimates of α and P are only based on observations of y up to y_{t-1}, and have not been updated to reflect information gained by y_t. To incorporate the new information gained from the current observation of dissolved oxygen, y_t, the Kalman filter updates the estimates of the predicted values by accounting for the current observation and the relative uncertainty surrounding the predictions and the observations – this process is akin to a weighted average of the prediction and the observation using precision (inverse of variance) as the weights. The updating equations are as follows:

$$E_t = P_{t|t-1} + H \quad [6]$$

$$\alpha_t = \alpha_{t|t-1} + P_{t|t-1} * (y_t - \alpha_{t|t-1}) * E_t^{-1} \quad [7]$$

$$P_t = P_{t|t-1} - E_t * (P_{t|t-1})^{-2} \quad [8]$$

In this implementation of the Kalman filter, we initiate $P_{t=1}$ with Q, and $\alpha_{t=1}$ with $y_{t=1}$. The parameters to be estimated are Q, H, ι, and ρ. The negative log likelihood, L, of the data given the current parameter estimates is

$$L = \Sigma(t=1 \text{ to } t=N)\ 0.5*\log_e(2*\pi) + 0.5*\log(E_t) + 0.5*(y_t - \alpha_{t|t-1})^2*E_t \qquad [9]$$

Having fit ι and ρ, they are multiplied by PAR and $\log_e$(temperature) at each time step, and summed up over the course of the day, yielding estimates of GPP and R in mmol O_2 m^{-3} d^{-1}, respectively. NEP was calculated as the sum of GPP and R on a given day. These parameters were fit separately for each day of data, and by convention ι is positive and ρ is negative; when these parameters take on the opposite sign, the estimates no longer are ecologically meaningful. On days where either ι or ρ had the wrong sign, that days estimates of GPP, R, and NEP were discarded from further analysis and did not contribute to seasonal estimates of metabolism.

Sample Collection for Isotope Analysis

Water was sampled from the epilimnion (at 0.5 m) and the metalimnion every month from May through August in 2010, and June through August in 2012. The samples were taken from 5 horizontally distributed locations in 2010, and 3 locations in 2012. The metalimnetic sampling depth was defined as the depth of the maximum saturation of dissolved oxygen (DO) below the mixed layer (Z_{mix}). Sample filtrate (Whatman GF/F filters) was analyzed for water deuterium (δ^2H of H_2O) and the δ^{13}C, δ^{15}N, and δ^2H of dissolved organic matter (DOM). Solid samples of DOM were obtained by evaporating the acidified filtrate (1mL 1N H_2SO_4 in 1L of filtrate) in a glass petri dish. The material collected on the Whatman GF/F filters was used to measure the carbon and nitrogen stable isotopes of particulate organic matter (POM). Material for POM analysis of hydrogen stable isotopes was collected on a MicronSep Cellulosic filter,

washed off of the filter with a small amount of deionized water, and dried at 60 ºC. DOM, δ^2H_2O, and POM sample sizes were 5, 8, and 33 in 2010, and 6, 18, and 14 in 2012.

Algal end members included phytoplankton and benthic algae. Phytoplankton isotope values were computed from POM and δ^2H_2O, as described in the main text. Benthic algae were sampled from ceramic tiles submerged at 0.5 m and 0.25 m in 2010 and 2012, respectively (n = 6, 6; this notation henceforth represents sample sizes in 2010, 2012). Tiles were deployed at horizontally distributed locations in the littoral zone of the lake throughout both summers, and samples were scraped from the tiles on each sampling date. Benthic algae sampled from tiles served as a morphological and isotopic surrogate for attached algae that might be growing in the lake, and the use of tiles avoided the potential for contamination by natural substrates (e.g., wood or sediment).

Macrophytes and terrestrial plants comprised the other end members sampled for isotopes. Macrophytes were sampled throughout the lake and included taxa of floating-leafed (*Nymphaea odorata* [n = 5, 2], *Nuphar variegata* [n = 5, 2], *Brasenia schreberi* [n = 4, 2], *Potamogeton nodosus* [n = 0, 2]) and submersed (*Chara* sp. [n = 5, 1], *Najas flexilis* [n = 1, 3], *Potamogeton pusillus* [n = 5, 2], *Potamogeton amplifolius* [n = 0, 2]) morphologies. Macrophytes were thoroughly rinsed with tap water, and taxa with broad leaves were also gently scrubbed to remove any remaining epiphytic growth. Terrestrial vegetation (*Larix laricina*, *Carex* sp., *Alnus incana* subsp. *rugosa*) was collected from around the perimeter of the lake (total of 10 samples in 2010, 4 samples in 2012). We used our previously measured isotope values of several tree species sampled from the watershed (*Picea mariana*, *Abies balsamea*, *Acer rubrum*, *Acer saccharum*, *Thuja occidentalis*, *Betula alleghaniensis*) to form an average "tree" isotopic signature (Solomon et al. 2011, Cole et al. 2011). Although we sampled macrophytes and

terrestrial end members in both years, we pooled samples from both years for use in mixing models. Furthermore, the isotope values of each taxon (e.g., *Chara* sp.) were averaged, then this average was averaged across taxa to form the isotope value of the group (e.g., submersed macrophytes). Therefore, differences in the sample sizes of individual taxa did not result in taxa with larger sample sizes having a larger influence on the group isotope values. Analysis of variance was used to calculate the variance of the groups.

Consumers were sampled on approximately the same dates as end members. All consumers were sampled from locations that were horizontally distributed across the lake. The zooplankton *Skistodiaptomus oregonensis* was collected by pumping water from discrete depths in the epilimnion and metalimnion through a net (n = 34, 18). The zooplankton predator, *Chaoborus* spp., was sampled using nighttime oblique net tows through the epilimnion (n = 20, 7). The snail *Helisoma trivolvis* was collected from the littoral zone of the lake, and the foot of each animal saved for isotope analysis (n = 6, 6). Fishes were captured using hoop nets and minnow traps placed around the perimeter of the lake. The gut tissue of each fish was excised, and the rest of the body used for isotope analysis. Fish species included *Pimephales promelas* (fathead minnow; n = 12, 14), *Phoxinus* spp. (dace; n = 12, 12), *Umbra limi* (central mud minnow; n = 9, 12), and young of the year *Ameiurus melas* (black bullhead; n = 7, 5). After sampling, all solid samples were dried at 60 ºC, ground to a fine powder, and sent to the Colorado Plateau Stable Isotope Laboratory (CPSIL) for isotope analysis (Doucett *et al.* 2007). At CPSIL, a benchtop equilibration procedure was used to correct for the exchange of H atoms between a set of standards including ground algal material and ambient water vapor. Solid samples were pyrolysed to H_2 gas and analyzed using a Thermo-Finnigan TC/E and Delta^{PLUS}-XL (Thermo Electron Corporation, Bremen, Germany). Theδ^2H of water samples was analyzed

using cavity ring-down laser spectroscopy using Los Gatos Research Off-Axis Integrated Cavity Output coupled to a CTC LC-PAL liquid autosampler.

Model Selection

We explored models that differed in the sources for which their contribution to consumer biomass (Φ) was to be estimated. Possible sources in the model were terrestrial, phytoplankton, submersed macrophytes, floating macrophytes, all macrophytes, and periphyton. We restricted our sensitivity analysis to models that 1) had at least two but not more than four sources ($2 \leq S \leq 4$); 2) contained the terrestrial end member (S_1 was always terrestrial); 3) did not contain redundant sources (e.g., could not contain both floating-leafed macrophytes and all macrophytes as separate sources). In total, eighteen models were evaluated for each consumer in each year (252 distinct model runs).

We used known consumer feeding habits and deviance information criterion (DIC) (Spiegelhalter *et al.* 2002) to choose which end members were included as sources in the mixing models. We only considered models that contained the terrestrial source and at least one other source. For the pelagic invertebrates, the two sources were terrestrial and phytoplankton organic matter. For the snail, DIC was used to select between models that did not contain phytoplankton, and periphyton and floating-leafed macrophytes were selected in addition to terrestrial. Models for the fishes were guided by DIC and contained three or four sources, with model selection always including terrestrial and phytoplankton, and never including submersed macrophytes.

Our estimates of resource use were robust to model selection (Fig. S1). However, comparing across models requires care when the exclusion of a certain group of resources can cause another source to become the only source that bounds consumers in one or more dimensions of isotope space. In this case, the contribution (Φ) of the remaining source would be

higher than in models containing other groups that could bound consumer isotope values. For example, phytoplankton and periphyton were the two sources with the lowest values of δ^2H (Fig 3). The isotope values of several invertebrates (Fig. 3C) and fishes (Fig. 3E) could not easily be explained by a model that contained neither phytoplankton nor periphyton, because these algal end members were the only sources that had lower δ^2H values. In other words, at least one of the algal sources was necessary for bounding consumers in the δ^2H dimension of isotope space. As a result, if a consumer with a low δ^2H value truly relied on phytoplankton, a model that did not contain phytoplankton might erroneously estimate a large contribution by periphyton, even if a model containing both end members estimates low periphyton contribution. For example, the final model for *U. limi* did not contain periphyton, but the average contribution of periphyton to *U. limi* across all models containing periphyton was 30% in 2010 and 34% in 2012. However, averaged across all models containing periphyton *and* phytoplankton, periphyton support of *U. limi* was 8% in 2010 and 7% in 2012. Similarly, for *P. promelas* and *Phoxinus* spp., periphyton support in the selected model was lower than that averaged across all models (Figure S1, median relative to circles); however, the average support by periphyton in models containing both algal end members was nearly identical to that in the selected model (Fig. S1, median relative to squares).

Size of POC and DOC pools

The sizes of the particulate and dissolved organic carbon (POC and DOC) pools were similar between years in Ward Lake and in Paul Lake. In Paul Lake, POC was 0.42 ± 0.16 mg L^{-1} in 2010 and 0.45 ± 0.17 mg L^{-1} in 2012 (annual mean ± standard deviation), and in Ward Lake POC was 0.85 ± 0.17 mg L^{-1} in 2010 and 1.0 ± 0.31 mg L^{-1} in 2012. DOC concentrations followed the same pattern, with Paul Lake (4.8 ± 0.81 mg L^{-1} in 2010, 4.5 ± 0.32 mg L^{-1} in 2012)

and Ward Lake (9.6 ± 2.7 mg L^{-1} in 2010, 10.6 ± 1.3 mg L^{-1} in 2012) both having similar DOC concentrations between years.

Biomasses of Copepod Zooplankton

Copepods are the dominant group of zooplankton in Ward Lake. We analyzed one species of calanoid copepod, *S. oregonensis*. The zooplankton biomass in Ward Lake decreased between years, while zooplankton biomass in Paul Lake remained similar (Main Text). However, the change in the seasonal average of zooplankton biomass in Ward Lake (from 0.88 g/m^2 in 2010 to 0.52 g/m^2) was not attributable to a decline in *S. oregonensis* adults (Fig. S2, Calanoid), but rather to a 0.20 g/m^2 decrease in copepod larvae (Fig. S5, Nauplii) and a 0.15 g/m^2 decrease in the copepod *Mesocyclops* (Fig. S2).

Aquashade and DOM Isotope Values

Our goal in analyzing the composition of DOM was to estimate the relative contributions of macrophytes, phytoplankton, periphyton, and terrestrial end members to this pool. However, our experimental manipulation introduced Aquashade to the DOM pool. Therefore, the composition of DOM was estimated after algebraically correcting for the influence of Aquashade on the isotope values of DOM by using measured concentrations, isotope values, and the C:N:H stoichiometry of the dye and of DOM. We estimated the concentration of Aquashade in Ward Lake and corrected for its influence on the isotope value of DOM. Aquashade concentration was estimated using spectrophotometry. Each week we measured the absorbance of lake water between 300 nm and 900 nm, using wavelengths near Aquashade's peak absorbance at 625 nm to estimate dye concentration. Absorbances at longer wavelengths (700 nm to 900 nm, far from the peak of Aquashade absorbance) were used to correct the rest of the spectrum for shifts in absorbance that were not caused by a change in Aquashade concentration. We then estimated the

volume fraction (ppm) of Aquashade in water by comparing the corrected spectrum to that of a known concentration of Aquashade. To convert the volume fraction of Aquashade to a concentration (mg L^{-1}), we used a density of 1 g mL^{-1}, which is within the range reported in the Material Safety Data Sheet for Aquashade.

We used the elemental stoichiometries of DOM and Aquashade to estimate the concentration of DOM from the concentration of DOC, and to estimate the proportion of Aquashade that contributed to the mass of C, N, and H in DOM. The DOM stoichiometry was empirically derived as part of the same mass spectrometry analysis that yielded isotope values, which reported DOM (in 2012) as 10% C, 0.4% N, and 2.3% H by mass. The Aquashade product contains ingredients other than the dyes (combined dye formula is $C_{53}H_{51}N_8Na_3O_{18}S_5$, 46.46% C, 8.5% N, 3.9% H by mass; the ratio of dyes is 9.9:1, giving the dye portion of Aquashade a composition of 54.20% C, 4.17% N and 4.09% H by mass), therefore we used the empirical stoichiometry, which was similar to that of the dyes (49.31% C, 4.39% N, 4.2% H). In 2012 the DOC concentration averaged 10.6 mg L^{-1}, making the DOM concentration 106 mg L^{-1}. The concentration of Aquashade was typically near 1.5 mg L^{-1}, or 1.4% of the DOM pool. Therefore, Aquashade comprised 6.9%, 15.5%, and 2.6% of the C, N, and H of the DOM pool.

The $\delta^{13}C$, $\delta^{15}N$, and $\delta^{2}H$ of Aquashade were -26.82‰, -0.02‰, and -65.4‰, respectively. The $\delta^{13}C$, and $\delta^{15}N$ values are similar to those of other end members and consumers in the study. The $\delta^{2}H$ of Aquashade is similar to that of water, which is highly enriched relative to the other pools we analyzed. As a pre-manipulation reference, the isotope values of DOM in 2010 were $\delta^{13}C$ = -28.2‰, $\delta^{15}N$ = -3.7‰, and $\delta^{2}H$ = -116.1‰. In 2012, DOM $\delta^{13}C$ = -19.5‰, $\delta^{15}N$ = 0.1‰, and $\delta^{2}H$ = -156.9‰. After correcting for the contribution of Aquashade to DOM, the DOM isotope values become DOM $\delta^{13}C$ = -18.9‰, $\delta^{15}N$ = 0.1‰, and $\delta^{2}H$ = -159.3‰. The isotope

values of DOM changed substantially between years, and this large change was not driven by the influence of Aquashade isotope values. To summarize, Aquashade was a minor portion of the DOM pool and had a minimal impact on our analysis of DOM composition, even if a correction had not been performed.

Literature Cited in the Appendix to Chapter 3

Batt, R. D., and S. R. Carpenter. 2012. Free-water lake metabolism: Addressing noisy time series with a Kalman filter. Limnology and Oceanography: Methods 10:20–30.

Carpenter, S. R., J. J. Cole, J. R. Hodgson, J. F. Kitchell, M. L. Pace, D. L. Bade, K. L. Cottingham, T. E. Essington, J. N. Houser, and D. E. Schindler. 2001. Trophic cascades, nutrients, and lake productivity: Whole-lake experiments. Ecological Monographs 71:163–186.

Carpenter, S. R., and J. F. Kitchell (Eds.). 1993. The trophic cascade in lakes. Carmbridge University Press, Cambridge, UK.

Cole, J. J., N. F. Caraco, G. W. Kling, and T. K. Kratz. 1994. Carbon dioxide supersaturation in the surface waters of lakes. Science 265:1568–70.

Cole, J. J., S. R. Carpenter, J. Kitchell, M. L. Pace, C. T. Solomon, and B. Weidel. 2011. Strong evidence for terrestrial support of zooplankton in small lakes based on stable isotopes of carbon, nitrogen, and hydrogen. Proceedings of the National Academy of Sciences of the United States of America 108:1975–1980.

Doucett, R. R., J. C. Marks, D. W. Blinn, M. Caron, and B. A. Hungate. 2007. Measuring terrestrial subsidies to aquatic food webs using stable isotopes of hydrogen. Ecology 88:1587–1592.

Downing, J. A., and F. H. Rigler (Eds.). 1984. A Manual on Methods for the Assessment of Secondary Productivity in Fresh Waters. Page 675 The Journal of Animal Ecology. Second edition. Blackwell Scientific Publications, Oxford, England.

Harvey, A. C. 1989. Forecasting, Structural Time Series Models and the Kalman Filter. Cambridge University Press, Cambridge.

Kalman, R. E. 1960. A New Approach to Linear Filtering and Prediction Problems. Journal of Basic Engineering 82:35–45.

Read, J. S., D. P. Hamilton, A. R. Desai, K. C. Rose, S. MacIntyre, J. D. Lenters, R. L. Smyth, P. C. Hanson, J. J. Cole, P. a. Staehr, J. a. Rusak, D. C. Pierson, J. D. Brookes, A. Laas, and C. H. Wu. 2012. Lake-size dependency of wind shear and convection as controls on gas exchange. Geophysical Research Letters 39.

Read, J. S., D. P. Hamilton, I. D. Jones, K. Muraoka, L. a. Winslow, R. Kroiss, C. H. Wu, and E. Gaiser. 2011. Derivation of lake mixing and stratification indices from high-resolution lake buoy data. Environmental Modelling & Software 26:1325–1336.

Solomon, C. T., S. R. Carpenter, M. K. Clayton, J. J. Cole, J. J. Coloso, M. L. Pace, M. J. Vander Zanden, and B. C. Weidel. 2011. Terrestrial, benthic, and pelagic resource use in lakes: results from a three-isotope Bayesian mixing model. Ecology 92:1115–1125.

Spiegelhalter, D. J., N. G. Best, B. P. Carlin, and A. van der Linde. 2002. Bayesian measures of model complexity and fit. Journal of the Royal Statistical Society: Series B (Statistical Methodology) 64:583–639.

Stainton, M. P. 1973. A syringe gas-stripping procedure for gas-chromatographic determination of dissolved inorganic and organic carbon in fresh water and carbonates in sediments. Journal of the Fisheries Board of Canada 30:1441–1445.

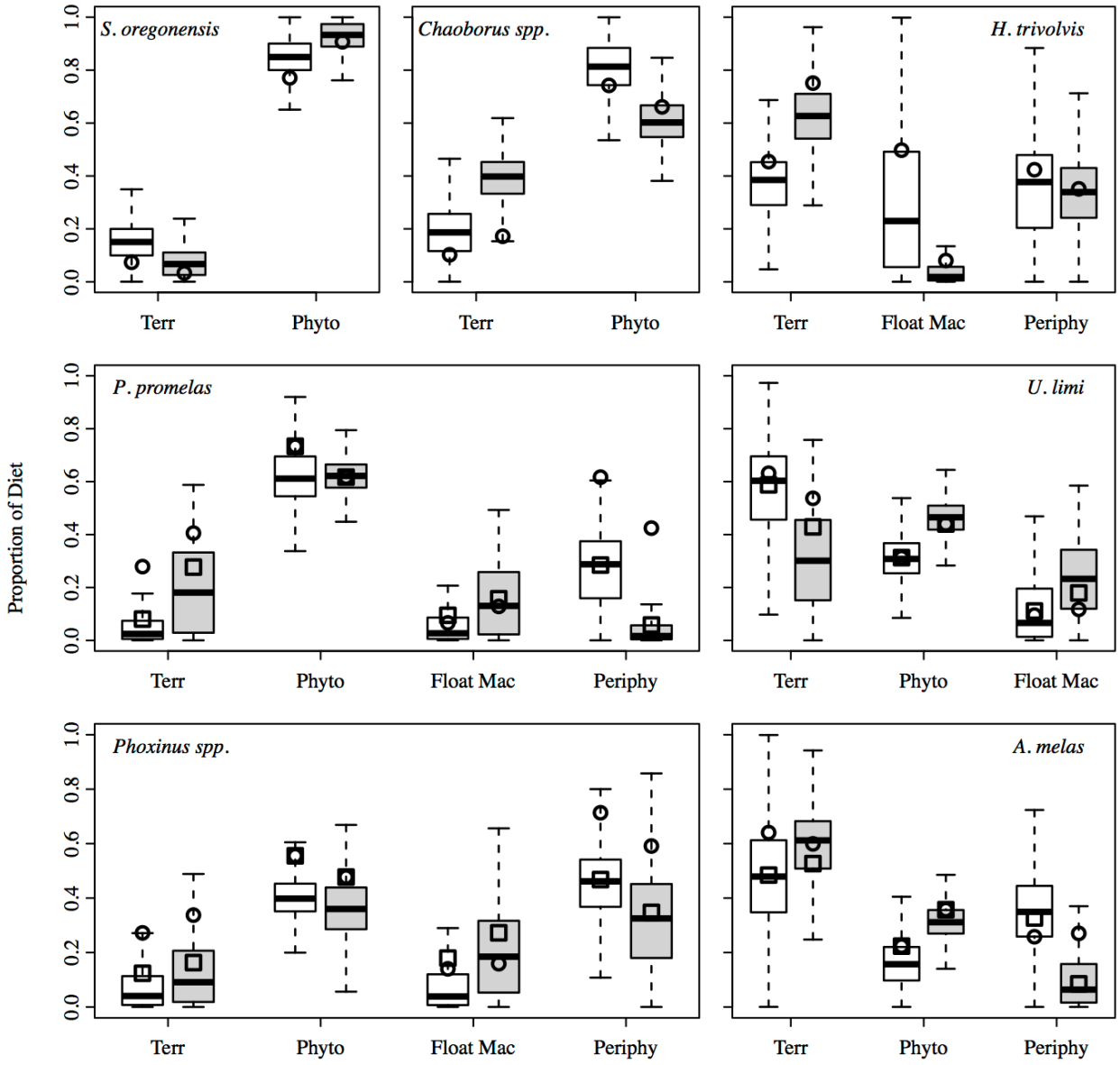

Figure S1. Boxplots of the proportional contributions of resources to consumers (posterior of Φ) supported by each resource in Ward Lake in 2010 (open) and 2012 (shaded). Boxes bound 25-75 percentiles. Each whisker extends beyond its respective quartile by a factor of 1.5*(interquartile range), and the dark line designates the median. All data were included in statistical calculations, but outliers are not displayed. The boxes, whiskers, and medians reflect the posterior for the final model. Circles show the average estimate for that resource in any of the 18 models from the sensitivity analysis (which included different combinations of resources) containing that resource.

Squares are the average estimate for that resource in any of the 18 models containing that resource *and* the phytoplankton resource.

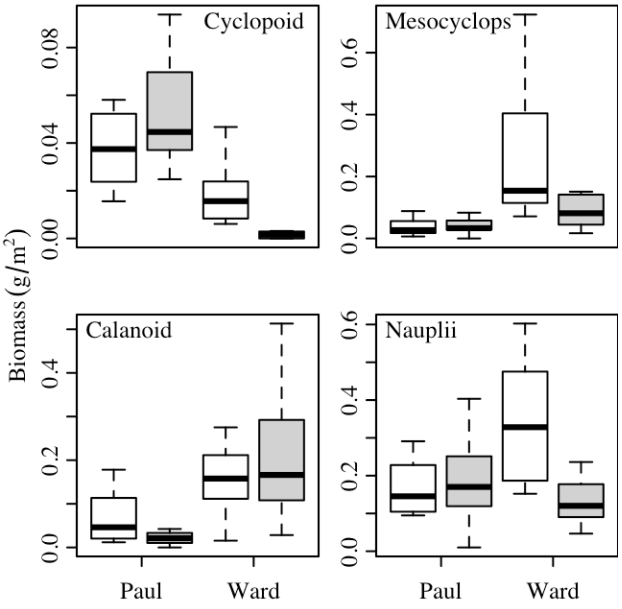

Figure S2. Biomasses of copepod zooplankton in Ward and Paul lakes in 2010 and 2012. Boxplot conventions as in Figure S1.

Chapter 4: Changes in ecosystem resilience detected in automated measures of ecosystem metabolism during a whole-lake manipulation*

Abstract

Environmental sensor networks are developing rapidly to assess changes in ecosystems and their services. Some ecosystem changes involve thresholds, and theory suggests that statistical indicators of changing resilience can be detected near thresholds. We examined the capacity of environmental sensors to assess resilience during an experimentally-induced transition in a whole-lake manipulation. A trophic cascade was induced in a planktivore-dominated lake by slowly adding piscivorous bass, while a nearby bass-dominated lake remained unmanipulated and served as a reference ecosystem during the four-year experiment. In both the manipulated and reference lakes, automated sensors were used to measure variables related to ecosystem metabolism (dissolved oxygen (DO), pH, and chlorophyll *a* concentration (Chl-*a*)) and to estimate gross primary production (GPP), respiration (R), and net ecosystem production (NEP). Thresholds were detected in some automated measurements more than a year before the completion of the transition to piscivore dominance. Directly measured variables (DO, pH, Chl-*a*) related to ecosystem metabolism were better indicators of the approaching threshold than were the estimates of rates (GPP, R, and NEP); this difference was likely a result of the larger uncertainties in the derived rate estimates. Thus, relatively simple characteristics of ecosystems that were observed directly by the sensors were superior indicators of changing resilience.

---

* Published as: Batt, R.D., S.R. Carpenter, J.J. Cole, M.L. Pace, R.A. Johnson. 2013. Changes in ecosystem resilience detected in automated measures of ecosystem metabolism during a whole-lake manipulation. *Proceedings of the National Academy of Sciences of the United States of America* **110**: 17398-17403, doi: 10.1073/pnas.1316721110

Models linked to thresholds in variables that are directly observed by sensor networks may provide unique opportunities for evaluating resilience in complex ecosystems.

Significance Statement

Large changes can occur when ecosystems cross certain thresholds. Crossing such thresholds poses a challenge to ecosystem management because the positions of the threshold are uncertain and change over time. However, as an ecosystem approaches a threshold its resilience declines, resulting in changes in system dynamics that increase variance and autocorrelation. Calculating these statistics requires frequent and sustained sampling efforts. Our study detected an approaching threshold by computing the statistical indicators from data collected by automated sensors, which are far less labor-intensive than comparable manual methods. Thus it may be feasible to monitor for approaching ecosystem thresholds using automated methods. This finding highlights a powerful use of modern sensor technology.

Introduction

In the 20th century, changes in land use, nutrient mobilization and species invasion altered Earth's ecosystems more than in any previous century of human history (1). Changing climate and expanding human population and consumption are likely to exacerbate ecosystem change in the future. Ecosystem changes have significant effects on human well-being through benefits that people receive from nature. To assess and anticipate environmental changes, observation networks are expanding for hydrology, biogeochemistry of air and water, land cover, and other relevant features of ecosystems (2–5). The observed variables are often designed to address trends in particular resources or pollutants such as water flow, contaminant concentrations, ecosystem metabolism, carbon storage or living resources. While some applications of environmental observations are straightforward, rapid expansion of sensor networks, information management and analysis (6–8) may create new opportunities for detecting, anticipating or forecasting fundamental changes such as ecosystem regime shifts.

Ecosystem thresholds are associated with large changes that can involve a significant loss of resources, or in other cases, trigger the restoration of desired conditions (9). Thresholds are uncertain, change over time, are not preceded by obvious changes in state, and are therefore difficult to anticipate. However, an ecosystem near a threshold has low resilience, and therefore is relatively sensitive to small perturbations and recovers slowly from these perturbations (10). Therefore, statistics related to variance or autocorrelation could be indicators of declining resilience or approaching thresholds (10, 11). Experimental tests of declining resilience in living systems are rare (12–17), especially in large-scale field settings. In terrestrial ecosystems such as forests and grasslands, changing resilience has been measured by analyzing the spatial patterns of vegetation maps obtained by satellite remote sensing (18, 19). In other cases, resilience has

been assessed using time series data (17, 20), though acquisition of appropriate data is challenging. Resilience indicators for time series such as variance, spectral power, and autocorrelation require high-frequency and long-term data sets. The intensity of sampling needed to acquire such data sets can be costly, and this cost is amplified if multiple variates must be monitored. Modern sensor technology permits automated, in situ, high frequency, long duration, and real time data collection that is less labor-intensive than comparable manual methods (6). Although automated sensors are promising for meeting intensive data requirements, it is not known whether variables measured by such sensors are suitable for assessing resilience or thresholds in complex ecosystems under field conditions.

Sensor data are often used to estimate metabolic rates (e.g., primary production) at the ecosystem scale (21–23). Primary production and respiration are fundamental ecosystem variables, closely related to carbon balance, and have been the focus of extensive research in diverse ecosystems for many decades. Furthermore, metabolism is closely tied to primary producer biomass and life form, which have been used to detect changing resilience in both terrestrial (18, 19, 24) and aquatic systems (13, 17, 25). So far, however, it is unknown whether metabolism can be used to detect changes in ecosystem resilience.

The objective of this study was to determine if automated measures of ecosystem metabolism could be used to detect declining resilience in a lake approaching a regime shift. We deployed automated sensors in Peter and Paul lakes from 2008 to 2011. Peter Lake experienced a regime shift due to an experimentally-induced trophic cascade, and Paul Lake was an unmanipulated reference lake. At the start of the experiment the lakes were in different stable states—the food web of the manipulated lake was dominated by planktivorous fishes and contained few largemouth bass (*Micropterus salmoides*), and the reference lake was dominated

by bass and contained few planktivorous fishes (Fig. 1). In one stable state, which we refer to as the "planktivore-dominated state", the number of adults in a bass population is small and unable to recruit because their young are consumed or out-competed by other fishes. In the alternative stable state, which we call the "bass-dominated state", a large population of adult bass limits the planktivore population. These two sets of feedbacks form the mechanistic basis for the alternative attractors (26–28). We added bass to the manipulated lake to induce a trophic cascade, pushing the manipulated lake toward the bass-dominated state that characterized the reference lake throughout the experiment. This critical transition shifts the ecosystem from a planktivore-dominated state to a bass-dominated state when bass abundance passes a critical threshold (27). Resilience declines as the ecosystem approaches this critical threshold. The aim was to approach the unknown critical bass abundance slowly so that the ecosystem would be in transition long enough to assess indicators of changing resilience. Bass were added to the manipulated lake in several small stocking events over the course of four years: 12 bass were added on day 189 of 2008, 15 on days 169 and 202 of 2009, none in 2010, and 32 on day 174 of 2011.

Leading indicators, such as variance or autocorrelation, are statistics computed from time series of ecosystem variables that are affected by an approaching threshold. Trophic cascades affect gross primary production (GPP) and algal biomass, which in turn influence other metabolic rates (respiration (R), net ecosystem production (NEP)) and other variables associated with metabolism (e.g., pH and dissolved oxygen saturation (DO)). Automated measurements of these six variables (derived estimates = GPP, R, and NEP; direct measurements = chlorophyll-*a* concentration (Chl-*a*), pH, and DO) can be made more frequently and easily than their manually-measured counterparts. Previous analyses of this experiment found that the variance and autocorrelation of manually-collected time series, including algal biomass, increased prior to day

230 of 2010, which was when the food webs of the two lakes became similar (17, 29, 30). Here we address whether or not automated measurements of three directly measured variables and three derived estimates of metabolism could be used to detect the loss of resilience in the manipulated ecosystem. We expected that the warning statistics computed from the time series of these six quantities would signal the approaching threshold before the manipulated lake became bass-dominated, but that there would be no such signal in the reference lake (Fig. 1).

Results & Discussion

Surprisingly, the calculated rates of metabolism (GPP, R, and NEP) did not provide consistent signals of the approaching threshold (Fig 2, Fig. S1). We used the quickest detection method to define the day of first alarm (DoFA)—the day when a statistical indicator, standard deviation (SD) or autocorrelation time (AcT), first became high enough to signal a nearby threshold (*Materials and Methods*). No alarms of the approaching threshold were detected in GPP. Alarms were detected in the AcT of R and NEP (DoFA in 2008 and 2009, respectively), but neither of these signals was corroborated by a change in SD.

In contrast to the calculated rates of metabolism, automated measurements of the three directly measured variables (Chl-*a*, pH, DO) detected the approaching threshold more than a year in advance of its arrival (Fig. 3, Fig. S1). These three directly measured variables performed similarly—most of the DoFAs were in 2009 (the DoFA in the AcT of pH was in 2008, the DoFA in the SD of DO was in 2010). The DoFA for the SD of Chl-*a*, pH, and DO coincided with increases in low-frequency variability in the manipulated lake relative to the reference lake (Fig. 4). The DoFAs in the directly measured variables were as early as the DoFAs in manual samples of chlorophyll (Fig. S1), which we analyzed as a benchmark because its SD and autocorrelation

are known to be indicators of this trophic cascade (17, 29, 30). Additionally, the directly measured variables were better correlated with manual daily chlorophyll concentrations than the calculated rates of metabolism, which had relatively noisy time series (Fig. S2,3).

In summary, not all variables perform equally well when monitoring for changes in resilience. We detected consistent signals of declining resilience in directly measured variables that were associated with metabolism; we did not see consistent signals in the derived estimates of metabolism. Some regime shifts may involve mechanisms that obscure signals of declining resilience in aggregated system variables like NEP (31), but measurement error or other sources of noise could have a similar effect. In lakes, estimates of GPP, R, and NEP often exhibit high day-to-day variability (32, 33) and are often poorly correlated with potential driver variables (34, 35). Sensor measurements are subject to measurement errors related to spatial heterogeneity and other processes (32, 36, 37). These measurement difficulties affect metabolism estimates (GPP, R, NEP) because these rates are calculated by fitting models to sensor data, and therefore incorporate uncertainty from both measurement and model errors (21, 36). The directly measured variables are subject only to measurement error. Therefore, additional noise in the model-derived estimates of metabolism may have obscured the signals of declining resilience that were detectable in the directly measured variables.

Our findings suggest that monitoring for changes in the resilience of complex systems such as lakes requires a careful choice of variables, based on theory as well as field trials. Depending on the particular ecosystem under study, certain variables might be expected to signal several kinds of critical transitions. For example, aquatic ecosystem regime shifts that are driven by nutrient loading, organic matter loading, and changes in top predator abundance all affect metabolism (16, 38–40). Therefore, variables related to metabolism might be useful to monitor.

However, even variables with similar drivers can perform differently when used to compute resilience indicators. We found that direct measurements of variables related to metabolism were more accurate than estimates of metabolism for signaling changes in resilience.

Emerging sensor technology and networks are improving capabilities for environmental monitoring (6, 8). These technologies hold considerable promise for data-intensive and spatially extensive studies of ecosystem processes, such as metabolism, ecosystem stability, resilience, and threshold detection. Organizations such as the Global Lake Ecological Observatory Network (4), the National Ecological Observatory Network (2), and the Ocean Observatory Initiative (5) reflect the well-established and growing interest in using automated sensors that are similar to those used in this study. Our results suggest that considerable research is needed to determine the monitoring strategies and variables that are most useful for measuring and comparing resilience in a wide range of ecosystems.

The susceptibility of an ecosystem to changing drivers or random events depends on the characteristics of critical thresholds (41). Crossings of some thresholds are unwanted, such as loss of a coral reef or rangeland, while others are deliberately sought, as in restoration of productive vegetation on degraded lands (42, 43). Moreover, fundamental progress in ecology requires better understanding of thresholds and the tempo of change in ecosystems. Thus we expect that field studies of resilience and thresholds will continue to be important in ecology as well as in environmental sciences in general. Emerging technology for observing time series data and for detecting warnings of change will make growing contributions to this field.

Materials & Methods

Fish Communities. At the beginning of the experiment, Peter Lake had a small population of the piscivorous largemouth bass (*Micropterus salmoides*), and the fish community was

dominated by small fishes such as the pumpkinseed sunfish (*Lepomis gibbosus*), golden shiner (*Notemigonus crysoleucas*), central mud minnow (*Umbra limi*), fathead minnow (*Pimephales promelas*), brook stickleback (*Culaea inconstans*), and dace (*Phoxinus* spp.). To strengthen the planktivore-dominance of Peter Lake, we added 1200 golden shiners to Peter Lake on day 149 of 2008. Conversely, Paul Lake was in a bass-dominated state throughout the experiment, with only a small number of *L. gibbosus* present. No manipulations were made in Paul Lake.

Automated Sensor Data. Peter and Paul lakes were each monitored with two YSI multiparameter sondes (model 6600 V2-4) fitted with optical dissolved oxygen (DO) (model 6150), pH (6561), optical chlorophyll-*a* (Chl-*a*; 6025), and conductivity-temperature (6560) probes. Sensor measurements were made at 0.7 m every 5 min and were calibrated weekly. Wind speed and mixed layer depth (z_{mix}; shallowest depth below which temperature changes by at least 1 ºC m^{-1}) data supplemented other sensor data as input to calculate ecosystem metabolism.

Statistical Indicators. Three statistical indicators were computed for each of the variables using programs written by the authors in the R programming language (44). Increasing standard deviation (45), increasing autocorrelation time (15, 20), and increasing spectral ratio (variance spectrum of the manipulated lake relative to that in the reference lake) at low relative to high frequencies (46) are signals of an approaching threshold. Standard deviation and autocorrelation time, $-\log_e(\text{autocorrelation})^{-1}$ (15), were computed for manual samples of Chl-*a* (μg L^{-1}), daily averages of the three directly measured variables collected by automated sensors (pH, DO (percent saturation), and Chl-*a* (μg L^{-1})), and the three calculated metabolism rates (GPP, R, and NEP; mmol O_2 m^3 d^{-1}) (*Supplemental Information*). Spectral ratio was computed only for the three direct measures of metabolism that were collected by automated sensors. Indicators were computed in 28-day rolling windows. We expected to detect signals of low resilience in the

manipulated lake in the form of the three indicators increasing prior to the regime shift in late 2010. We expected no signals in the reference lake.

Quickest Detection. To determine when the change in an indicator first became large enough to constitute a signal of low resilience, we employed the "quickest detection" (QD) method for detecting state changes (47–49). In our application, the QD method uses two probability distributions for an indicator: a baseline state where the indicator has low values (far from tipping point), and a critical state where the indicator has a high value (close to tipping point). Indicator x in lake i on day t ($x_{i,t}$) follows probability density $f(x_{i,t})$ for the baseline state and $g(x_{i,t})$ for the critical state. The likelihood for the indicator being in either state is updated each time the systems are observed, and the ratio of these likelihoods is $g(x_{i,t})/f(x_{i,t}) = \Lambda_t$. The detection statistic for the QD method is R_t, and R_t is updated as new Λ_t arrive: $R_t = (1 + R_{t-1}) \times \Lambda_t$. When the indicator is more likely to be in the critical state than the baseline state, Λ_t is greater than one, which increases the rate at which R_t rises. The day of first alarm (DoFA) is when R_t first reaches a predefined threshold, A. We used the same formulation for calculating the parameters of $f(x_{i,t})$ and $g(x_{i,t})$ for all variables and indicators, and over broad ranges the DoFA was not sensitive to the value of these parameters or to our choice of A (*Supplemental Information*). The QD method is particularly useful for detecting approaching thresholds because observations after the shift to the new state are not needed to signal the alarm.

Acknowledgements

We thank Tim Cline, James Coloso, Jason Kurtzweil, David Seekell, Laura Smith, Grace Wilkinson, and the University of Notre Dame Environmental Research Center staff for their assistance, and the referees for their helpful comments. This work was supported by the National Science Foundation (DEB 0716869, DEB 0917696).

Literature Cited in Chapter 4

1. Millenium Ecosystem Assessement (2005) *Ecosystems and human well-being: Current states and trends* (Island Press, Washington, D.C., USA).
2. Kampe TU, Johnson BR, Kuester M, Keller M (2010) NEON: The first continental-scale ecological observatory with airborne remote sensing of vegetation canopy biochemistry and structure. *J Appl Remote Sens* 4(043510):1–24.
3. Porter JH et al. (2009) New eyes on the world: Advanced sensors for ecology. *Bioscience* 59(5):385–397.
4. Hanson PC (2007) A grassroots approach to sensor and science networks. *Front Ecol Environ* 5(7):343–343.
5. Cowles T, Delaney J, Ocrutt J, Weller R (2010) The ocean observatories initiative: Sustained ocean observing across a range of spatial scales. *Mar Technol Soc J* 44(6):54–64.
6. Porter J et al. (2005) Wireless sensor networks for ecology. *Bioscience* 55(7):561–572.
7. Hampton SE et al. (2013) Big data and the future of ecology. *Front Ecol Environ* 11(3):156–162.
8. Collins SL et al. (2006) New opportunities in ecological sensing using wireless sensor networks. *Front Ecol Environ* 4(8):402–407.
9. Groffman PM et al. (2006) Ecological thresholds: The key to successful environmental management or an important concept with no practical application? *Ecosystems* 9(1):1–13.
10. Scheffer M et al. (2009) Early-warning signals for critical transitions. *Nature* 461(7260):53–9.
11. Scheffer M et al. (2012) Anticipating critical transitions. *Science* 338(6105):344–348.

12. Drake JM, Griffen BD (2010) Early warning signals of extinction in deteriorating environments. *Nature* 467(7314):456–459.

13. Veraart AJ et al. (2012) Recovery rates reflect distance to a tipping point in a living system. *Nature* 481(7381):357–9.

14. Dai L, Korolev KS, Gore J (2013) Slower recovery in space before collapse of connected populations. *Nature* 496(7445):355–8.

15. Dai L, Vorselen D, Korolev KS, Gore J (2012) Generic indicators for loss of resilience before a tipping point leading to population collapse. *Science* 336(6085):1175–1177.

16. Sirota J, Baiser B, Gotelli NJ, Ellison AM (2013) Organic-matter loading determines regime shifts and alternative states in an aquatic ecosystem. *Proc Natl Acad Sci USA* 110(19):7742–7.

17. Carpenter SR et al. (2011) Early warnings of regime shifts: A whole-ecosystem experiment. *Science* 332(6033):1079–1082.

18. Hirota M, Holmgren M, Van Nes EH, Scheffer M (2011) Global resilience of tropical forest and savanna to critical transitions. *Science* 334(6053):232–235.

19. Staver AC, Archibald S, Levin SA (2011) The global extent and determinants of savanna and forest as alternative biome states. *Science* 334(6053):230–2.

20. Dakos V et al. (2008) Slowing down as an early warning signal for abrupt climate change. *Proc Natl Acad Sci USA* 105(38):14308–14312.

21. Stæhr PA et al. (2010) Lake metabolism and the diel oxygen technique: State of the science. *Limnol Oceanogr Methods* 8:628–644.

22. Canadell JG et al. (2000) Commentary: Carbon Metabolism of the Terrestrial Biosphere: A Multitechnique Approach for Improved Understanding. *Ecosystems* 3(2):115–130.

23. Rundel PW, Graham EA, Allen MF, Fisher JC, Harmon TC (2009) Environmental sensor networks in ecological research. *New Phytol* 182(3):589–607.

24. Kéfi S et al. (2007) Spatial vegetation patterns and imminent desertification in Mediterranean arid ecosystems. *Nature* 449(7159):213–7.

25. Wang R et al. (2012) Flickering gives early warning signals of a critical transition to a eutrophic lake state. *Nature* 492(7429):419–22.

26. Walters CJ, Kitchell JF (2001) Cultivation/depensation effects on juvenile survival and recruitment: implications for the theory of fishing. *Can J Fish Aquat Sci* 58(1):39–50.

27. Carpenter SR, Brock W a, Cole JJ, Kitchell JF, Pace ML (2008) Leading indicators of trophic cascades. *Ecol Lett* 11(2):128–38.

28. Seekell DA, Cline TJ, Carpenter SR, Pace ML (2013) Evidence of alternate attractors from a whole-ecosystem regime shift experiment. *Theor Ecol* 6(3):385–394.

29. Seekell DA, Carpenter SR, Cline TJ, Pace ML (2012) Conditional Heteroskedasticity Forecasts Regime Shift in a Whole-Ecosystem Experiment. *Ecosystems* 15(5):741–747.

30. Pace ML, Carpenter SR, Johnson RA, Kurtzweil JT (2013) Zooplankton provide early warnings of a regime shift in a whole lake manipulation. *Limnol Oceanogr* 58(2):525–532.

31. Boulton CA, Good P, Lenton TM (2013) Early warning signals of simulated Amazon rainforest dieback. *Theor Ecol* 6(3):373–384.

32. Van de Bogert MC et al. (2012) Spatial heterogeneity strongly affects estimates of ecosystem metabolism in two north temperate lakes. *Limnol Oceanogr* 57(6):1689–1700.

33. Solomon CT et al. (2013) Ecosystem respiration: Drivers of daily variability and background respiration in lakes around the globe. *Limnol Oceanogr* 58(3):849–866.

34. Stæhr PA, Sand-Jensen K (2007) Temporal dynamics and regulation of lake metabolism. *Limnol Oceanogr* 52(1):108–120.

35. Coloso JJ, Cole JJ, Pace ML (2011) Difficulty in discerning drivers of lake ecosystem metabolism with high-frequency data. *Ecosystems* 14(6):935–948.

36. Batt RD, Carpenter SR (2012) Free-water lake metabolism: Addressing noisy time series with a Kalman filter. *Limnol Oceanogr Methods* 10:20–30.

37. Coloso JJ, Cole JJ, Hanson PC, Pace ML (2008) Depth-integrated, continuous estimates of metabolism in a clear-water lake. *Can J Fish Aquat Sci* 65(4):712–722.

38. Scheffer M, Hosper SH, Meijer M-L, Moss B, Jepessen E (1993) Alternative equilibria in shallow lakes. *Trends Ecol Evol* 8(8):276–279.

39. Genkai-Kato M, Vadeboncoeur Y, Liboriussen L, Jeppesen E (2012) Benthic – planktonic coupling, regime shifts, and whole-lake primary production in shallow lakes. *Ecology* 93(3):619–631.

40. Carpenter SR et al. (2001) Trophic cascades, nutrients, and lake productivity: Whole-lake experiments. *Ecol Monogr* 71(2):163–186.

41. Scheffer M (2009) *Critical Transitions in Nature and Society* (Princeton University Press, Princeton, NJ).

42. Walker B, Salt D (2013) *Resilience Practice* (Island Press, Washington, D.C., USA).

43. Hobbs RJ, Suding KN (2009) *New Models for Ecosystem Dynamics and Restoration* (Island Press, Washington, D.C., USA).

44. R Development Core Team (2012) *R: A Language and Environment for Statistical Computing* (R Foundation for Statistical Computing, Vienna, Austria).

45. Carpenter SR, Brock WA (2006) Rising variance: a leading indicator of ecological transition. *Ecol Lett* 9(3):311–8.

46. Kleinen T, Held H, Petschel-Held G (2003) The potential role of spectral properties in detecting thresholds in the Earth system: application to the thermohaline circulation. *Ocean Dyn* 53(2):53–63.

47. Shiryaev AN (2010) Quickest Detection Problems: Fifty Years Later. *Seq Anal* 29(4):345–385.

48. Polunchenko AS, Tartakovsky AG (2011) State-of-the-art in sequential change-point detection. *Methodol Comput Appl Probab* 14(3):649–684.

49. Carpenter SR, Brock WA, Cole JJ, Pace ML (2013) A new approach for rapid detection of nearby thresholds in ecosystem time series. *Oikos*.

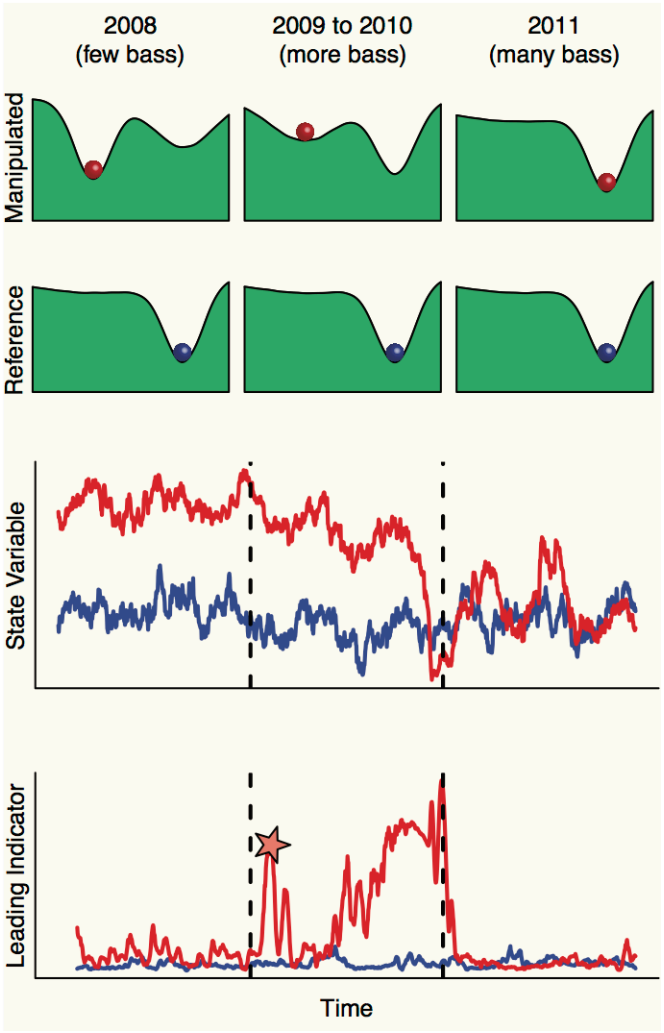

Fig. 1. Conceptual diagram outlining the experimental design and hypotheses. The first two rows are ball and cup diagrams, where the balls represent the state of the system, and the steepness of the cups is related to the stability of the system—a ball nestled in a deep cup is stable. In 2008, the manipulated lake (red) is stably situated in a basin characterized by few bass, and the reference lake (blue) is stable with many bass. In 2008 the lakes are in different stable states, but the manipulated lake begins to change as bass are added to it. The third row shows one variable representing the state of the two systems over time (e.g., chlorophyll concentration), and the fourth row shows leading indicators over time (e.g., autocorrelation time). In 2009 and 2010, the manipulated lake is not yet bass-dominated, but the system becomes unstable and the leading

indicator rises. The star indicates the day of the “first alarm” of the approaching regime shift, as computed from the leading indicators by the quickest detection method. The elevated leading indicator and the first alarm precede the transition of the manipulated lake to a bass-dominated state. In 2011 both lakes are in a stable, bass-dominated state.

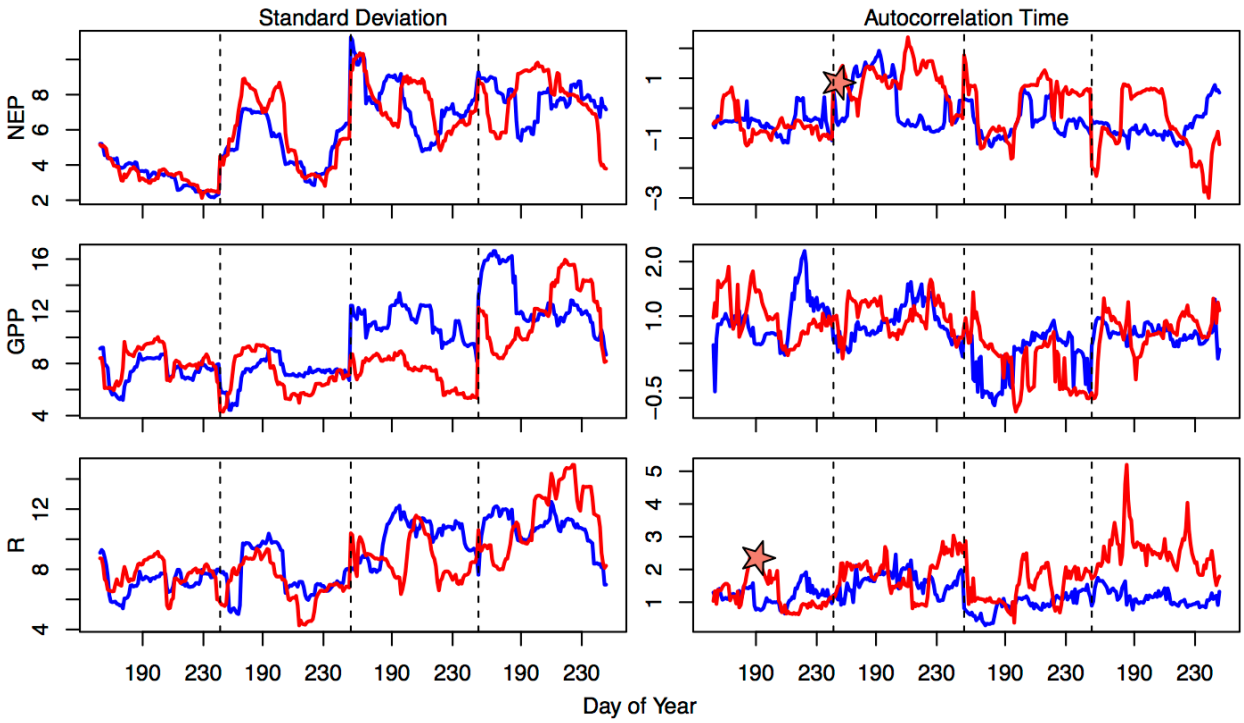

Fig. 2. Values of leading indicators (columns) computed from calculated rates of metabolism (rows) over time. Red lines are the manipulated lake, blue lines are the reference lake. Vertical dashed lines separate years (2008-2011). Bass were first added to the manipulated lake on day 189 of 2008, and the regime shift completed near day 230 of 2010. Stars indicate the day of the first alarm, computed from a particular leading indicator-variable combination using the quickest detection method. Daily averages of calculated metabolism rates (mmol O_2 m^{-3} d^{-1}) were used to compute the leading indicators in the first (NEP), second (GPP), and third (R) rows.

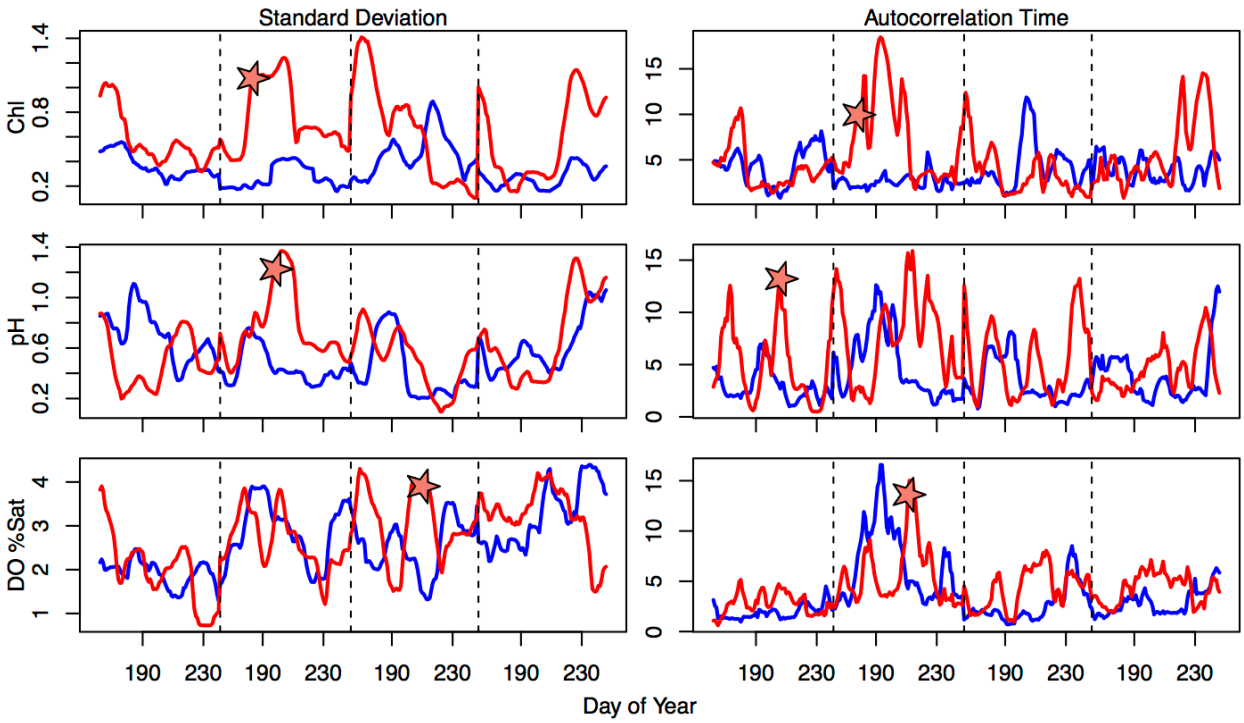

Fig. 3. Values of leading indicators (columns) computed from directly-measured sensor variables (rows) over time. Red lines are the manipulated lake, blue lines are the reference lake. Vertical dashed lines separate years (2008-2011). Bass were first added to the manipulated lake on day 189 of 2008, and the regime shift completed near day 230 of 2010. Stars indicate the day of the first alarm, computed from a particular leading indicator-variable combination using the quickest detection method. Daily averages of measurements made by automated sensors were used to compute the leading indicators in the first (chlorophyll, µg/L), second (pH), and third (dissolved oxygen percent saturation) rows.

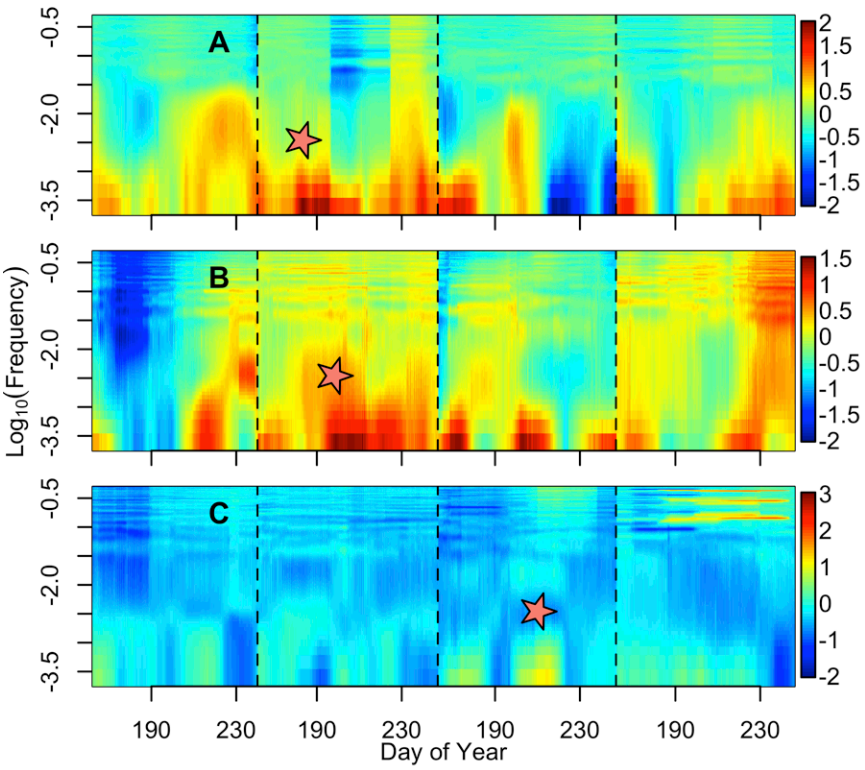

Fig. 4. Time series of the log-ratio of the variance spectrum of the manipulated lake to that of the reference lake, computed from automated high-frequency (5-min) observations of (A) chlorophyll-*a*, (B) pH, (C) percent saturation of dissolved oxygen. The colors represent log-ratio, such that warm colors indicate that the manipulated lake is more variable at that frequency than the reference lake. Note that the log-ratio of variance (color) is scaled differently for each variable. The vertical axis is the log10(frequency) of the signal computed within the rolling window, such that a fortnightly variance signal is at -3.61, weekly = -3.30, daily = -2.46, and hourly = -1.08. The stars indicate the first alarms computed from the standard deviations of the daily averages of each variable (Figure 2). The horizontal placement of the stars indicates the day of the first alarm, and the vertical placement is at the daily frequency. Bass were first added to the manipulated lake on day 189 of 2008, and the regime shift completed near day 230 of 2010. Vertical dashed lines separate years (2008-2011).

Appendix to Chapter 4

Study Systems. This study was conducted over four summers from 2008 to 2011 in Peter Lake and Paul Lake, located at the University of Notre Dame Environmental Research Center in the upper peninsula of Michigan (89°32' W, 46°13' N). Peter and Paul are small lakes (2.7 and 1.7 ha, respectively). The two lakes were originally one hourglass shaped lake that was separated by an earthen dike in the 1940's (1). Thus, Peter and Paul have similar chemical and limnological characteristics. Fish communities and manipulations are described in the main text. The Paul Lake zooplankton community was dominated by the large-bodied cladocerans *Daphnia* spp. and *Holopedium gibberum* throughout the experiment (2). Initially, the Peter Lake zooplankton community had a mixture of large and small zooplankton, including *Bosmina* sp., *Diaphanosoma birgei*, *Daphnia* spp., and *H. gibberum*. However, the taxa in Peter Lake shifted to larger-bodied species over the course of the experiment as a result of the fish manipulation. For example, the small-bodied *D. parvula* and *D. dubia* comprised the *Daphnia* in Peter Lake in 2008, but the large-bodied *D. rosea* and *D. pulex* had much higher relative abundance by 2010. Both lakes are thermally stratified during summer and relatively unproductive: between 2008 and 2011 the total P concentration ($\mu g\ L^{-1}$) was 4.90 ± 2.52 (mean ± standard deviation) in Paul Lake and 5.96 ± 3.83 in Peter Lake, and the chlorophyll *a* concentration ($\mu g\ L^{-1}$) was 3.48 ± 1.77 in Paul Lake and 4.71 ± 2.52 in Peter Lake. Detailed descriptions of both lakes are provided in Carpenter & Kitchell (1993) (1).

Sensor Observations. To ensure the quality of time series prior to statistical analysis, raw sensor observations were inspected for missing values, outliers, and other possible deviations from statistical assumptions. The sensor time series included direct measurements of chlorophyll *a* concentration (Chl-*a*; $\mu g\ L^{-1}$), pH, and dissolved oxygen (DO; percent saturation). The sensor

DO and temperature data were used to estimate gross primary production (GPP), respiration (R), and net ecosystem production (NEP) – all in units of mmol O_2 m^{-3} d^{-1}. Missing values (0.5% of data) were handled by computing statistics from the incomplete time series (e.g., computing variance from 27 instead of 28 days). If greater than 3 hr of data was missing during a day (0.9% of days), the entire day was treated as missing. Time series of DO, Chl-*a*, and pH were examined for outliers (greater than three standard deviations from annual mean), and were treated as missing data when detected (0.24% of data). Time series were inspected and corrected for mean shifts due to calibration of sensors or other differences between instruments (which were rotated among lakes weekly). To account for any between-lake difference in buffering capacity, annual time series of pH were scaled to have a mean of 0 and a standard deviation of 1. Quantile-quantile plots of variables were consistent with a normal distribution.

In total, we analyzed time series of seven variables collected from two lakes over four years (Fig. S2). In addition to the six sensor-based variables, we also analyzed manual measurements of Chl-*a*, which were obtained from laboratory analysis of daily samples of surface water (3). Missing values in the manual Chl-*a* time series were handled in the same manner as the sensor-based time series.

Metabolism Calculations. Net ecosystem production (NEP) was estimated from time series of DO, water temperature, and wind speed using a simple variation of the Odum (1956) model which is widely used in limnology (5–7). The model attributes changes in DO concentration (mmol O_2 m^{-3}) between time steps of duration Δt (Δt = 5 min) to the metabolic processes of gross primary production (GPP) and respiration (R), and to exchange with the atmosphere (F):

$$(DO_t - DO_{t-1}) \times (\Delta t)^{-1} = (GPP_{t-1} + R_{t-1}) + F_{t-1} \quad (1)$$

Estimates of atmospheric flux were based on the disequilibrium between DO and atmospheric oxygen:

$$F_t = k_t \times (DO_{Sat,t} - DO_t) \times (z_{mix,t})^{-1} \quad (2)$$

where DO_{Sat} is the oxygen concentration at atmospheric equilibrium. The piston velocity k (m^{-1}) drives DO to atmospheric equilibrium, and was calculated from k_{600}, which in turn was estimated from measurements of water temperature and wind speed (8, 9). NEP (mmol O_2 m^3 d^{-1}) is the change in DO after accounting for atmospheric flux. R was computed each day as the 24-hr extrapolation of NEP during the nights (darkness) surrounding the daylight period. GPP was computed as the sum of R and NEP.

Statistical Indicators and Correlations between Variables. All statistics were computed in the R programming language (10). Statistical indicators were calculated over 28-day rolling windows within each year. The 28-day window was shifted by increments of one day for computing autocorrelation time (AcT) and standard deviation (SD) from daily time series, and by twelve hours for computing spectral ratio from high frequency time series. The spectral ratio was calculated as the ratio of the spectral density in the manipulated lake to that in the reference lake, and spectra were computed from the autocorrelation function. Autocorrelation time was computed from first order autocorrelation (AR1). Before computing AR1, time series were linearly detrended to achieve stationarity (11, 12). Autocorrelation time was computed as $-\log_e(AR1)^{-1}$ (13).

All seven variables were either estimates of, or closely related to, metabolism. We expected that these variables would respond similarly to the manipulations, and therefore would yield similar temporal patterns in the statistical indicators. However, the patterns in the statistical indicators differed among the variables (Fig. S1). Signals of declining resilience were detected in

the manual Chl-*a* measurements and in the directly measured sensor variables (Chl-*a*, pH, DO), but not in the time series of metabolism estimates (GPP, R, NEP).

Variables that are highly correlated should show similar patterns in statistical indicators. We compared the correlation of daily time series of sensor-based variables to the daily time series of manually sampled Chl-*a*. We used manual Chl-*a* as the independent variable in these regressions because in the past it has responded to trophic cascades in these lakes (1, 14), and because previous analyses of this experiment have used it to detect changes in resilience (3, 15, 16). Variables that gave the clearest signals of changing resilience were also those that were best correlated with manual Chl-*a* (Fig. S3). Perhaps unsurprisingly, sensor Chl-*a* was better correlated with manual Chl-*a* than the other sensor variables. DO and pH were also correlated with manual Chl-*a*. However, despite being largely based on DO dynamics, the metabolism estimates (GPP, R, NEP) were not correlated with manual Chl-*a*. All variables were subject to observation error, but metabolism estimates were influenced by both observation error and process (i.e., model) errors. The presence of this additional source of uncertainty in the metabolism estimates could have reduced their correlation with driver variables and obscured signals of changing resilience that might otherwise have been detectable in their time series.

Compared to manual Chl-*a* in the manipulated lake, manual Chl-*a* in the reference lake rarely extended beyond a limited range of low concentrations, which would have contributed to the low R^2 values for the reference lake compared to those for the manipulated lake (Fig. S3).

Quickest Detection. To determine when the change in an indicator first became large enough to constitute a signal of low resilience, we employed the "quickest detection" (QD) method for detecting state changes (17–19). The QD method defines two probability densities for $x_{M,t}$, the observation of indicator x on day t in the manipulated lake: $f(x_{M,t})$ is the probability

density of x_t if the system was in the baseline state (far from tipping point), and $g(x_{M,t})$ is the probability density of x_t if the system was in the critical state (close to tipping point). Their ratio is $g(x_{M,t})/f(x_{M,t}) = \Lambda_t$. The detection statistic for the QD method is R_t, and R_t is updated as new Λ_t arrive: $R_t = (1 + R_{t-1}) \times \Lambda_t$. When the indicator is more likely to be in the critical state than the baseline state, Λ_t is greater than one, which increases the rate at which R_t rises. The day of first alarm (DoFA) is when R_t first reaches a predefined threshold, A.

Implementing QD requires defining $f(x_{M,t})$, $g(x_{M,t})$, and A. The functions for the probability densities were two normal distributions:

$$f(x_{M,t}) \sim N(\mu = x_{C,t} - \Delta_f, \sigma_{f,g}) \quad (3)$$

$$g(x_{M,t}) \sim N(\mu = x_{C,t} + \Delta_g, \sigma_{f,g}) \quad (4)$$

where $x_{C,t}$ is the value of the indicator in the reference lake on day *t*. The mean of $f(x_{M,t})$ is the current value of the indicator in the reference lake minus Δ_f, a baseline difference between the indicator in the two lakes. The mean of $g(x_{M,t})$ is the current value of the indicator in the reference lake plus Δ_g, which was formulated so that $x_{M,t}$ in the critical state would be higher than $x_{C,t}$: $\Delta_g = |\Delta_f| + 2 \times |x_{C,t}|$. The standard deviations of $f(x_{M,t})$ and $g(x_{M,t})$, $\sigma_{f,g}$, were equivalent and calculated as twice the standard deviation of the first 28 values of $x_{C,t}$. Δ_f was calculated as the mean difference in the two lakes for the first 28 values of indicator in 2008 (up to day 189). All variable – indicator combinations used the same value for A (10^7), the same formulation for Δ_f, Δ_g, and $\sigma_{f,g}$.

The DoFA detected in manual Chl-*a*, sensor Chl-*a*, pH, and DO showed little change over wide ranges of these parameter choices (Fig. S4-7). The parameter A describes the threshold amount of evidence that needs to be accumulated to signal entry to the critical state. Increasing the value of A will never reduce the time until alarm, and only in cases where a large

amount of evidence is accumulated in a single time step is it possible for increasing A to have no affect on the DoFA. We tested the sensitivity of the DoFA to our choice of A by varying it across 13 orders of magnitude. For the manual and sensor Chl-*a*, increasing A over 13 orders of magnitude increased the DoFA by a few days (Fig. S4,5). The DoFA of the SD of DO changed little across A, but the AcT of DO and both indicators computed from pH had DoFA that increased suddenly at particular values of A (Fig. S6,7). However, the values of A that we used in our analysis were far from these abrupt shifts in DoFA, and in no case did our choice of A lead to a particular DoFA that was only observed for a narrow range of A. Therefore, the DoFA was robust to our choice of A over many orders of magnitude, and the results are representative of what would have been obtained for a wide choice of A values.

The parameters Δ_f and Δ_g are used as offsets that are applied to the statistics computed from the reference lake, the sum of which can the be used to form an expectation of the value of the statistic in the manipulated lake in the baseline and critical states. Our method for calculating Δ_f and Δ_g was general enough to be used for all variables and statistics. The sensitivity of DoFA to Δ_f and Δ_g was assessed by varying these parameters over a range of values that were appropriate for each variable: the nominal values were multiplied by a sequence of coefficients ranging from 0 to 2. However, as was the case with A, a moderate increases or decreases in the values of Δ_f and Δ_g in the neighborhood of our nominal values changed the DoFA by only a few days.

The uncertainty around the value of the indicator in the baseline state and critical state is represented by σ_f and σ_g, respectively. In our formulation, these two variables have the same value. Varying $\sigma_{f,g}$ by a factor of 0.01 to 2 caused the DoFA of manual and sensor Chl-*a* to increase by a few days with increasing $\sigma_{f,g}$ (Fig. S4,5). The DoFA of the SD of pH and DO

responded similarly to the Chl-a variables. The DoFA of their AcT showed abrupt shifts but nonetheless the nominal value of the parameter was not in the region of rapid change (Fig. S6,7). In general the DoFA was robust to $\sigma_{f,g}$, with the exception that lowest value of $\sigma_{f,g}$ lead to an early DoFA for each combination of variables and statistics. This low value was one tenth of the value that we used for determining the DoFA in Fig. 2 and Fig. S2.

In all cases, the nominal values of A, Δg, Δf, and σf,g resulted in DoFA that were similar to those found for a range of other parameter choices. Varying these four parameters tended result in either a "plateau" of DoFA (the DoFA was nearly constant across a range of parameter values), or a slowly-changing DoFA. Importantly, the nominal value used for all parameters was always situated in slowly changing region of a plateau of the DoFA.

Literature Cited in the Appendix to Chapter 4

1. Carpenter SR, Kitchell JF eds. (1993) *The trophic cascade in lakes* (Carmbridge University Press, Cambridge, UK).
2. Pace ML, Carpenter SR, Johnson RA, Kurtzweil JT (2013) Zooplankton provide early warnings of a regime shift in a whole lake manipulation. *Limnol Oceanogr* 58(2):525–532.
3. Carpenter SR et al. (2011) Early warnings of regime shifts: A whole-ecosystem experiment. *Science* 332(6033):1079–1082.
4. Odum HT (1956) Primary production in flowing waters. *Limnol Oceanogr* 1(2):102 – 117.
5. Coloso JJ, Cole JJ, Pace ML (2011) Difficulty in discerning drivers of lake ecosystem metabolism with high-frequency data. *Ecosystems* 14(6):935–948.

6. Cole JJ, Pace ML, Carpenter SR, Kitchell JF (2000) Persistence of net heterotrophy in lakes during nutrient addition and food web manipulations. *Limnol Oceanogr* 45(8):1718–1730.

7. Stæhr PA et al. (2010) Lake metabolism and the diel oxygen technique: State of the science. *Limnol Oceanogr Methods* 8:628–644.

8. Jahne B et al. (1987) On the parameters influencing air-water gas-exchange. *J Geophys Res C: Oceans* 92(C2):1937–1949.

9. Cole JJ, Caraco NF (1998) Atmospheric exchange of carbon dioxide in a low-wind oligotrophic lake measured by the addition of SF6. *Limnol Oceanogr* 43(4):647–656.

10. R Development Core Team (2012) *R: A Language and Environment for Statistical Computing* (R Foundation for Statistical Computing, Vienna, Austria).

11. Dakos V et al. (2008) Slowing down as an early warning signal for abrupt climate change. *Proc Natl Acad Sci USA* 105(38):14308–14312.

12. Dakos V et al. (2012) Methods for detecting early warnings of critical transitions in time series illustrated using simulated ecological data. *PLoS One* 7(7):e41010.

13. Dai L, Vorselen D, Korolev KS, Gore J (2012) Generic indicators for loss of resilience before a tipping point leading to population collapse. *Science* 336(6085):1175–1177.

14. Carpenter SR et al. (2001) Trophic cascades, nutrients, and lake productivity: Whole-lake experiments. *Ecol Monogr* 71(2):163–186.

15. Seekell DA, Carpenter SR, Cline TJ, Pace ML (2012) Conditional Heteroskedasticity Forecasts Regime Shift in a Whole-Ecosystem Experiment. *Ecosystems* 15(5):741–747.

16. Carpenter SR, Brock WA (2011) Early warnings of unknown nonlinear shifts: a nonparametric approach. *Ecology* 92(12):2196–2201.

17. Shiryaev AN (2010) Quickest detection problems: Fifty years later. *Seq Anal* 29(4):345–385.

18. Polunchenko AS, Tartakovsky AG (2011) State-of-the-art in sequential change-point detection. *Methodol Comput Appl Probab* 14(3):649–684.

19. Carpenter SR, Brock WA, Cole JJ, Pace ML (2013) A new approach for rapid detection of nearby thresholds in ecosystem time series. *Oikos*.

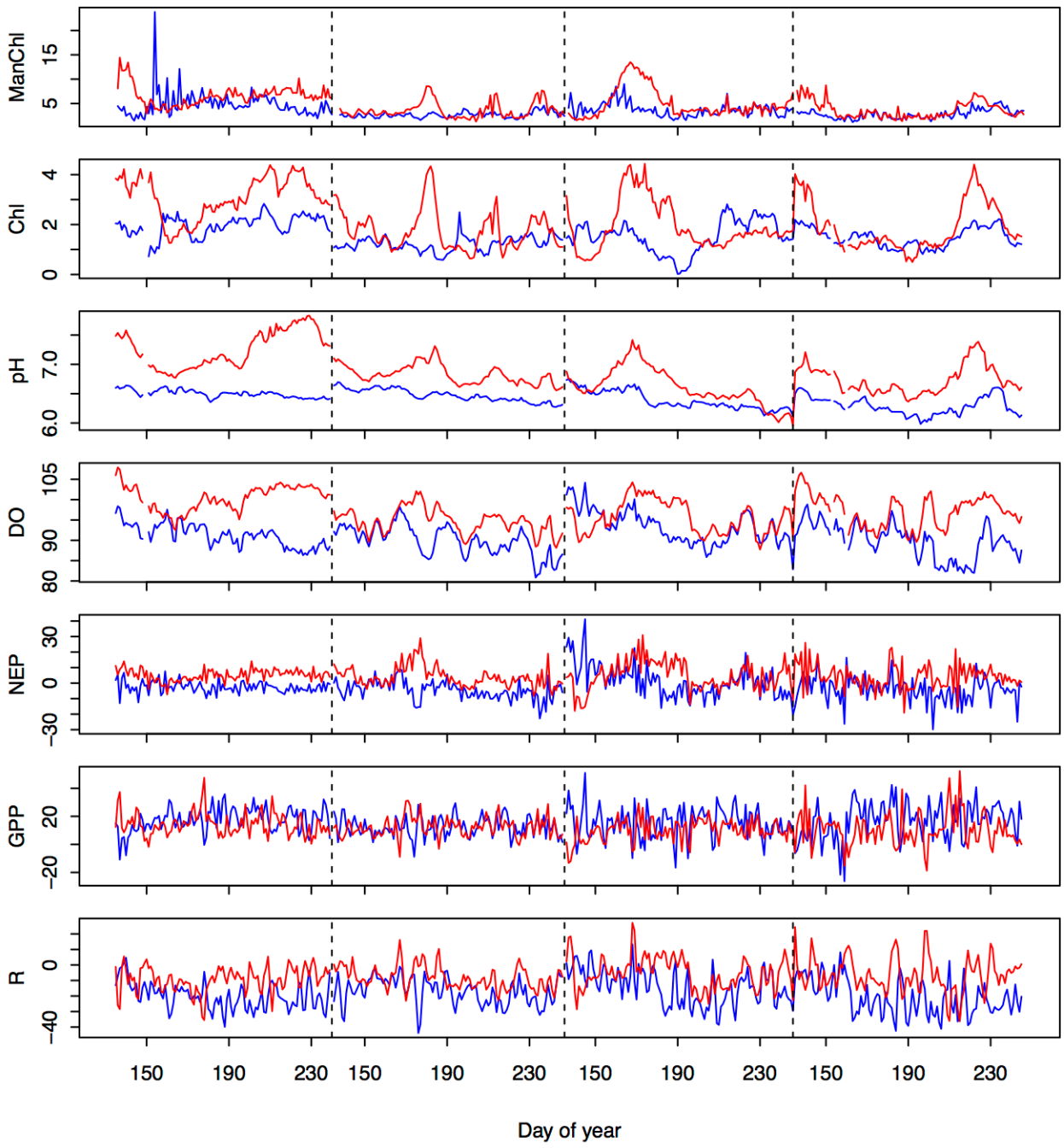

Fig. S1. Values of leading indicators (columns) computed from each variable (rows) over time. Red lines are the manipulated lake, blue lines are the reference lake. Vertical dashed lines separate years (2008-2011). Bass were first added to the manipulated lake on day 189 of 2008, and the regime shift completed near day 230 of 2010. Red circles indicate alarms, computed from a particular leading indicator- variable combination using the quickest detection method.

The chlorophyll concentration in the first row was manually sampled. Daily averages of measurements made by automated sensors were used to compute the leading indicators in the second (chlorophyll, μg L^{-1}), third (pH), and fourth (dissolved oxygen percent saturation, DO) rows. The three bottom rows show estimates of net ecosystem production (NEP, μmol O_2 L^{-1} d^{-1}), gross primary production (GPP, μmol O_2 L^{-1} d^{-1}), and respiration (R, μmol O_2 L^{-1} d^{-1}). Metabolism values were estimated from automated measurements of water temperature, DO, and wind speed.

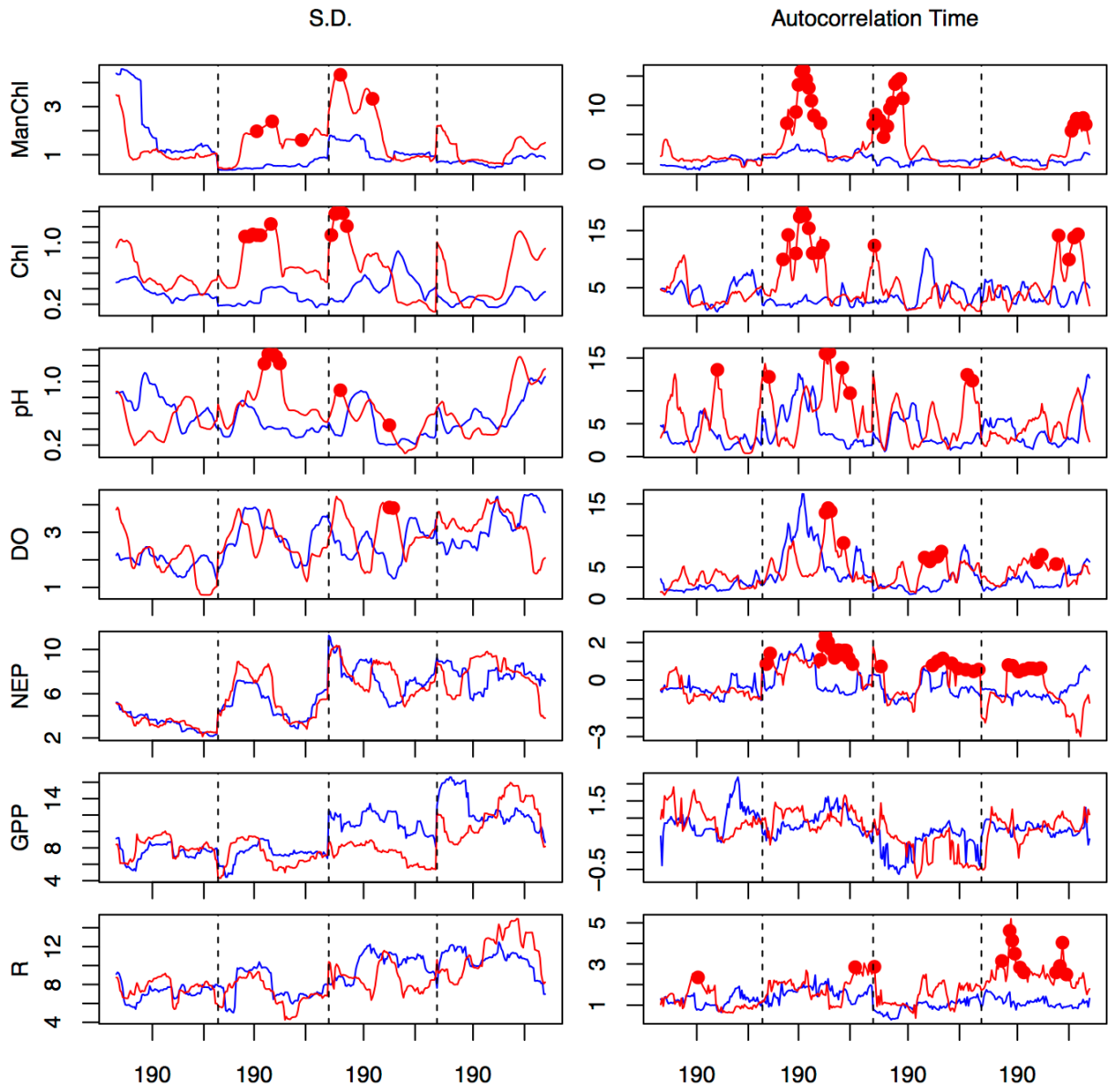

Fig. S2. Daily time series of the six automated high-frequency measures and one daily manual measurement collected from both the manipulated lake (red line) and the reference lake (blue line) over the four years of the experiment. Manually sampled chlorophyll (ManChl; µg L^{-1}) is related to metabolism. Directly measured variables collected by automated sensors include chlorophyll *a* (Chl-*a*; µg L^{-1}), dissolved oxygen (DO; percent saturation), and pH. Gross primary

production (GPP; mmol O_2 m^{-3} d^{-1}), respiration (R), and net ecosystem production (NEP) are model estimates of metabolism that are derived from data collected by automated sensors.

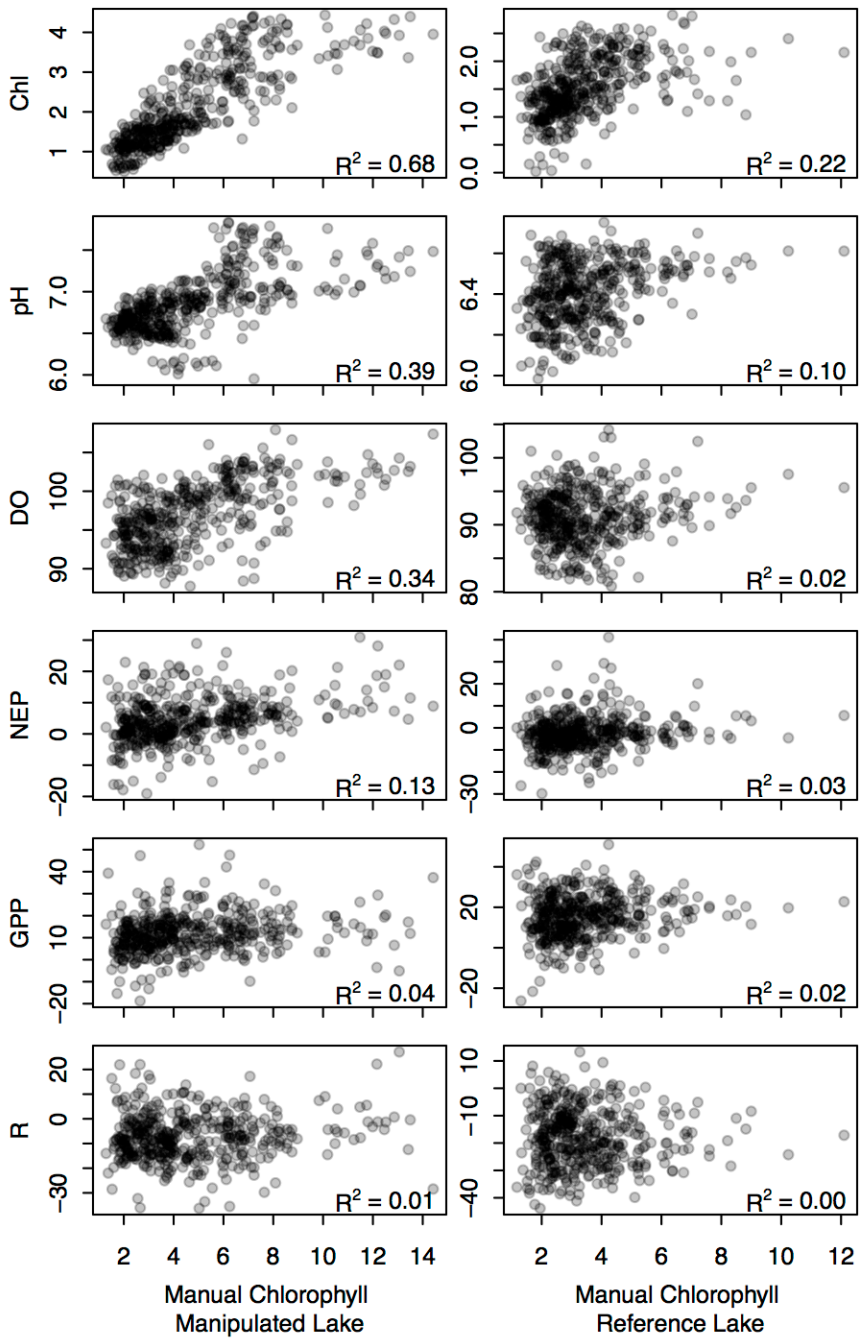

Fig. S3. Comparison of the daily means of chlorophyll *a* (Chl-*a*), pH, dissolved oxygen (DO; percent saturation), net ecosystem production (NEP; mmol O_2 m^{-3} d^{-1}), respiration (R), and gross primary production (GPP) to the manual samples of Chl-*a* in Peter Lake (the manipulated lake) and Paul Lake (the reference lake) from the four years of the experiment. The italicized value in the bottom right corner of each panel is the R^2 value from a linear regression of the two variables

in that panel. The scatter plots and linear regressions in the second column of panels excluded a single outlier from the time series of manual Chl-*a* (value of 23.8 μg L^{-1}).

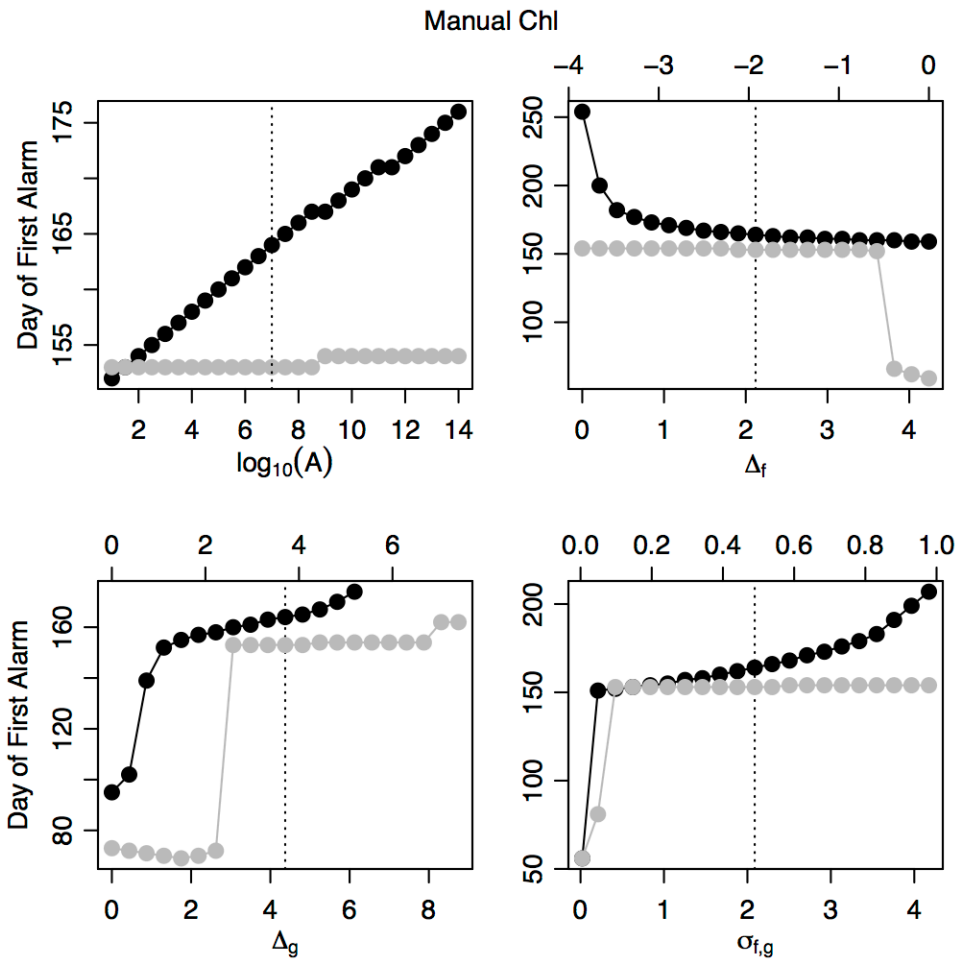

Fig. S4. Sensitivity of the day of first alarm (left axis) to parameters of the quickest detection algorithm (QD) when QD was as applied to the standard deviation (black points) and autocorrelation time (grey points) of manually-sampled Chl-*a* time series. The sensitivity analysis was conducted for the alarm threshold (A), the shift of the leading indicator in manipulated lake below that in the reference lake during the baseline state (Δ_f), the average shift of the leading indicator in the manipulated lake above that in the reference lake during the critical state (Δ_g), and the standard deviation of the leading indicator in the manipulated lake during either state ($\sigma_{f,g}$). The day of first alarm was computed across the same values of A for both leading indicators, with a nominal value of 10^7 (vertical dotted line). The day of first alarm was computed for values of Δ_f and Δ_g that ranged from 0 to 2 times the nominal value used with

the standard deviation (bottom axis) or autocorrelation time (top axis), and $\sigma_{f,g}$ ranged from 0.01 to 2 times the nominal value used with each leading indicator.

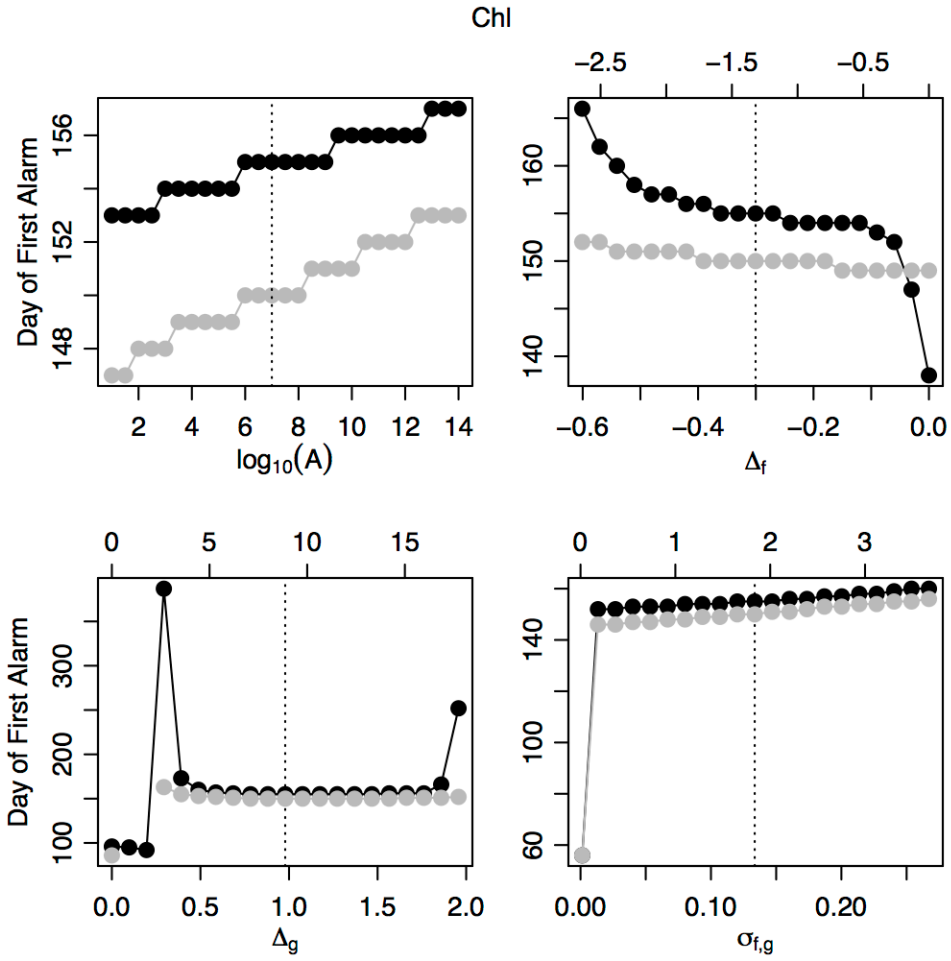

Fig. S5. Sensitivity of the day of first alarm (left axis) to parameters of the quickest detection algorithm (QD) when QD was as applied to the standard deviation (black points) and autocorrelation time (grey points) of time series of the daily averages of chlorophyll concentration measured by automated sensors. The sensitivity analysis was conducted for the alarm threshold (A), the shift of the leading indicator in manipulated lake below that in the reference lake during the baseline state (Δ_f), the average shift of the leading indicator in the manipulated lake above that in the reference lake during the critical state (Δ_g), and the standard deviation of the leading indicator in the manipulated lake during either state ($\sigma_{f,g}$). The day of first alarm was computed across the same values of A for both leading indicators, with a nominal value of 10^7 (vertical dotted line). The day of first alarm was computed for values of Δ_f and Δ_g

that ranged from 0 to 2 times the nominal value used with the standard deviation (bottom axis) or autocorrelation time (top axis), and $\sigma_{f,g}$ ranged from 0.01 to 2 times the nominal value used with each leading indicator. No point was plotted if an alarm was not detected in a leading indicator for a given parameter value.

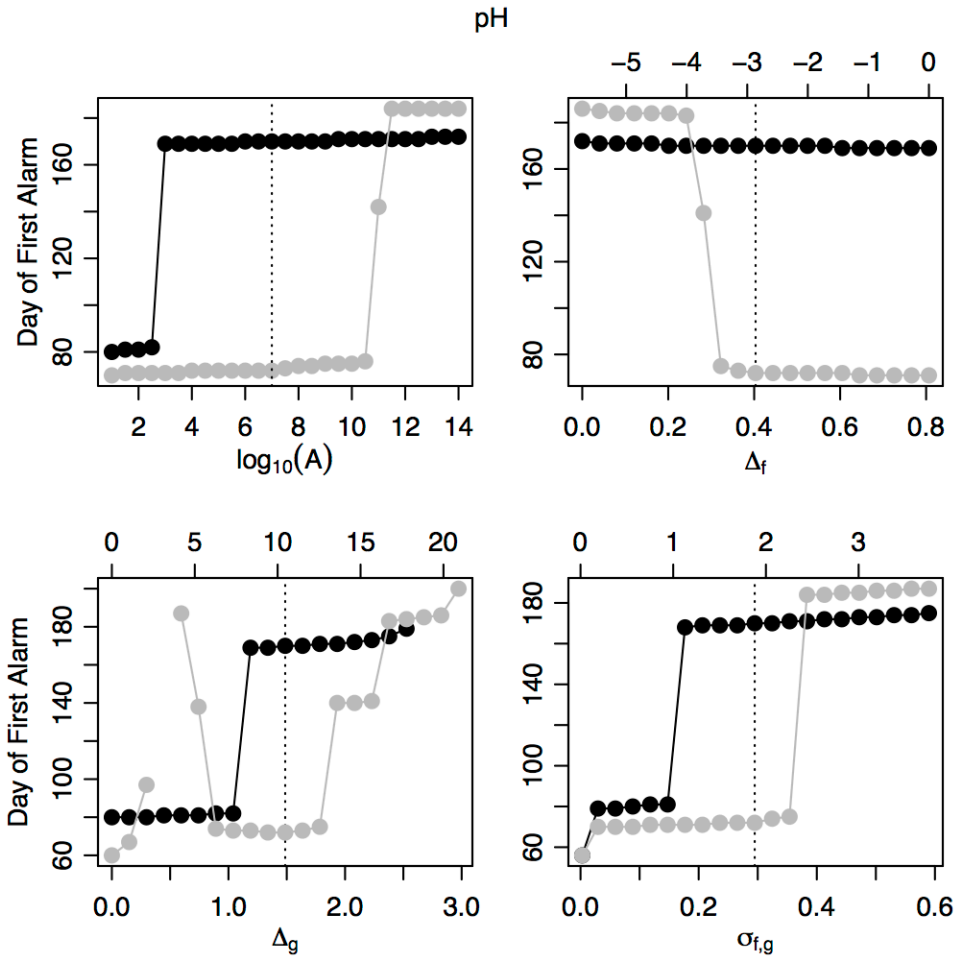

Fig. S6. Sensitivity of the day of first alarm (left axis) to parameters of the quickest detection algorithm (QD) when QD was as applied to the standard deviation (black points) and autocorrelation time (grey points) of time series of the daily averages of pH measured by automated sensors. The sensitivity analysis was conducted for the alarm threshold (A), the shift of the leading indicator in manipulated lake below that in the reference lake during the baseline state (Δ_f), the average shift of the leading indicator in the manipulated lake above that in the reference lake during the critical state (Δ_g), and the standard deviation of the leading indicator in the manipulated lake during either state ($\sigma_{f,g}$). The day of first alarm was computed across the same values of A for both leading indicators, with a nominal value of 10^7 (vertical dotted line). The day of first alarm was computed for values of Δ_f and Δ_g that ranged from 0 to 2 times the

nominal value used with the standard deviation (bottom axis) or autocorrelation time (top axis), and $\sigma_{f,g}$ ranged from 0.01 to 2 times the nominal value used with each leading indicator. No point was plotted if an alarm was not detected in a leading indicator for a given parameter value.

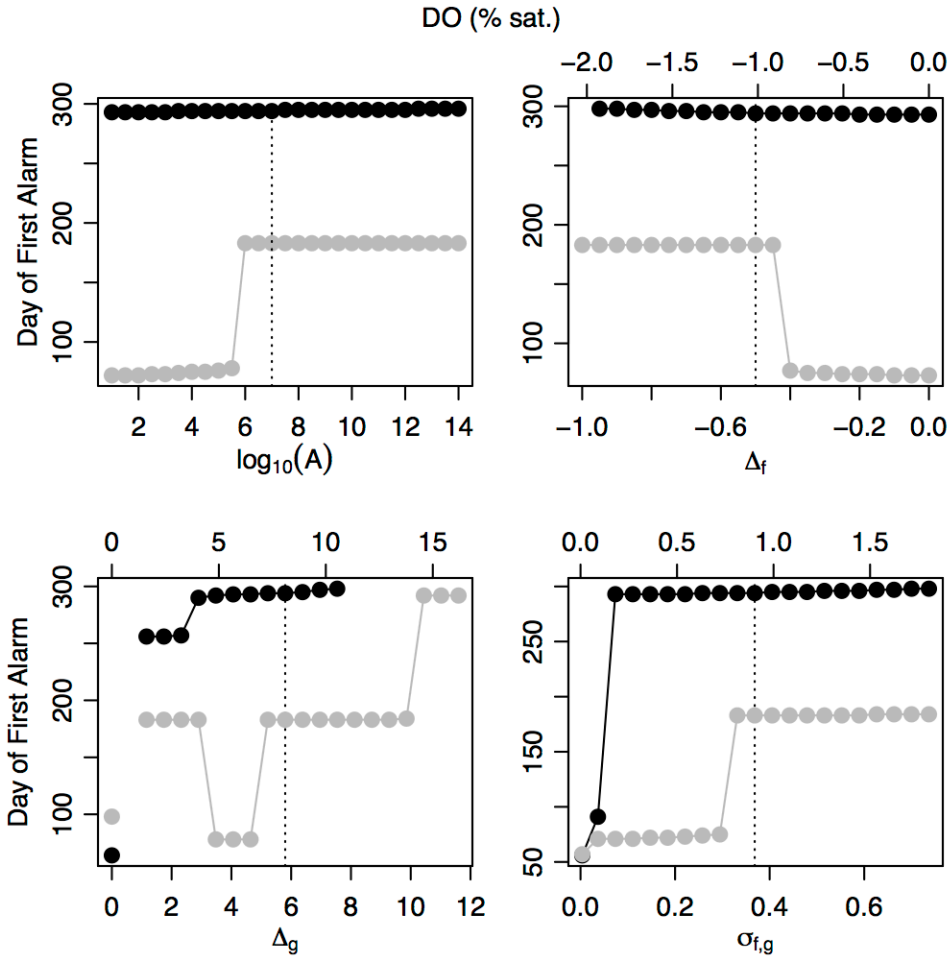

Fig. S7. Sensitivity of the day of first alarm (left axis) to parameters of the quickest detection algorithm (QD) when QD was as applied to the standard deviation (black points) and autocorrelation time (grey points) of time series of the daily averages of dissolved oxygen (percent saturation) measured by automated sensors. The sensitivity analysis was conducted for the alarm threshold (A), the shift of the leading indicator in manipulated lake below that in the reference lake during the baseline state (Δ_f), the average shift of the leading indicator in the manipulated lake above that in the reference lake during the critical state (Δ_g), and the standard deviation of the leading indicator in the manipulated lake during either state ($\sigma f_{,g}$). The day of first alarm was computed across the same values of A for both leading indicators, with a nominal value of 10^7 (vertical dotted line). The day of first alarm was computed for values of Δ_f and Δ_g

that ranged from 0 to 2 times the nominal value used with the standard deviation (bottom axis) or autocorrelation time (top axis), and $\sigma_{f,g}$ ranged from 0.01 to 2 times the nominal value used with each leading indicator. No point was plotted if an alarm was not detected in a leading indicator for a given parameter value.

Chapter 5: Tails of extremes in biotic and abiotic ecological time series*

An ecosystem can be greatly impacted by a single, large event. Massive events are more likely to be present in time series with extremes that follow fat-tailed probability distributions. As a result, scientists have stressed the importance of the thickness of the tails of a distribution (tailedness) for gauging the size and frequency of abiotic perturbations to ecosystems[1–3]. However, the tailedness of biological time series is not well characterized, which exposes us to being surprised by the extremes of these variables. We analyzed 595 long-term lake time series spanning meteorological, physical, chemical, and biological variables, and show that a range of tailedness can be found in all variable types. Biological variables were the most fat-tailed time series in our data set, and were estimated to exceed their historical records more frequently than the other categories. Furthermore, we found that presuming a normal or log-normal distribution for ecological time series can result in a skewed perception of the time that will pass between record breaking events. Ecological extremes may be made less surprising by accounting for possible fat tails in variables like biological populations.

---

*To be submitted for publication with the following coauthors: Stephen R. Carpenter, Anthony R. Ives

Extreme events are the largest or smallest values expressed by a variable over time (e.g., annual maxima), and a single extreme can change an ecosystem drastically. Compared to variables with extremes following probability distributions with thin or bounded upper tails, fat-tailed variables have a greater capacity to massively exceed historical precedent. The tail thickness of the distribution of a variable's extremes (i.e. the shape of the distribution of maxima, henceforth tailedness) can be quantified using extreme value theory, which is commonly applied to abiotic perturbations, such as natural disasters[2,4–7]. The statistics of extremes can be used to estimate how often flood stage breaches a levee[5], temperature crosses the lethal limit for limpets, or waves dislodge mussels[3]. Even when a threshold lies far beyond a variable's historical maximum, a threshold need only be crossed once to incite massive change. Therefore, it is crucial to know what types of variables can be fat-tailed.

Although fat tails have been found in a variety of variables, very few studies have evaluated their existence in the extremes of biological time series. To our knowledge, the empirical precedent for fat-tailed biological extremes is provided by a single time series of copepod zooplankton[8]. Such examples may be rare because some patterns common to biological time series, like autoregressive moving average (ARMA) models with Gaussian errors, are unlikely to produce fat-tailed extremes. However, a variety of nonlinear processes can produce fat-tailed distributions[9,10]. Nonlinear processes are prevalent in biological time series[11], and fat-tailed fluctuations (but not densities) have been observed in several biological populations[12]. For example, populations with nonlinear responses contingent upon rare conditions (i.e., the 'perfect storm') may have fat-tailed extremes (Fig. 1). Like ARMA models, jump-diffusion models are generic time series models and are commonly applied to financial time series; unlike ARMA,

jump-diffusion models involve chance multiplicative processes that are capable of producing fat-tailed returns and prices[13–15]. Although jump-diffusion models are rarely applied to ecological time series, their essential elements are chance events and multiplicative processes, which are considered commonplace in the natural world. Thus it is plausible for fat tails to be present in the extremes of both abiotic and biotic ecosystem time series.

Here we analyze 595 long-term lake time series (median duration of 29 years) from the North Temperate Lakes Long Term Ecological Research (NTL LTER) database to characterize the tailedness of biological, chemical, physical, and meteorological variables (Methods). The generalized extreme value distribution (GEV) is the limiting distribution for maxima[16], and its shape parameter (ξ) is a measure of tail thickness – negative ξ indicates a bounded upper tail, ξ near 0 indicates a thin tail, and positive ξ indicates that the maxima are fat-tailed.

We found a wide range of ξ in each variable category, but the biological variables were more fat-tailed than the other types of variables (Fig. 2A), which had significantly thinner tails (Methods). Under the null hypothesis that ξ was not different from 0 (two-tailed t-test, $p > 0.1$), we used the estimates of ξ and associated standard errors to calculate the frequency of each category of tailedness (bounded, thin, fat) for each variable type. Of the 283 biological time series, 38% had a ξ greater than 0 – by far the largest frequency of fat-tailedness among variable types (13% for chemical, 4% for physical, 0% for meteorological). Only 1% of biological time series had a bounded tail, which was the lowest frequency among variable types (22% for chemical, 51% for physical, 42% for meteorological). The fish with the largest estimate of ξ were *Lepomis* spp. in Lake Mendota ($\xi = 1.2$; 90% CI: $0.7 < \xi < 1.8$), the fattest-tailed zooplankton were *Kellicottia*

spp. in Crystal Bog ($\xi = 1.2$; 90% CI: $0.7 < \xi < 1.7$), and Crystal Lake had the most fat-tailed chlorophyll time series ($\xi = 0.5$; 90% CI: $0.2 < \xi < 0.8$). As estimates of ξ increase, the statistical moments $\geq 1/\xi$ become undefined[16] – therefore the estimated ξ of *Lepomis* spp. in Mendota and *Kellicottia* spp. in Crystal Bog imply that the average of their annual maxima will not converge to a long-term mean as more data are collected. Similarly, the long-term variance of chlorophyll concentration in Crystal Lake will not converge with additional data. To our knowledge this analysis provides the first evidence that the extremes of vertebrate time series can be fat-tailed, and that the tailedness of biological variables is larger than other types of variables in the same ecosystems.

Estimates of tailedness can provide valuable information on the size and frequency of large events. Record-breaking events are generally regarded as rare occurrences, but the difference in ξ across variables suggests that some types of variables may break records more often than others. We used the GEV fits to calculate the expected waiting time (years) until each time series broke its current record by at least 10%. Waiting time is heavily influenced by the value of ξ, but also depends on the other GEV parameters (μ and σ). The pattern in waiting times across variable types was similar to that in ξ: biological variables are likely to break their current records sooner than other categories of variables (Fig. 2B). In other words, not accounting for the distribution of extremes could lead to surprises in how often biological variables produce massive events.

Comparing waiting times derived from the GEV to waiting times derived from normal and log-normal distributions illustrates how these distributions can lead to vastly different expectations for the future (Fig. 3). When a variable has a bounded upper tail, the normal and log-normal

distributions both predict shorter waiting times than the GEV. As tail thickness increases, the normal distribution predicts waiting times that are much longer than those estimated from the log-normal or GEV. The GEV and log-normal estimate similar waiting times for most fat-tailed variables; however, in many cases the log-normal estimates waiting times several orders of magnitude longer than those estimated by the GEV. For example, the longest log-normal waiting time for a fat-tailed biological variable was 2,177 years for chlorophyll concentration in Crystal Lake, but the GEV estimate was only 103 years. By contrast, the longest GEV waiting time for a fat-tailed biological variable was 973 years for the zooplankton *Mesocyclops* spp. in Lake Monona, and the log-normal estimate was 256 years. It is difficult to know which distribution provides the most accurate estimate of waiting time for a given time series. Selecting among the three distributions by Akaike information criterion indicates that the log-normal was best-fitting for 60% of the time series and the GEV for 29%, which suggests that a single distribution is unlikely to give the best estimate of waiting time for all time series. Therefore, it may be risky to form intuition of future extremes without considering several distributions, including those that permit more flexibility in tail thickness, like the GEV.

Our analysis clearly identified fat tails in several biological time series, but we were largely unable to explain the variability of ξ across time series. For example, time series ξ did not show a strong relationship with the number or eigenvalue of ARMA parameters, nor with the ξ of the ARMA residuals. The time series of fish (n=111) and zooplankton (n=165) spanned 28 and 34 genera, respectively, but taxonomic classification was not strongly associated with ξ (Supplementary Notes, Extended Data Figs. 1-5). Although ξ was significantly different between variable categories, this pattern may change if our analysis were expanded to include variables

not present in our data set. Estimating a statistic based on rare events requires long time series[1,7], and estimates of ξ may improve with continued data collection. Therefore we suggest that continuing long-term monitoring of ecological variables and characterizing the tailedness of additional time series is critical for understanding ecological extremes.

It is dangerous to consider the future as a set of norms[17,18], and forecasting future events, especially extreme events, is difficult. However, tailedness and related statistics may enhance our ability to prepare for an uncertain future by offering an approach to gauge the scale and frequency of large events that lie on the horizon. Furthermore, global environmental change is increasing the prevalence of extremes in some abiotic variables[6,19], but it is unclear how global change might be influencing the tailedness of biological variables. The presence of fat-tailed biological variables could profoundly affect how we manage for ecosystem resilience, particularly because a variety of ecosystems are subject to regime shifts triggered by critical densities of biological populations[20,21]. Managing for ecosystem resilience could be facilitated by investigating the mechanisms that generate fat tails, and by recognizing that fat tails exist in a variety of ecosystem variables, including biological populations.

Methods Summary

Data were obtained through the NTL LTER database, and included data from 11 lakes and 2 regions of Wisconsin, USA. Extremes were defined via the block-maximum method[7], which yielded annual maxima. Each time series of extremes contained between 15 and 158 annual maxima (median = 29), and was categorized as biological (n=283 lake time series, including chlorophyll, 28 fish genera, and 34 zooplankton genera), chemical (n=220, e.g. ion

concentration), physical (n=80, e.g. water temperature), or meteorological (12 regional time series, e.g. mean daily wind speed).

The GEV has three parameters, location (μ), scale (σ), shape (ξ)[1], and its cumulative distribution function is

$$F(x;\mu,\sigma,\xi)=\begin{cases}\exp\{-[1+\xi(x-\mu)/\sigma]^{-1/\xi}\}, & \xi\neq 0\\ \quad 1+\xi(x-\mu)/\sigma>0 & \\ \exp\{-\exp[-(x-\mu)/\sigma]\} & \xi=0.\end{cases}$$

The GEV parameters were fit using maximum likelihood after removing a linear temporal trend from time series of maxima[1]. Parameters for the normal and log-normal distributions were estimated from the means and standard deviations of the detrended time series of annual maxima and their logarithms, respectively.

Waiting is the inverse probability (P; calculated from the cumulative distribution function) of observing a value ≥ 10% over the current record, multiplied by the observation frequency (F, years^{-1}) of maxima in the time series (F was usually 1): Waiting Time = 1/P*F. Statistical analyses were performed in R[22].

AR(1) were simulated from:

$$x_t = \varphi x_{t-1} + \varepsilon_t$$

where x is the state at time t, φ=0.5 is the autoregressive coefficient, and ε are normal errors. Jump-diffusion models were simulated from[13–15]:

$$r_{t+\Delta} - r_t = \mu(r_t)\Delta + \sigma(r_t)\varepsilon_{t+\Delta}\sqrt{\Delta} + J_{t+\Delta}Z_{t+\Delta}$$

$$J_{t+\Delta}Z_{t+\Delta} = \sum_{i=1}^{n(t+\Delta)} N(0,\sigma_Z\sqrt{n(t+\Delta)})_i$$

$$n(t+\Delta) = Pois(\lambda\Delta)$$

$$S(T) = \prod_{t=1}^{T} \exp(r_t\Delta)$$

where r is the change in state, μ=0, the size of each time step is Δ=1, σ=0.1, ε ~N(0,1) is a Weiner process, jump J of size Z has intensity λ=0.1 and is the sum of n(t+Δ) normal shocks with standard deviation (σ_Z=0.1)*n(t+Δ)$^{0.5}$. The state variable S (S_0=1) at time T is the product of exp(r) from times t to T.

Acknowledgements We thank J. Gaeta, A. Latzka, J. Kurtzweil, S. Oliver, L. Winslow, C. Herren, J. Magnuson, M. Turner, and students in Zoology 955/6 (Spring 2013) and 995 (Spring 2014) at UW-Madison for discussions and comments on the manuscript. We thank the North Temperate Lakes Long-Term Ecological Research program for providing the data. We thank the National Science Foundation for funding.

Author Contributions RDB and SRC conceived the study. RDB, SRC, and ARI designed the study. RDB wrote the R code and analyzed the data; analysis was guided by feedback from SRC and ARI. RDB, SRC, and ARI wrote the manuscript.

Literature Cited in Chapter 5

1. Katz, R. W., Brush, G. S. & Parlange, M. B. Statistics of extremes: modeling ecological disturbances. *Ecology* **86,** 1124–1134 (2005).

2. Gaines, S. D. & Denny, M. W. The largest, smallest, highest, lowest, longest, and shortest: extremes in ecology. *Ecology* **74,** 1677–1692 (1993).

3. Denny, M. W., Hunt, L. J. H., Miller, L. P. & Harley, C. D. G. On the prediction of extreme ecological events. *Ecol. Monogr.* **79,** 397–421 (2009).

4. Malamud, B. D. Tails of natural hazards. *Phys. World* **17,** 31–35 (2004).

5. Katz, R. W., Parlange, M. B. & Naveau, P. Statistics of extremes in hydrology. *Adv. Water Resour.* **25,** 1287–1304 (2002).

6. Grinsted, a., Moore, J. C. & Jevrejeva, S. Projected Atlantic hurricane surge threat from rising temperatures. *Proc. Natl. Acad. Sci.* **110,** (2013).

7. Palutikof, J. P., Brabson, B. B., Lister, D. H. & Adcock, S. T. A review of methods to calculate extreme wind speeds. *Meteorol. Appl.* **6,** 119–132 (1999).

8. Schmitt, F. G., Molinero, J. C. & Brizard, S. Z. Nonlinear dynamics and intermittency in a long-term copepod time series. *Commun. Nonlinear Sci. Numer. Simul.* **13,** 407–415 (2008).

9. Newman, M. Power laws, Pareto distributions and Zipf's law. *Contemp. Phys.* **46,** 323–351 (2005).

10. Barabási, A.-L. The origin of bursts and heavy tails in human dynamics. *Nature* **435,** (2005).

11. Hsieh, C., Glaser, S. M., Lucas, A. J. & Sugihara, G. Distinguishing random environmental fluctuations from ecological catastrophes for the North Pacific Ocean. *Nature* **435,** 336–40 (2005).

12. Segura, A. M., Calliari, D., Fort, H. & Lan, B. L. Fat tails in marine microbial population fluctuations. *Oikos* **122,** 1739–1745 (2013).

13. Tankov, P. & Voltchkova, E. Jump-diffusion models: a practitioner's guide. *Banq. Marchés* **99,** 1–24 (2009).

14. Brigo, D., Dalessandro, A., Neugebauer, M. & Triki, F. A stochastic processes toolkit for risk management: mean reverting processes and jumps. *J. Risk Manag. Financ. Institutions* **3,** 65–83 (2009).

15. Johannes, M. The statistical and economic role of jumps in continuous-time interest rate models. *J. Finance* **59,** 227–260 (2004).

16. Coles, S. *An introduction to statistical modeling of extreme values*. (Springer, 2001).

17. Oppenheimer, M., O'Neill, B. C., Webster, M. & Agrawala, S. The limits of consensus. *Science (80-.).* **317,** 1505–6 (2007).

18. Burgman, M. *et al.* Modeling extreme risks in ecology. *Risk Anal.* **32,** 1956–66 (2012).

19. IPCC. *Managing the Risks of Extreme Events and Disasters to Advance Climate Change Adaptation*. 582 (Cambridge University Press, 2012). doi:10.1017/CBO9781139177245

20. Carpenter, S. *et al.* General Resilience to Cope with Extreme Events. *Sustainability* **4,** 3248–3259 (2012).

21. Folke, C. *et al.* Regime Shifts, Resilience, and Biodiversity in Ecosystem Management. *Annu. Rev. Ecol. Evol. Syst.* **35,** 557–581 (2004).

22. R Core Team. *R: A Language and Environment for Statistical Computing*. (R Foundation for Statistical Computing, 2014).

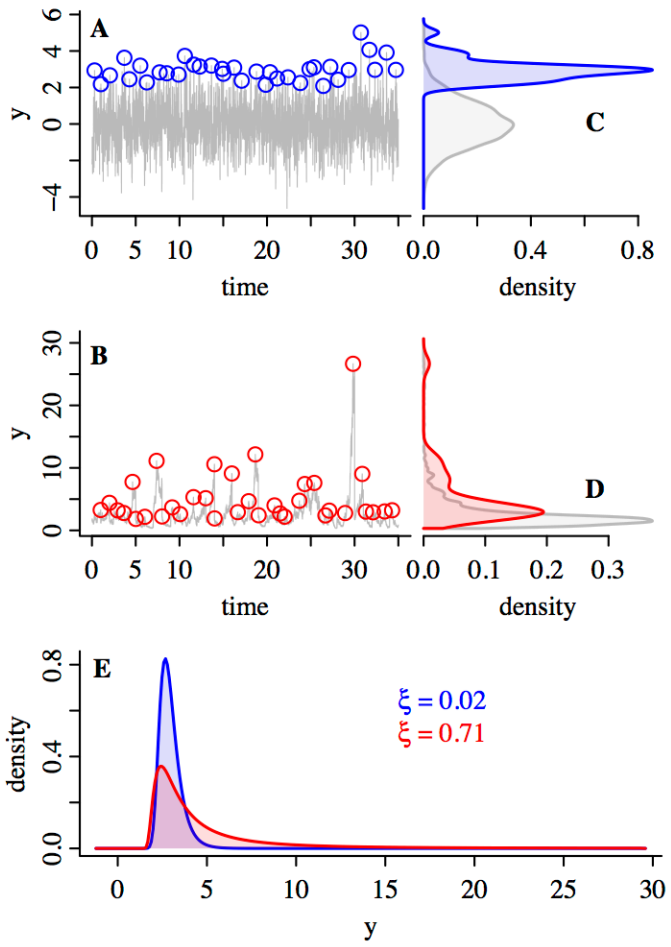

Figure 1. An AR(1) model (A) and a jump-diffusion model (B) were used to simulate 35 separate years of time series, each year with 100 observations. The AR(1) model evolves additively with normal errors (gray line in A), and the jump-diffusion model evolves geometrically with normal errors (diffusion) and a Pois(λ) chance of additional normal errors (jump) at each time step (gray line in B). Taking the maxima of each of the 35 short time series that comprise the gray lines yields annual maxima (circles in A, B). The empirical distributions of the full time series (i.e., parent distributions) are shown in gray, and the empirical distributions of the largest annual observations (extremes) are in blue and red (C,D). Fitting the GEV to the annual maxima reveals that the distribution of the extremes in A has a thin upper tail (E, blue distribution), whereas the distribution of extremes in B has a fat upper tail (E, red distribution).

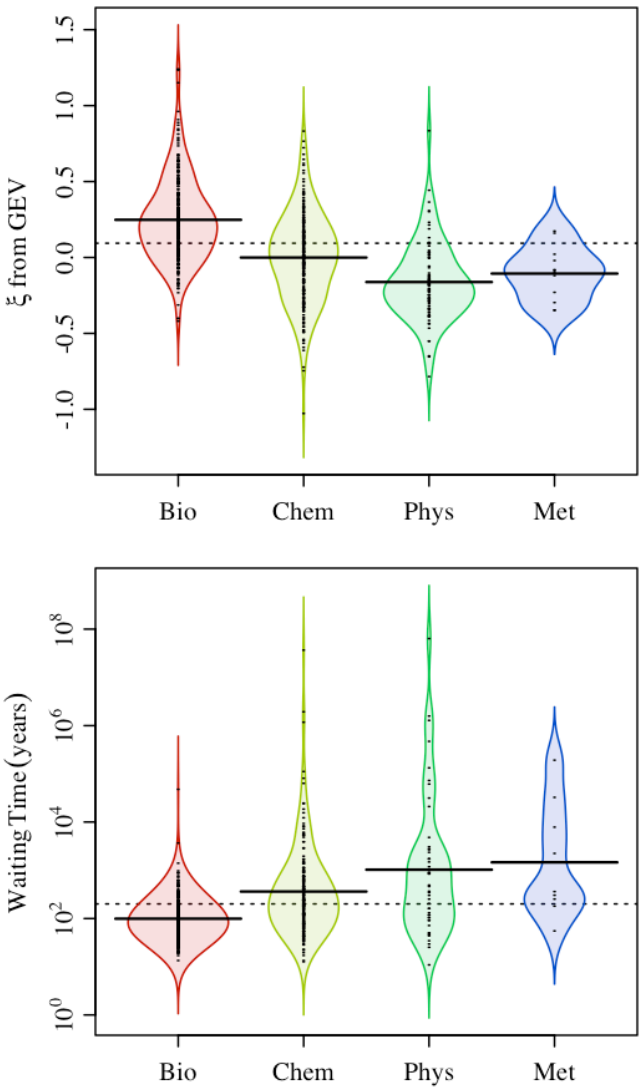

Figure 2. Bean plots of ξ estimated from the GEV (top), and waiting times (years) estimated from the GEV fits (bottom). Waiting times are the time until the maximum observation in a time series is broken by at least 10%. Each "bean" consists of a mirror image of the density plot of ξ or of the waiting times in each category (red = biological, yellow = chemical, green = physical, blue = meteorological). The values of individual observations are indicated by the small black dashes inside each bean. Horizontal dotted line is the mean across all categories. Solid horizontal lines are the means within each category.

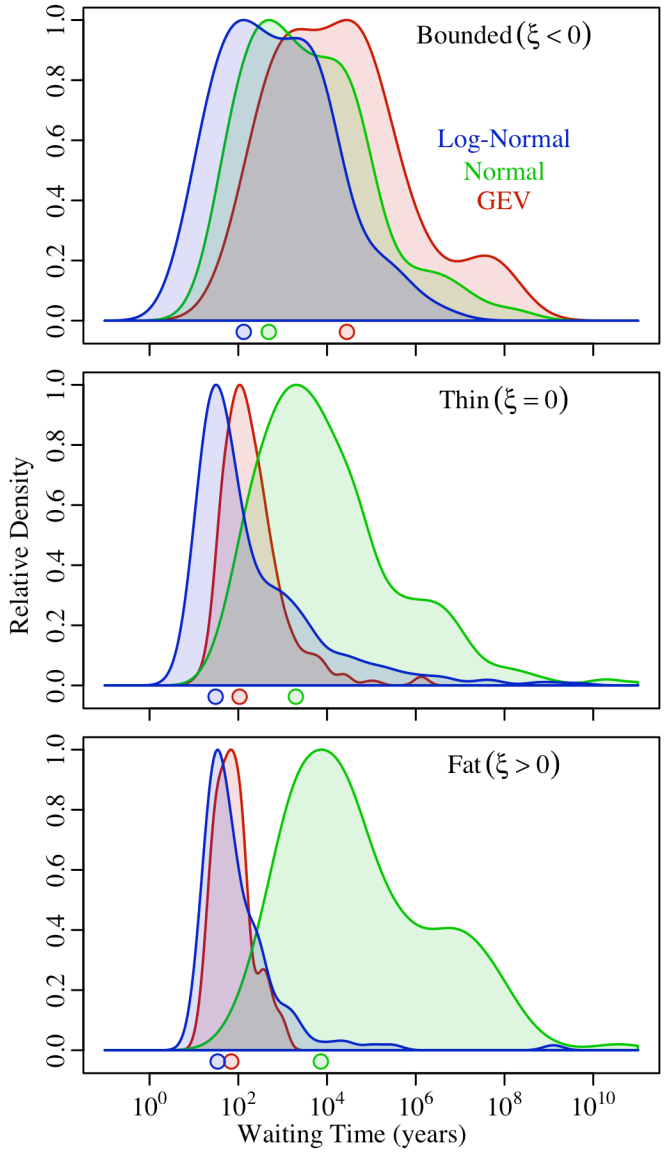

Figure 3. Density plots of waiting times for record-breaking events. Estimates from the GEV (red), log-normal (blue), and normal distributions (green) fitted to time series reflect the time until the next record-breaking event. Small circles indicate modes. All densities were scaled to a maximum of 1, and truncated at waiting times $< 10^{-1}$ or $> 10^{11}$ years. Panels distinguish ranges of ξ estimated from GEV fits to the time series under the null hypothesis that $\xi = 0$ ($p > 0.1$), and represent time series with a bounded (top), thin (middle), or fat (bottom) upper tail.

APPENDIX 1 TO CHAPTER 5: METHODS

Variables Analyzed. Raw data were downloaded from the online databases of the North Temperate Lakes Long-Term Ecological Research (NTL LTER) program (lter.limnology.wisc.edu/). Data were downloaded on April 18, 2013, except wind data, which were downloaded on March 30, 2014. Most time series from the northern lakes begin in 1981. Most time series from the southern lakes begin in 1996, except fish time series begin in 1995, zooplankton in 1976, and three ice cover time series that begin in 1851, 1852, and 1877. Most time series end between 2010 and 2012. Northern lakes include Allequash Lake, Big Muskellunge Lake, Crystal Bog, Crystal Lake, Little Rock Lake, Sparkling Lake, Trout Bog, and Trout Lake. The only time series from Little Rock Lake is ice cover. Southern lakes include Fish Lake, Lake Mendota, Lake Monona, and Lake Wingra.

Meteorological variables included air temperature (daily minimum, maximum, range), sum daily precipitation, snow depth, and daily average wind speed. These metrics were available for two regions: northern and southern. Northern meteorological measurements were made at the Minocqua Dam, with the exception of wind speed, which was measured at the Minocqua Airport. Southern meteorological measurements were made in Madison, WI. Southern wind speed measurements were corrected for changes in anemometer location.

Physical variables variable included epilimnetic averages for the following variables measured across a depth profile: dissolved oxygen concentration, dissolved oxygen percent saturation, water temperature, and the fraction of light at depth relative to light at surface. Physical variables also included non-profile variables: light extinction coefficient, Secchi depth (no viewer), lake

level, duration of the ice-free season (number of days), and the depth of the epilimnion. Epilimnetic depth (Z_{mix}) was defined as the shallower of two consecutive temperature measurements in a depth profile that had an average decrease in temperature (ºC) per meter of at least 2 (ºC m^{-1}). For variables measured over depth, epilimnetic averages were taken before cross-site measurements. If a depth profile was taken during mixis the average was taken across all depths, and the shallowest value of a profile was used on dates when Z_{mix} could not be calculated (e.g. because temperature profile unavailable).

Chemical variables included alkalinity, bicarbonate reactive silica (unfiltered), calcium, chloride, conductivity, dissolved inorganic carbon, dissolved organic carbon, dissolved reactive silica (filtered), iron, potassium, magnesium, manganese, sodium, ammonium, nitrate plus nitrite, pH, sulfate, total inorganic carbon, total organic carbon, total nitrogen (unfiltered), total phosphorus (unfiltered), and total particulate matter.

Biological variables included the abundance of fishes and zooplankton, and epilimnetic chlorophyll concentration. Each genus of fish or zooplankton comprised its own time series. Therefore, each fish or zooplankton time series was the sum of several unique taxonomic identifiers – e.g., summing across identifiers corresponding to different species in the same genus, hybrids, and taxa identified to the genus level. Fishes included the following genera: *Ambloplites*, *Ameiurus*, *Amia*, *Aplodinotus*, *Catostomus*, *Coregonus*, *Cottus*, *Cyprinus*, *Esox*, *Etheostoma*, *Labidesthes*, *Lepisosteus*, *Lepomis*, *Lota*, *Luxilus*, *Micropterus*, *Morone*, *Notemigonus*, *Notropis*, *Osmerus*, *Perca*, *Percina*, *Percina*, *Percopsis*, *Pimephales*, *Pomoxis*, *Salvelinus*, *Sander*, and *Umbra*. Crustacean zooplankton included the following genera: *Acanthocyclops*,

Aglaodiaptomus, *Bosmina*, *Ceriodaphnia*, *Chydorus*, *Daphnia*, *Diacyclops*, *Diaphanosoma*, *Diaoptomus*, *Eubosmina*, *Holopedium*, *Leptodiaptomus*, *Leptodora*, *Mesocyclops*, *Sinobosmina*, *Skistodiaptomus*, *Tropocyclops*. Rotifer zooplankton included the following genera: *Ascomorpha*, *Asplancha*, *Collotheca*, *Conochiloides*, *Conochilus*, *Filinia*, *Gastropus*, *Kellicottia*, *Keratella*, *Lecane*, *Lepadella*, *Monostyla*, *Notholca*, *Ploesoma*, *Polyarthra*, *Synchaeta*, *Trichocera*.

Fish catch per unit effort (number of individuals per hour trap set, CPUE) data were available for several methods: beach seines, electrofishing, fyke nets, gill nets (several mesh sizes), trammel nets. For a given lake, the availability of method-specific CPUE was typically consistent among years. However, in some cases a particular method was missing in a few years, or only present in a few years. Data from a particular method (per lake-year) could be missing either because the method did not capture any fish, or because it was not used. For gill nets, we assumed that an observation for at least 1 mesh size in a lake-year indicated that the full range of mesh sizes was deployed, as would be in accordance with NTL LTER protocol as indicated in the corresponding meta data. Thus, gill net catch was summed across mesh sizes, and gill net treated as a single method. For each lake we only used data observed with methods that were present in >95% of years for which data were available, and any methods that did not meet this criterion were removed from further consideration in our analysis. We defined the methods that met the aforementioned criteria in each lake as the "gear types" for that lake. Taxon-specific CPUE was calculated as the sum of CPUE across gear types. If a gear type was missing for a lake in a particular year, the CPUE of any taxa in that lake that had ever been caught by that gear type was designated as a missing value for that year, and therefore did not contribute to our analysis. This

procedure avoided erroneous fluctuations in species abundance that could be driven by interannual differences in methods used.

Data quality assurance. Prior to performing any calculations, two methods of quality assurance were implemented to remove erroneous entries from the data set. First, most values flagged in the North Temperate Lakes Long Term Ecological Research database were removed from analysis. An exception was made for the chlorophyll data set, which included elements that were flagged because they were measured during a transient method change. For these flagged data, "uncorrected" values were used instead of "corrected" values, as recommended by the database meta data. In addition to removing flagged data, each parent time series (i.e., full time series of all observations, not just annual maxima) was manually scanned for erroneous values, which were removed when found. Values were declared erroneous if they violated the sign convention of the measurement (e.g., negative concentrations), or were not plausible given measurement conventions (e.g., fraction of light at depth relative to surface greatly exceeding 1 [due to measurement error induced by variable cloud cover]). Removing these values was taken as an extra precaution, although in most cases the manually removed values were negative and would not have been included in the set of annual maxima, and thus the results of our analyses unaffected by their presence or absence.

Distribution fitting and waiting times. Time series were excluded from analysis if any of its annual maxima were less than 0, as this prevented comparison of waiting times with the log-normal distribution (2 time series were excluded for this reason). In some cases (79 of the 595

time series), waiting times were undefined because the value 10% over the record was outside the support of the generalized extreme value distribution (GEV):

$$x \in [\mu - \sigma/\xi, +\infty) \quad when\ \xi > 0,$$
$$x \in (-\infty, +\infty) \quad when\ \xi = 0,$$
$$x \in (-\infty, \mu - \sigma/\xi] \quad when\ \xi < 0.$$

For example, the return level could be outside support if ξ is less than zero, and the return level is greater the limit of the upper tail ($\mu - \sigma/\xi$). Undefined waiting times were excluded from comparisons of waiting time between variable types and distribution types.

ARMA Models. Autoregressive moving average (ARMA) models were fit to time series of detrended annual maxima using restricted maximum likelihood following the methods of [1,2]. Because these likelihood surfaces are known to be rough, we used the differential evolution optimization algorithm as implemented in the DEoptim package in R[3]. We fit 12 possible combinations of ARMA(p,q) models, with AR(p) components ranging between p=1 to p=3, and MA(q) components ranging between q=0 to q=3. Model selection was performed using the corrected Akaike Information Criterion (AICc). We fit the GEV to the Cholesky residuals of the most parsimonious ARMA model for each time series. We refer to the order of the ARMA model as the sum p+q of the most parsimonious ARMA model, and the eigenvalue of the parameters is the maximum of the absolute values of the eigenvalues of the AR parameter matrix.

Literature cited in Appendix 1 to Chapter 5: Methods

1. Ziebarth, N. L., Abbott, K. C. & Ives, A. R. Weak population regulation in ecological time series. *Ecol. Lett.* 13, 21–31 (2010).

2. Ives, A. R., Abbott, K. C. & Ziebarth, N. L. Analysis of ecological time series with ARMA(p,q) models. *Ecology* 91, 858–71 (2010).

3. Mullen, K., Ardia, D., Gil, D., Windover, D. & Cline, J. "DEoptim": An R package for global optimization by differential optimization. *J. Stat. Softw.* 40, 1–26 (2011).

APPENDIX 2 TO CHAPTER 5: EXTENDED DATA

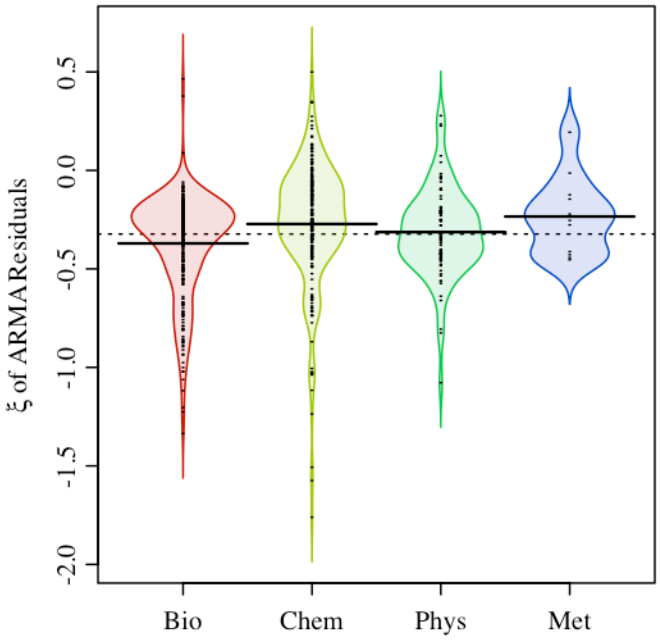

Extended Data Figure 1. Beanplots of the shape (ξ) of the ARMA residuals. Each "bean" consists of a mirror image of the density plot of ξ or of the waiting times in each category (red = biological, yellow = chemical, green = physical, blue = meteorological). The values of individual observations are indicated by the small black dashes inside each bean. Horizontal dotted line is the mean across all categories. Solid horizontal lines are the means within each category.

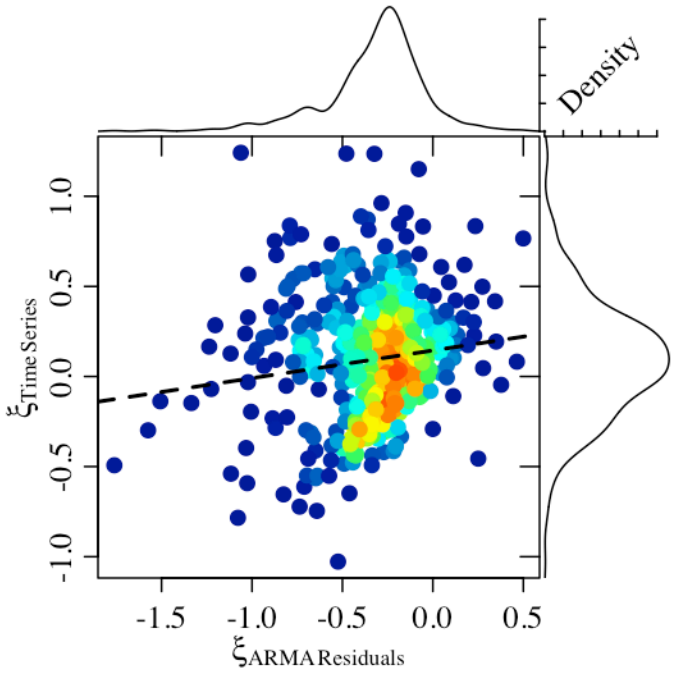

Extended Data Figure 2. The distributions and relationship between ξ of time series and ξ of the residuals of ARMA fits. Density plots in the margins reflect the distribution of the parallel axis. The color of the points in the scatter plot is proportional to the number of points in that coordinate region, with red colors in regions overlain with many points. The dashed line is a linear regression that provides a visual reference for the relationship between the axes.

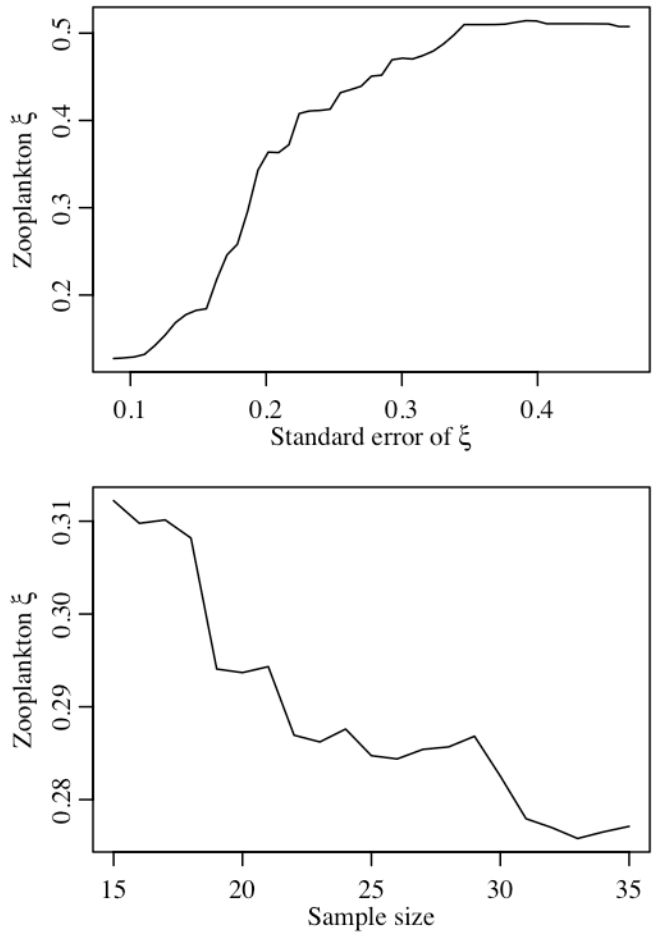

Extended Data Figure 3. Marginal effects of top two predictor variables on ξ from random forest constructed from zooplankton data. Vertical axes indicate values for zooplankton ξ (conditioned on the other predictor variables) found in the random forest across the range of the standard error of ξ (top) or across the range of sample sizes (bottom).

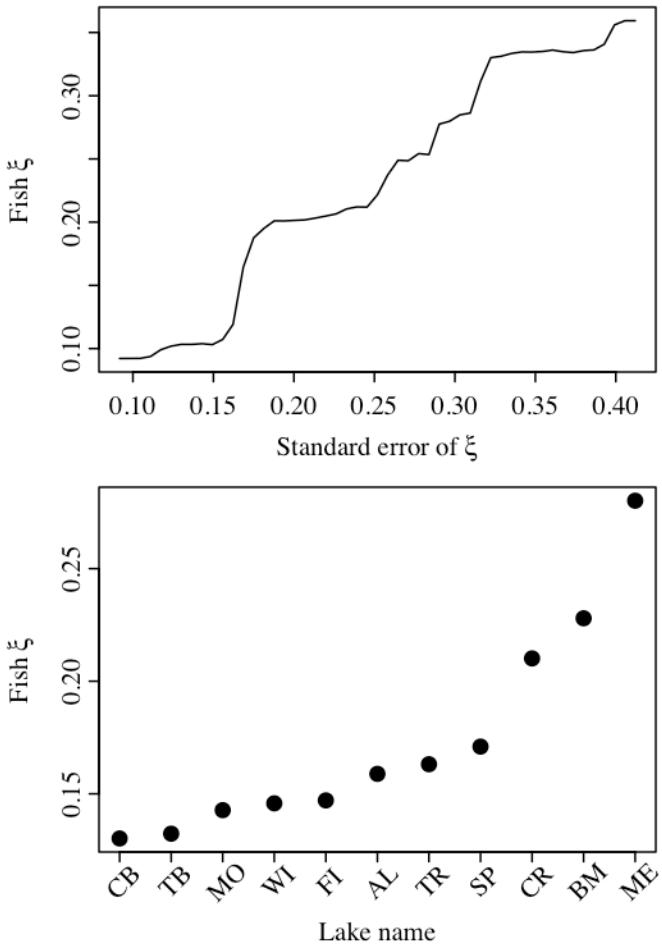

Extended Data Figure 4. Marginal effects of top two predictor variables on ξ from random forest constructed from fish data. Vertical axes indicate values for fish ξ (conditioned on the other predictor variables) found in the random forest across the range of the standard error of ξ (top) or across lakes (bottom). Lake names are as follows: CB = Crystal Bog, TB = Trout Bog, MO = Lake Monona, WI = Lake Wingra, FI = Fish Lake, AL = Allequash Lake, TR = Trout Lake, SP = Sparkling Lake, CR = Crystal Lake, BM = Big Muskellunge Lake, ME = Lake Mendota.

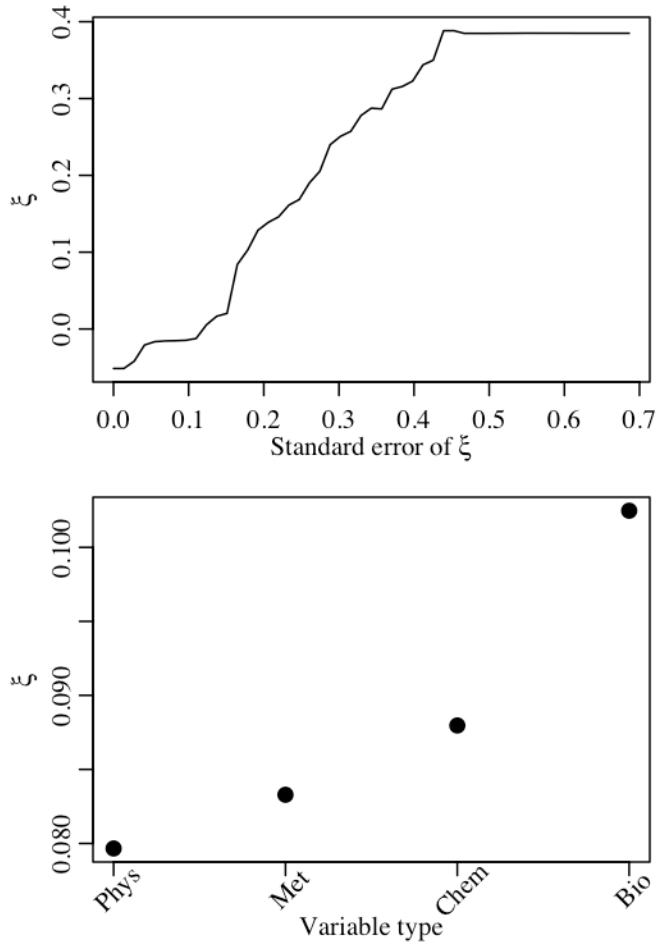

Extended Data Figure 5. Marginal effects of top two predictor variables on ξ from random forest constructed from all data. Vertical axes indicate values of ξ (conditioned on the other predictor variables) found in the random forest across the range of the standard error of ξ (top) or across variable types (bottom). Variable types are as follows: Phys = physical, Met = meteorological, Chem = chemical, Bio = biological.

APPENDIX 3 TO CHAPTER 5: SUPPLEMENTARY NOTES

Hypothesis testing. To estimate the standard errors of the ξ estimates, the covariance matrix from the GEV fit (thus parameter standard errors) was estimated from the solution to the Hessian computed by the optimization function. For optimization of the GEV, we used the Nelder Mead algorithm implemented in the optim function in R, which numerically derives the Jacobian of the algorithm gradient around optimized parameters. We identified a significant, positive correlation between the standard errors of the ξ estimates and ξ (linear regression between ξ as the response and standard errors plus intercept as predictors; regression multiple $R^2 = 0.22$ [0.219 for adjusted], $p < 2*10^{-16}$, $t = 12.94$, slope=2.0). Furthermore, there was evidence that the standard errors differed between categories (ANOVA, $F=9.2$, $p < 6.2*10^{-6}$), although the explained variance was low (multiple $R^2=0.04$, adjusted = 0.04).

Due to the relationship between the standard errors of ξ and the estimates of ξ and variables types, we compared estimates of ξ across variable types using both least squares regression and weighted least squares regression. The response variable was ξ, and the four variable types were used as categorical predictors, with the biological type serving as the reference level (intercept). The inverse of the square of the standard error of ξ was used as the weight in the weighted least squares regression. In both types of regression, the biological variable had ξ significantly greater than 0 (estimate = 0.25 for unweighted, 0.16 for weighted), and each of the other variables types had significantly lower ξ than the biological category (all $p \leq 2.08*10^{-5}$ for all categories and regression types). The linear regression $R^2=0.28$ (0.24 adjusted), and the weighted linear regression $R^2=0.64$ (0.64 adjusted). Contrasts were set up to define the null hypotheses that each difference between the following pairs of variable types was equal to zero: chemical - biological,

physical - biological, meteorological - biological. To maintain a significance level of 0.05, p-values for these multiple comparisons were corrected using the multcomp package in R, which we used to implement the Dunnett's many-to-one test[1]. After correction, all variable types in both models maintained a mean ξ that was significantly less than the mean ξ of the biological variable type (across models and factor levels, all $p \leq 0.0057$).

Random Forests. We constructed random forest regression trees[2] as a method for exploring relationships between ξ and other characteristics of the time series, as well as between ξ and the taxonomic classification of fish and zooplankton. Random forests used bootstrap aggregation ("bagging", sampling the data set with replacement), and each forest consisted of 2,000 trees. Random forests differ from other regression tree algorithms in that at each branch in each of the trees, a random subset of the predictor variables is selected (square root of the number of predictors, rounded up). By selecting a random subset of predictors, the algorithm limits the potential for a few highly predictive variables to dominate the formation of trees, thereby reducing the correlation among trees in the forest. The algorithm for generating random forests also avoids the problem of over-fitting, and the trees do not require "pruning". During forest fitting, out-of-bag error is calculated from the errors for predicting a given sample using only regression trees in the forest that did not include that sample (due to bootstrapping with replacement). The mean of these errors is the out-of-bag error for the sample. To determine variable importance, out-of-bag errors are calculated as above, except now observations of the predictor variable of interest are scrambled with respect to the observations of the response variable. The ratio of the out-of-bag error (which is measured per sample) before and after the scrambling of the predictor variable is a measure of the importance of the predictor variable to

estimating the sample. The mean of this ratio across all samples is a basic measure of the importance of the predictor variable. Because random forests are indeed random (due to bagging, randomizing subsets of predictors, and scrambling), results can vary between forests constructed using the same original data set. However, for a large number of trees, the results for the forest converge.

A random forest was constructed for the full data set, as well as for two subsets corresponding to the zooplankton and fish data. Fish and zooplankton were analyzed separately from the rest of the data set because taxonomic information could not be used as a predictor for the other variables. The number of possible splits in a tree increases exponentially with the number of factor levels (and therefore predictor variables). Therefore, fish and zooplankton were analyzed separately from each other to reduce the number of unique taxa for each level of taxonomic classification (e.g., reduce the number of families). Genus was not used as a factor for zooplankton because of the larger number of zooplankton genera.

All data sets included the following predictor variables: standard error of ξ, lake, sample size, μ (GEV location) of ARMA residuals, σ (GEV scale) of ARMA residuals, ξ of ARMA residuals, variance of ARMA residuals, variance of the MA component of the ARMA model (equal to residual variance when q=0), stationary variance of the ARMA process, MA order (q), AR order (p), eigenvalue of AR parameters, and the ratio of the stationary variance of the ARMA process to the variance of the MA component. Analysis of the full data set also included variable type (e.g., biological) as a predictor. Fish and zooplankton analyses also included taxonomic classification (order, family, and genus for fish; phylum, class, order, and family for

zooplankton). When constructing forests for the full data sets and the fish and zooplankton subsets, and missing values in response or predictor variables resulted in removal of that sample (i.e., row of data) from the analysis. Therefore, the full data set consisted of 587 samples (down from the 595 possible), the fish data set included 111 samples (no samples removed), and the zooplankton data set included 157 samples (165 possible).

We constructed random forests using the *randomForest*[3] in R. We checked the importance of predictor variables estimated by randomForest against those estimated from another package, *party*[4], which implements additional algorithms to correct for a bias in variable importance that can favor correlated, continuous, or many-level categorical predictors. We report rank variables and report their importance according to the *party* method. Both packages consistently indicated that the standard error of ξ was the most important predictor of ξ in forests constructed for fish, zooplankton, and for the entire data set.

For zooplankton, the two most important predictors were the standard error of ξ (importance = 0.03), and sample size (importance = 0.003). Estimates of the marginal effects (computed using the partialPlot function in *randomForest*) of these predictors on the tailedness of zooplankton indicates that zooplankton ξ increases from 0.13 to 0.51 across the range of standard errors, but ξ only changes from 0.31 to 0.28 across the range of sample sizes (Extended Data Fig. 3).

For fish, the two most important predictors were the standard error of ξ (importance = 0.023) and lake identification (importance = 0.0053). Across the range of standard errors, fish ξ increases from 0.09 to 0.34, and across lakes fish ξ ranged from 0.13 to 0.28 (Extended Data Fig. 4).

According to the random forest (produced by *randomForest*), the two lakes with the smallest fish ξ (conditional on values of all other predictor variables) were the two bog lakes in the data set (Extended Data Fig. 4). Sample size was the second most important predictor for zooplankton, and for fish it was the third most important predictor (importance of sample size to fish ξ = 0.002). Although lake identification was the second most important predictor for fish, it was the least important predictor for zooplankton (importance of lake to zooplankton ξ = -0.0005; negative importance means that the average out-of-bag error slightly increased when this predictor variable was scrambled).

The two most important variables for the full data set were the standard error of ξ (importance = 0.026) and variable type (importance = 0.014). Across the range of the standard error of ξ, tailedness increased from -0.05 to 0.38. Across variable types, ξ ranged from 0.08 for physical to 0.10 for biological (Extended Data Fig. 5).

Literature Cited in Appendix 3 to Chapter 5: Supplementary Notes

1. Hothorn, T., Bretz, F. & Westfall, P. Simultaneous inference in general parametric models. *Biometrical J.* 50, 346–363 (2008).
2. Breiman, L. E. O. Random Forests. 5–32 (2001).
3. Liaw, A. & Wiener, M. Classification and regression by randomForest. *R news* 2, 18–22 (2002).
4. Strobl, C., Boulesteix, A.-L., Kneib, T., Augustin, T. & Zeileis, A. Conditional variable importance for random forests. *BMC Bioinformatics* 9, 307 (2008).